Spring 2008

Derivation of new double-input DC-DC converters using the building block methodology

Karteek Gummi

Department:

DERIVATION OF NEW DOUBLE-INPUT DC-DC CONVERTERS USING THE BUILDING BLOCK METHODOLOGY

by

KARTEEK GUMMI

A THESIS

Presented to the Faculty of the Graduate School of the

MISSOURI UNIVERSITY OF SCIENCE AND TECHNOLOGY

In Partial Fulfillment of the Requirements for the Degree

MASTER OF SCIENCE IN ELECTRICAL ENGINEERING

2008

Approved by

_____	_____
Dr. Mehdi Ferdowsi, Advisor	Dr. Badrul Chowdhury

_____

Dr. Keith Corzine

ABSTRACT

In most power electronic systems, the instantaneous input and output power vary by time and are not exactly identical with each other. Hence, providing a good match between them is a complicated task to deal with if not impossible. Furthermore, due to the wide variation range of the processed power, the overall efficiency of the system is not high. The solution is to hybridize the system using an energy storage unit like in hybrid electric vehicles, power factor correction systems, and photovoltaic systems. Multi-input converters play a key role in such hybridized systems, where it is required to have more than one power source. Utilizing multi-input converters is preferred to using several independent converters (multiple converters) from efficiency, components count, size, cost, and performance points of view. Several types of multi-input converters have been proposed in the literature. However, there haven't been many systematic approaches to derive multi-input converter topologies. Furthermore, all possible topologies are not completely explored and it is difficult to derive new converters from the existing topologies. In this thesis, a systematic approach to derive several new double-input converters using H-bridge cells or single-pole triple-throw switches as building blocks is proposed. Different operating modes and the switch realization of the new converters are obtained and their corresponding voltage ratios are derived. Bidirectional power flow is also considered. All of the proposed converters consist of only one inductor; hence, the number of passive elements that are required is reduced. The operating characteristics of the new converters are verified using simulation results.

ACKNOWLEDGEMENTS

I would like to express my sincere gratitude and appreciation to Dr. Mehdi Ferdowsi for giving me an opportunity to work on this interesting project. He not only gave me valuable advices in academics, but also helped my transition into a different culture. His subtle guidance with unbelievable patience has made a great impact on this research and me. I would also like to thank Dr. Badrul Chowdhury and Dr. Keith Corzine for serving on my committee. All three have significantly impacted me as instructors and advisors, and I'm proud of the education I've received under their care.

I have also benefited from many stimulating discussions on the nature of research and academia with Asha Patel and Kai Wan. It is, at this time that I take extreme pleasure in thanking my roommates and friends for putting up with me and supporting me during my lows and highs. It would have been impossible to have achieved all these things without their understanding.

Special thanks goes to my family, my mother Shashikala and my father Muralidhar Reddy, as well as my brother and extended family who endowed me with the curiosity about the natural world. You have all helped shape me into what I am today, and your support has been indispensable. All in all, I would like to thank everyone who has made it possible for me to climb up the ladder of the graduate degree program.

TABLE OF CONTENTS

Page

LIST OF ILLUSTRATIONS

LIST OF TABLES

1. MULTIPLE CONVERTER SYSTEMS AND MULTI-INPUT CONVERTERS

1.1. MULTIPLE CONVERTER SYSTEMS

In most power electronic systems, input power, output demand, or both instantaneously change and are not exactly identical with each other at any time instant. Hence, providing a good match between them is a complicated task to deal with if not impossible. Furthermore, due to the wide variation of processed power, overall efficiency of the system is not high. Hence, additional energy sources are required to assist the main source in fulfilling the load demand. In that case, the operating point of the main source will have a much smaller variation window [1-6]. The additional energy sources may be energy storage devices which can be recharged in case they are out of power.

The conventional approach of connecting multiple energy sources is placing them either in series or parallel with each other. Sources that are placed in series have to conduct the same current which is not always desirable. Also, as different sources have different voltage levels, they cannot be directly connected in parallel. Hence, multiple power electronic converters are required to connect multiple sources in a single system in order to supply the load demand.

An example of a system which requires multiple converters is a photovoltaic (PV) system [7, 8], which is depicted in Figure 1.1. The system consists of two sources of power which are PV cells and battery pack. A solar powered system can supply energy only during the day time or in particular only during clear sky days. On a cloudy sky day or at night, they are not capable of supplying power that is required by the load. So the system requires an additional voltage sources e.g. batteries or ultracapacitors to fulfill the additional load demand. Also during clear sky days the excess power generated by the

solar power can be used to recharge the batteries. Hence, the use of multiple converters is inevitable for a photovoltaic system.

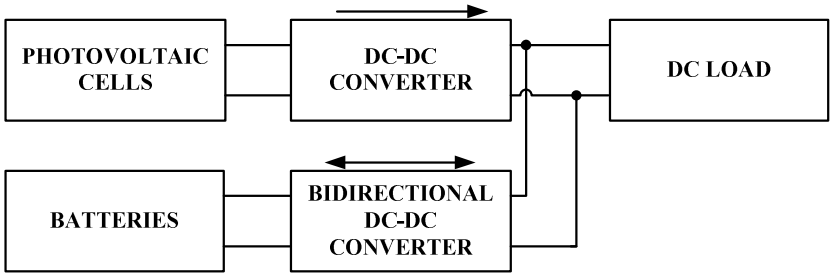

Figure 1.1. Photovoltaic system using multiple converters

Another example of a system which requires multiple converters is a hybrid electric vehicle (HEV). A basic hybrid vehicle consists of an internal combustion engine (ICE) and a battery pack. Batteries are used as an electric power source or as an energy storage unit. Other sources like ultracapacitors or flywheels can be used in place of batteries. To improve the performance and efficiency of an HEV, more than one of these sources may be used. Hence, the use of multiple converters is inevitable. Use of multiple converters makes it possible to run the ICE at optimal rating with maximum efficiency and any additional energy requirement (say during acceleration) can be made available by batteries and ultracapacitors. Block diagram of an HEV which consists of ultracapacitors and batteries is shown in Figure 1.2. One can observe that the system consists of two bidirectional dc-dc converters to connect batteries and ultracapacitors.

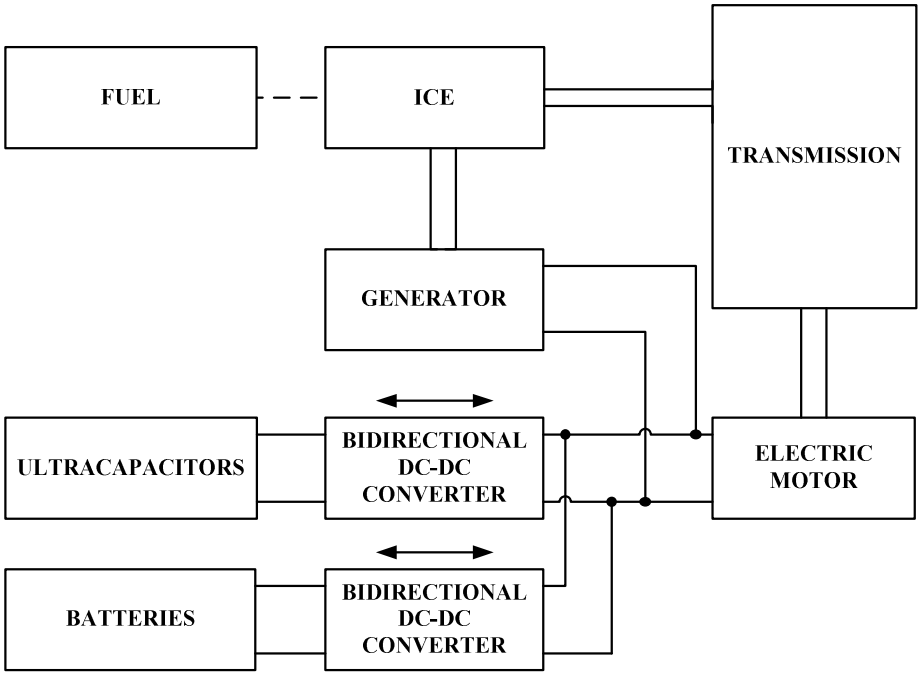

Figure 1.2. Hybrid Electric Vehicle system using multiple converters

It is more advantageous to use multi-input converters rather than several independent converters as it results in less number of components, simple control, more stability, and also lower losses in the system. An example of a system using multi-input converters is shown in Figure 1.3. This system consists of a single multi-input converter instead of using two separate converters.

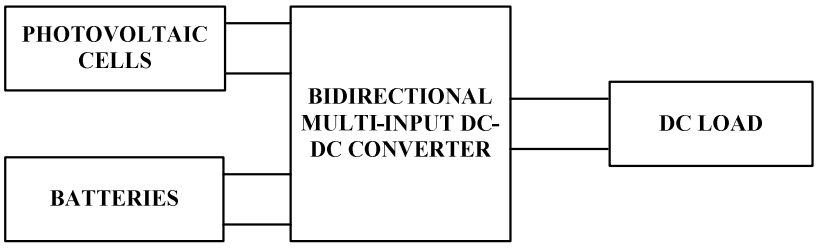

Figure 1.3. Photovoltaic system using a multi-input converter

In this chapter several multiple converter systems are discussed first followed by the existing multi-input converters.

1.2. CONVENTIONAL PARALLEL-CONNECTED CONVERTERS

Figure 1.4 shows the block diagram of a system in which converters are connected in parallel. Separate dc-dc conversion stages are employed for individual sources [9-16]. These converters are linked together at the dc bus and controlled independently. In some systems, a communication bus may be included to exchange information and manage power flow between the sources. Various examples of such converters are interleaved boost converter, current-fed push–pull converter, phase-shifted full-bridge converter, three-phase converter etc. The main drawback of such system lies in the fact that it is inherently complex and has a high cost due to the multiple conversion stages and communication devices between individual converters.

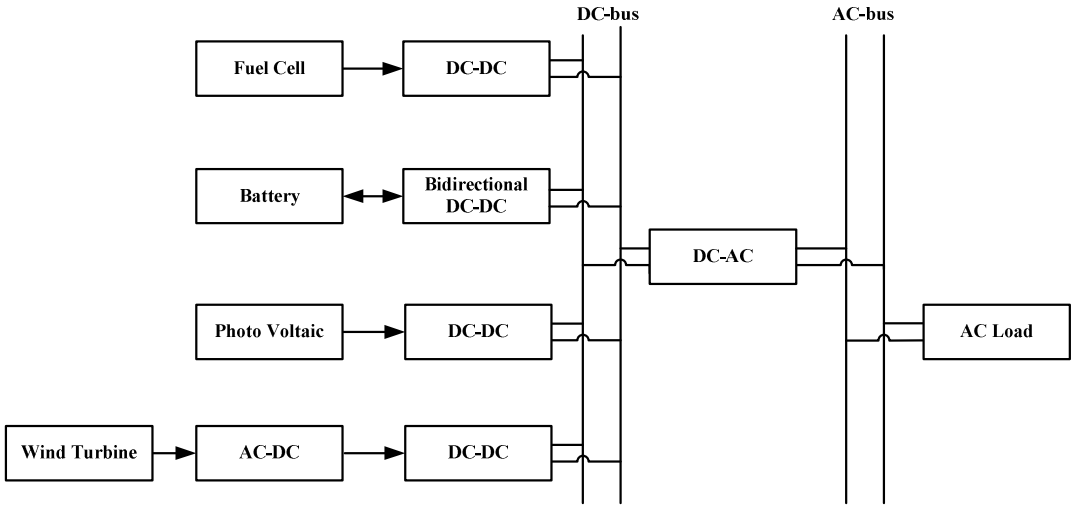

Figure 1.4. Parallel connected converter

1.3. CONVENTIONAL SERIES-CONNECTED CONVERTERS

An example of a system consisting series connected converters is shown in Figure 1.5. This type of configuration is used for low power wind and solar applications [17]. Such a converter layout results from the series connection of the output stages of two switch-mode dc-dc step-up converters. In this circuit configuration, output voltage and current regulation is difficult, since both of the sources used may have the intermittent nature. The main disadvantage of such systems is that output current flows through both converters hence power loss is high. Also, the gating signals for the two input voltage sources are conjunctive which may produce a circulating current in the two input sources.

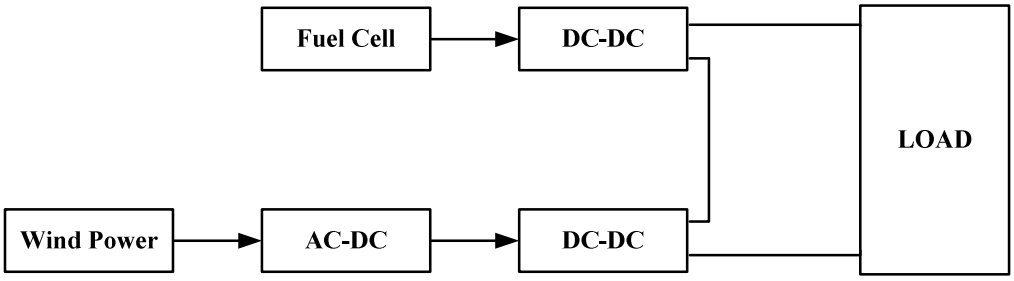

Figure 1.5. Series connected converters.

1.4. MULTI-INPUT CONVERTERS BASED ON FLUX ADDITIVITY

Placing converters either in parallel or series results in use of more number of components, more losses, and less efficiency. Hence, use of a single multi-input converter is preferred to using several multiple converters. One approach of deriving multi-input converters is using the principle of flux additivity [18-23]. In this method, sources are interconnected through a multi-winding transformer, so it is possible to

connect multiple sources having quite different voltage levels. Sources are galvanically isolated, which could be a compulsory requirement for safety reasons in some applications. In this type of systems, energy sources are combined in the magnetic form by adding up their produced magnetic flux together in the magnetic core of the coupled transformer instead of combining them in the electric form.

1.4.1. Simple Isolated Buck-Boost or Fly Back Converter: This is a simple type of multi-input converter which is shown in Figure 1.6. The converter uses the principle of magnetic coupling to combine two input sources [24-38]. This converter has no bi-directional power transfer capability. In general, as there are two primary windings which are coupled to single secondary the size is a bit big compared to conventional converters.

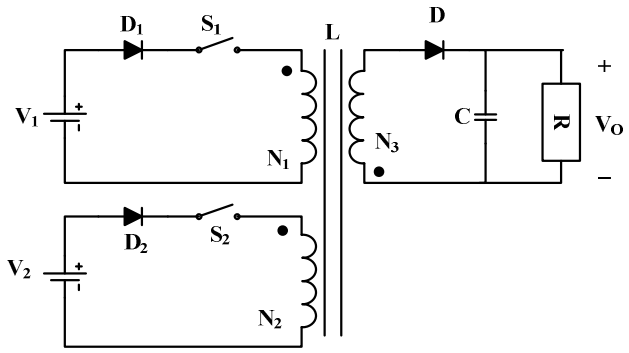

Figure 1.6. Simple isolated buck-boost multi-input converter

The converter in Figure 1.6 in general can have many inputs and many outputs like a multi-input-multi-output converter shown in Figure 1.7.

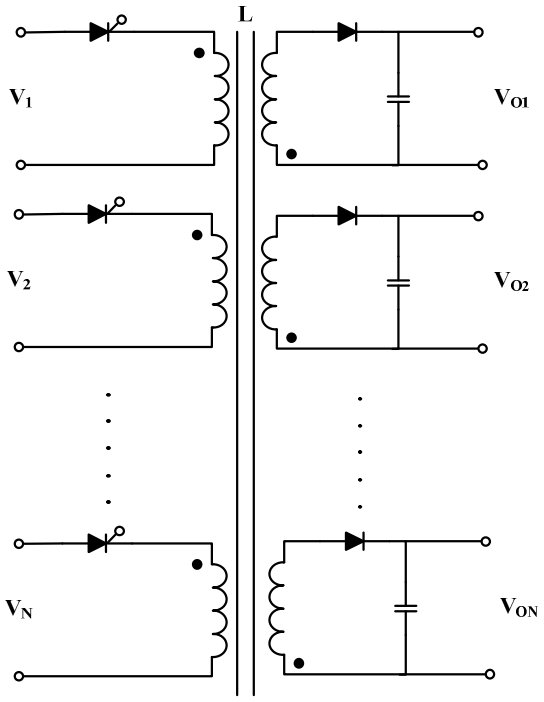

Figure 1.7. Multi-Input multi-output converter

1.4.2. Bi-directional Converters. A multi-input bidirectional dc-dc converter derived from a general topology is presented in [39, 40]. The topology shows a combination of dc-link and magnetic coupling. The dc-link is a method in which a number of different sources are linked together through switching cells to a dc bus where energy is buffered by means of capacitors. The resulting converters have the advantage of being simple in topology and have a minimum number of power devices.

Figure 1.8 shows a Multiple-input zero voltage switching (ZVS) bidirectional dc-dc converter [41, 42]. This converter has less switching losses and higher efficiency because the conduction loss due to input current in the boost and buck-boost converter is lower. During reverse power flow, this circuit cannot achieve zero voltage switching completely but it realizes reducing switching losses by the decrease of the switch voltage

at turn on. The low conduction loss can be achieved by using bi-directional two parallel boost converters instead of boost and buck-boost. Although this converter cannot achieve ZVS operation completely during reverse power flow, the switching loss is reduced by the effect of the auxiliary circuit.

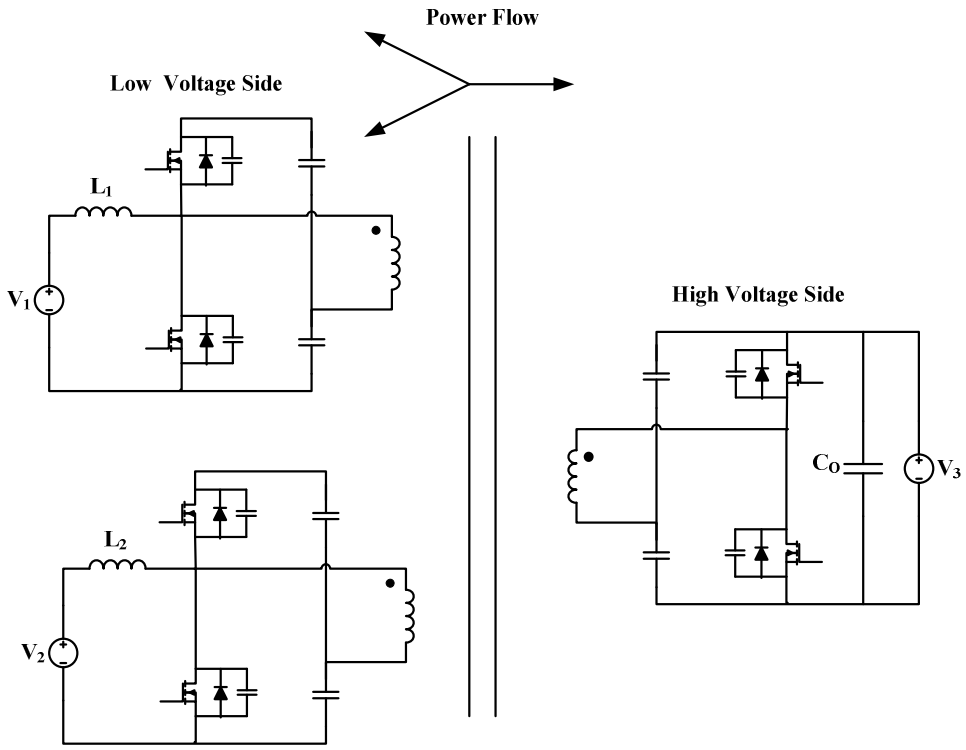

Figure 1.8. Multiple-input ZVS bidirectional dc-dc converter

1.4.3. Advanced Bi-directional Converter Combining DC-link and Magnetic Coupling. The converter obtained by combining dc-link and magnetic coupling [43] is shown in Figure 1.9, the voltage source and the storage are interconnected through a dc bus because they have nearly equal operating voltages, and the load is incorporated through a transformer winding. Six switches are used and all the three ports are

bidirectional. This system is suitable for applications in which the low operating voltage of the source and storage need to be boosted to match the load-side high voltage, which further feeds an inverter to generate an ac output.

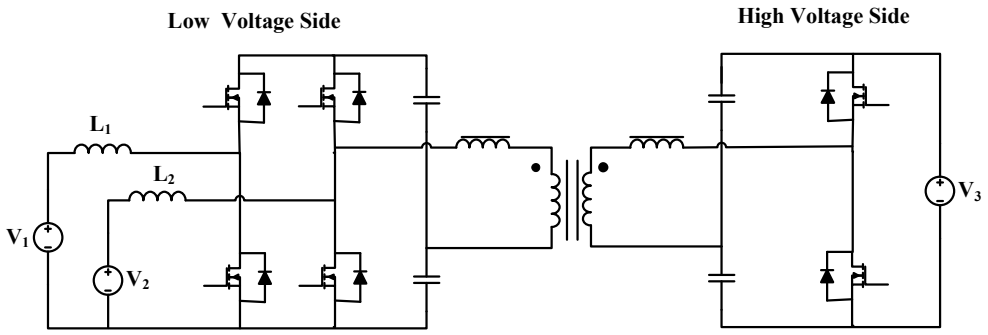

Figure 1.9. Three-port converter combining DC-link and magnetic coupling

The topology of Figure 1.9 looks similar to the topology given in [44] with the only difference being magnetic coupling. In addition to the converter circuit of Figure 1.9, Figure 1.10 shows the possibility of coupling the storage directly to the dc-bus, showing a simpler topology [45]. In this case, only four switches are needed. However, the performance of this converter may not be as good as the converter in Figure 1.9, since the dc-bus voltage (i.e. the terminal voltage of the storage) should not vary over a wide range. If a super capacitor is chosen as the storage, the energy storage capacity of the super capacitor cannot be fully utilized because the energy is proportional to the square of the terminal voltage.

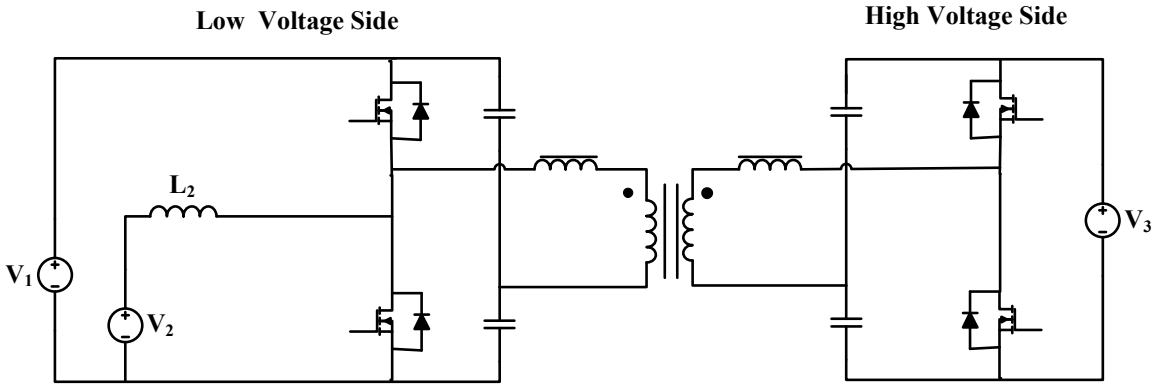

Figure 1.10. Three-port converter with storage directly coupled to DC-bus

1.5. MISCELLANEOUS TOPOLOGIES OF MULTI-INPUT CONVERTERS

The converter circuit which is shown in Figure 1.11 is a multi-input boost converter which consists of standard inverter phase leg connected to a dc bus capacitor, where in more phase legs can be paralleled to accommodate more sources. This can be used for bi-directional power flow as the switches used are bidirectional-conducting, forward-blocking with an anti parallel diode.

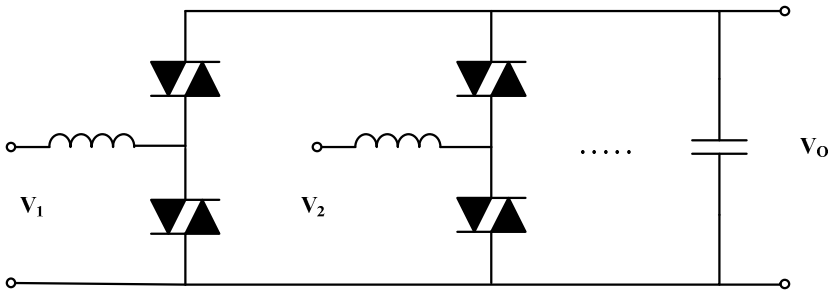

Figure 1.11. Three-port multi-input boost converter

Multi-input buck-boost converter, which is shown in Figure 1.12, is capable of interfacing sources of different voltage-current characteristics to a common load, while achieving a low part count [46, 47]. With multiple inputs, the energy source is diversified to increase reliability and utilization of renewable sources. The inputs are interfaced through a forward-conducting-bidirectional-blocking switch. However, it does not provide isolation between inputs, though isolation among outputs and inputs is optional. Bidirectional power flow to and from sources can be done extrinsically by using another converter connected from the output back to an input or by using the isolated multi-output where some outputs are used to feed back to some inputs. This configuration, allows for only unidirectional power flow. For sources such as primary batteries, solar cells, and fuel cells, this is sufficient. This type of converter can operate both in continuous and discontinuous conduction modes.

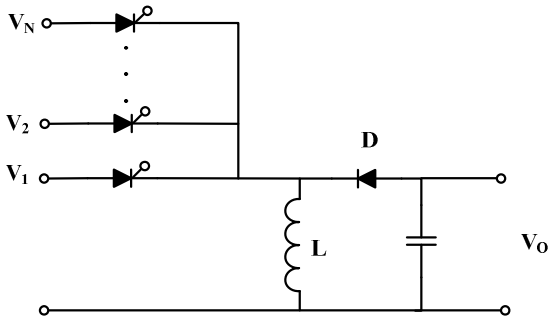

Figure 1.12. Multi-input buck-boost converter

Multi-input buck converter [46], which is shown in Figure 1.13, has dc sources that are placed in series with the diode like in the previous multi-input buck-boost

converter converter. This topology scales to more inputs as needed, but of course, is only capable of buck operations, which may be all that is needed in some applications.

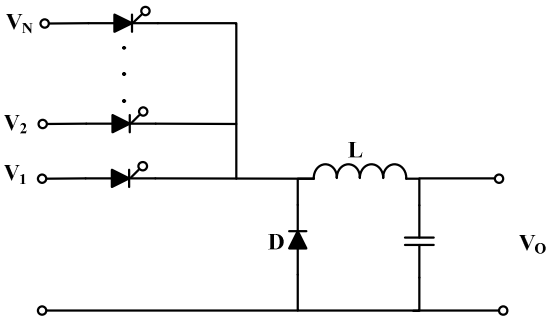

Figure 1.13. Multi-input buck converter

The multi-input buck-boost converter can have inverted, non-isolated output with respect to the inputs by replacing the inductor with coupled inductors to form a circuit as shown in Figure 1.14. This provides isolation between the input and the output sources. This circuit resembles a fly back converter. Hence, the name multi-input fly back converter.

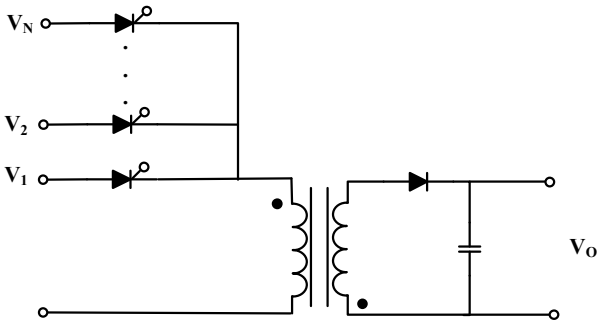

Figure 1.14. Multi-input flyback converter

Double-input integrated buck-buckboost converter, which is shown in Figure 1.15, is a simplified double-input converter with less number of switches, diodes, and inductors compared to the traditional multiple converters. It consists of switches, diodes equal to the number of input sources, an inductor and a capacitor [48-50]. The double-input dc-dc converter can draw power from two different voltage sources simultaneously or individually. This type of converter has no bi-directional power flow capability. This converter uses hard switching.

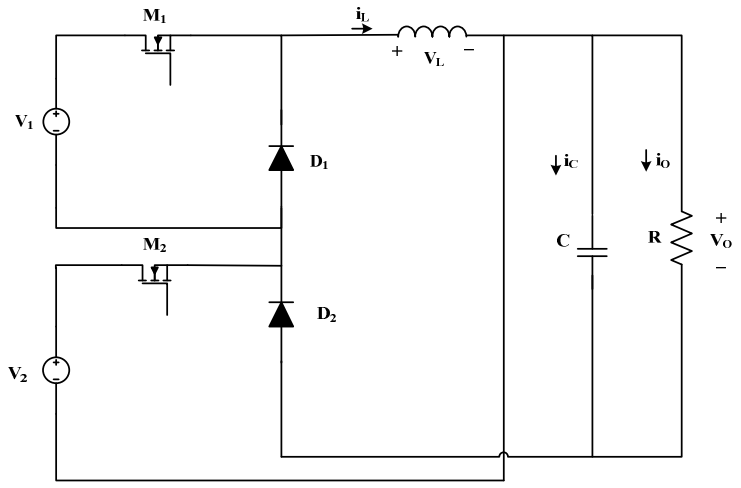

Figure 1.15. Integrated double-input buck-buckboost converter

Integrated buck-buck converter [50-53], which is shown in Figure 1.16, uses two bulk converters. This converter can also draw power from two different voltage sources simultaneously or individually. If each source operates individually the circuit operates as buck converter.

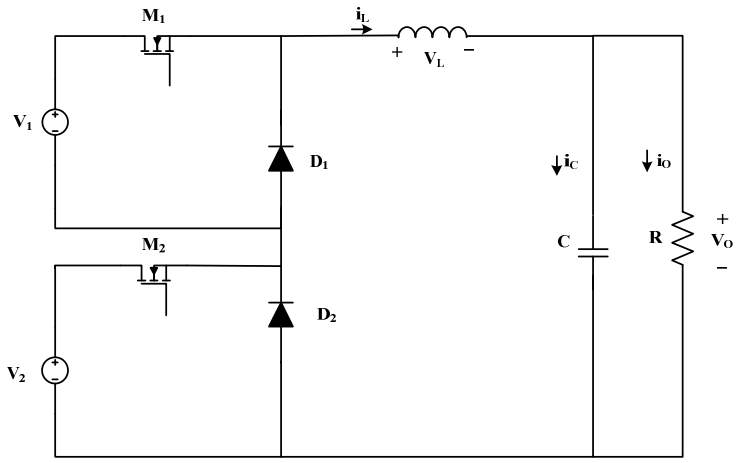

Figure 1.16. Integrated double-input buck-buck converter

Integrated buckboost-buckboost converter [50-53], as depicted in Figure 1.17, uses two bulk converters like the previous converter. The restriction of this converter is that both switches are not allowed to be turned on simultaneously; hence, each source can provide power to the load individually or can be supplemented with energy stored in the inductor supplied by the other source.

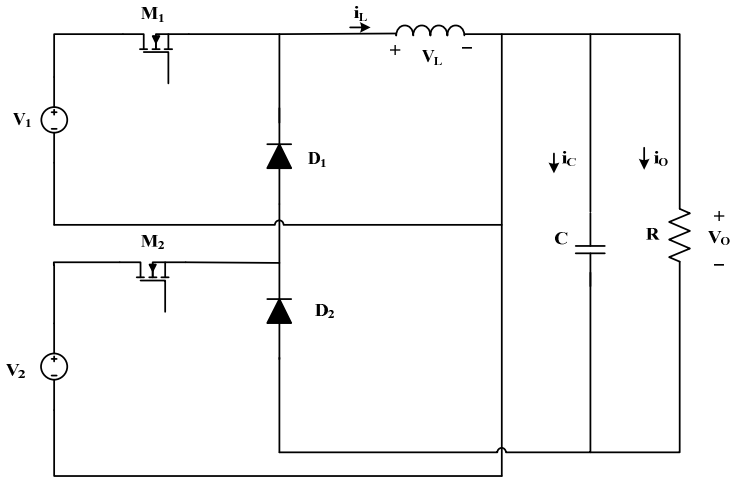

Figure 1.17. Integrated double-input buckboost-buckboost converter

An isolated half-bridge converter is proposed in [54-59] for grid-connected photovoltaic/wind application which interfaces three ports: a source, a bidirectional storage port, and an isolated load port. This multi-input converter, as depicted in Figure 1.18, utilizes three basic modes of operation within a constant-frequency switching cycle to provide two independent control variables. This allows tight control over two of the converter ports, while the third port provides the power balance in the system. The switching sequence ensures a clamping path for the energy of the leakage inductance of the transformer at all times. This energy is further utilized to achieve zero-voltage switching for all primary switches for a wide range of source and load conditions. This topology promises significant savings in component count and losses for power-harvesting systems.

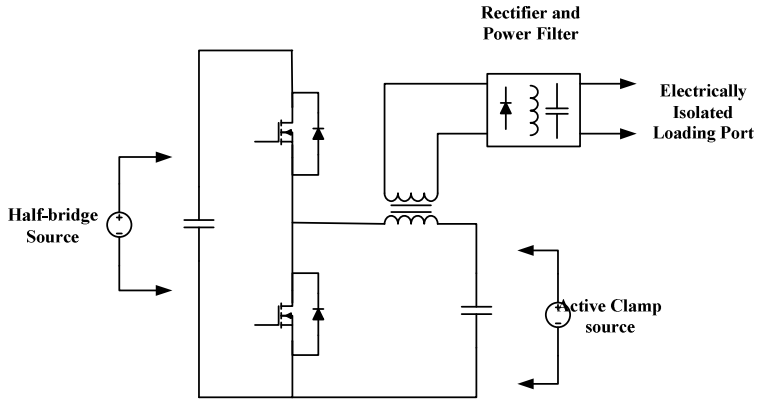

Figure 1.18. Half-bridge and active-clamp forward converter

As described earlier, multi-input converters can be implemented using either flux additivity or by combining the structure of the converters [60-63]. There is not a systematic approach to derive multi-input converters using building blocks until now. Also, all possible topologies are not completely explored and it is difficult to derive new converters from the existing topology. Hence, in this thesis, a systematic approach to derive multi-input converters by using H-bridge cells or single-pole triple-throw switches as building blocks is proposed.

In chapter two, new double-input dc-dc converter topologies are derived using H-bridge cells as building blocks and their operating modes and switch realization techniques are being discussed. In chapter 3, the voltage transfer ratios and the simulations of the new topologies are presented. In chapter 4, several other new double-input converter topologies are derived using a single-pole triple-throw switch as building block.

2. DERIVATION OF MULTI-INPUT DC-DC CONVERTERS USING H-BRIDGE CELLS

In modern power electronic systems, several power sources like batteries, ultracapacitors, PVs, fuel cells, generators etc. are used; therefore, utilization of multi-input converters is inevitable. The advantage of using such converters is that they integrate different power sources while each one is allowed to have different power rating. A general example of a multi-input converter is shown in Figure 2.1. Here any of the two input sources can be used to provide power by using only a single multi-input converter. This ultimately reduces the size, parts count, and cost and also it increases the efficiency of the system.

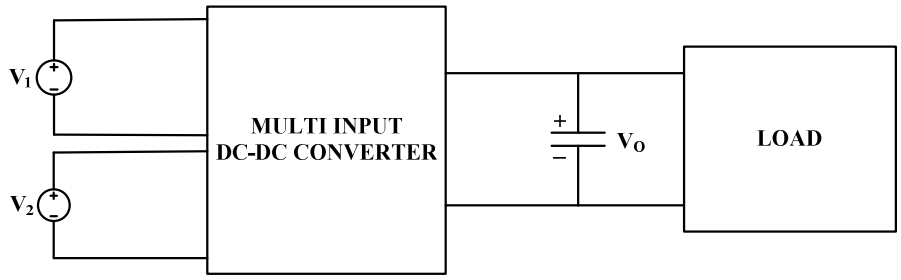

Figure 2.1. Multi-input dc-dc converter topology for two input dc sources

In this chapter, a general approach of synthesizing double-input converters using H-bridge cells as building blocks is introduced. Each H-bridge cell is then simplified based on the particular power flow. Switch realization for the remaining switches is also discussed.

2.1. INTRODUCTION TO H-BRIDGE CELLS

An H-bridge cell, as Figure 2.2 suggests, is comprised of four switches and a voltage source. The name 'H-bridge' is due to the physical appearance of the switches which resembles letter 'H'. The source included in the cell can be a battery, ultracapacitor, PV system, or fuel cell system. When switches S_1 and S_3 are turned on (and S_2 and S_4 are open), output voltage is equal to V. When switches S_2 and S_4 are turned on (and S_1 and S_3 are open), output voltage is equal to -V. The ideal switches used may be replaced by transistors, MOSFETs, or diodes according to the requirement of the system.

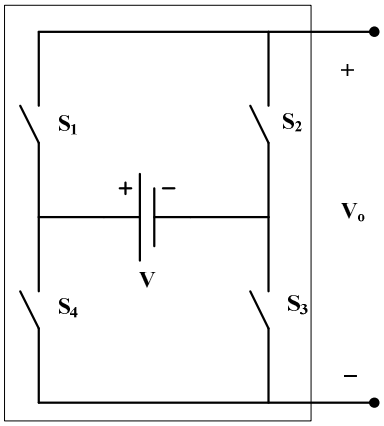

Figure 2.2. Circuit diagram of an H-bridge cell

Different modes of operation of an H-bridge cell are shown in Table 2.1. From the table one can see that some of the modes are undetermined, as the output voltage is not determined by voltage source V. Furthermore, some modes are not allowed, as this result in the voltage source to be shorted which is not permitted.

Table 2.1. Output voltage of an H-bridge cell

S_1	S_2	S_3	S_4	V_O
OFF	OFF	OFF	OFF	Undetermined
ON	OFF	OFF	OFF	Undetermined
OFF	ON	OFF	OFF	Undetermined
OFF	OFF	ON	OFF	Undetermined
OFF	OFF	OFF	ON	Undetermined
ON	OFF	ON	OFF	V
OFF	ON	OFF	ON	-V
ON	OFF	OFF	ON	0
OFF	ON	ON	OFF	0
ON	ON	OFF	OFF	Not allowed
OFF	OFF	ON	ON	Not allowed
ON	ON	ON	OFF	Not allowed
ON	OFF	ON	ON	Not allowed
ON	ON	OFF	ON	Not allowed
OFF	ON	ON	ON	Not allowed
ON	ON	ON	ON	Not allowed

In this thesis, an H-bridge cell with an inductor connected in series with its voltage source is called an enhanced H-bridge cell. An enhanced H-bridge cell, which is shown in Figure 2.3, consists of switch pairs S_1 & S_2 and S_3 & S_4 that cannot be open at the same time as this interrupts the continuous flow of the inductor current. One can observe from the different modes of operation of an enhanced H-bridge cell, given in Table 2.2, that some of the modes which are not allowed in the previous case are allowed in this case as there is an inductor in series with the source. Also current of the inductor is

assumed to be continuous and having switches of one leg to be on is assumed to be allowed in Table 2.2.

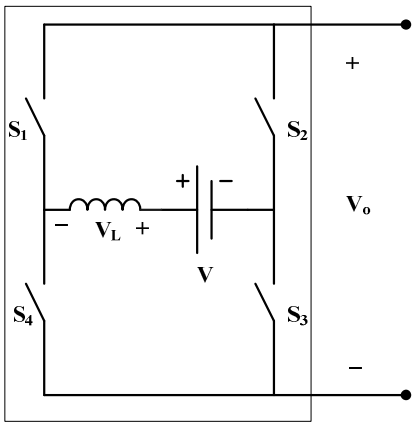

Figure 2.3. Circuit diagram of an enhanced H-bridge cell

Table 2.2. Voltage across the inductor of an enhanced H-bridge cell

S_1	S_2	S_3	S_4	V_L
OFF	OFF	OFF	OFF	Not allowed
ON	OFF	OFF	OFF	Not allowed
OFF	ON	OFF	OFF	Not allowed
OFF	OFF	ON	OFF	Not allowed
OFF	OFF	OFF	ON	Not allowed
ON	ON	OFF	OFF	V
OFF	OFF	ON	ON	V
ON	OFF	OFF	ON	Not allowed
OFF	ON	ON	OFF	Not allowed
ON	OFF	ON	OFF	$(V - V_O)$
OFF	ON	OFF	ON	$(V + V_O)$
ON	ON	ON	OFF	V

Table 2.2. Voltage across the inductor of an enhanced H-bridge cell (continued)

S_1	S_2	S_3	S_4	V_L
ON	OFF	ON	ON	V
ON	ON	OFF	ON	V
OFF	ON	ON	ON	V
ON	ON	ON	ON	V

2.2. DERIVATION OF DOUBLE-INPUT BUCK-BUCK CONVERTER USING H-BRIDGE CELLS

A simple outline of a new dc-dc converter using H-bridge cells as building blocks is shown in Figure 2.4. Topology introduced in Figure 2.4, herein after named as buck-buck converter, resembles the topology of a buck converter with two inputs. The advantage of this type of converter is that it contains only one inductor so the size, parts count, weight, and cost are reduced. By replacing H-bridge cells in a buck-buck converter with their circuit topology, one would obtain Figure 2.5.

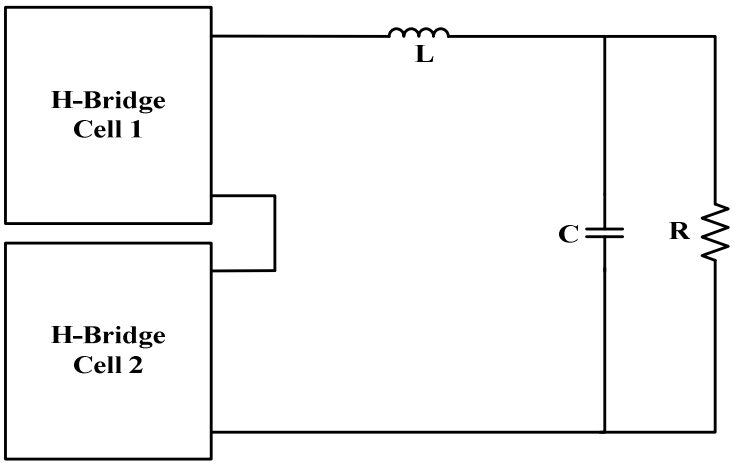

Figure 2.4. Outline of a buck-buck converter using H-bridge cells

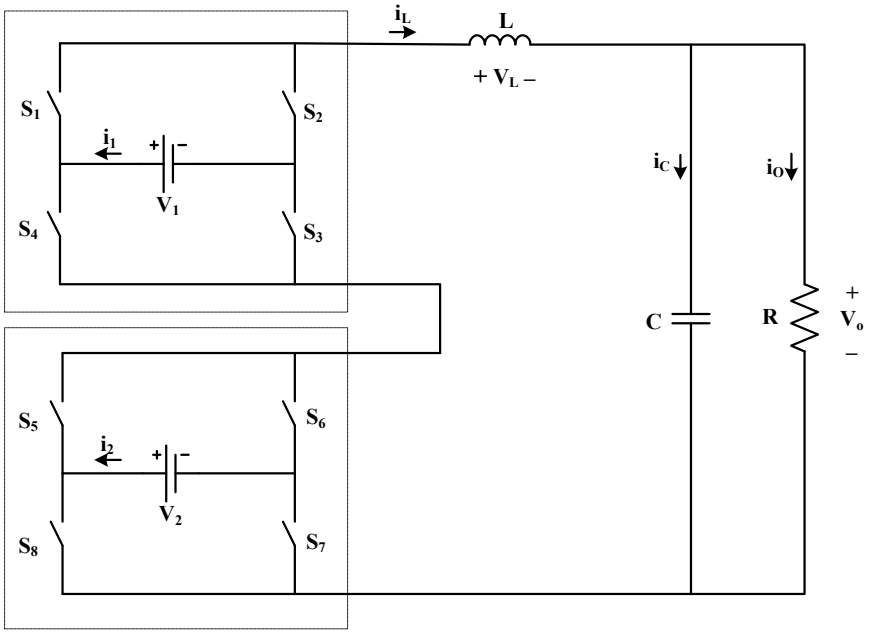

Figure 2.5. Double-input buck-buck converter using H-bridge cells

Four modes of operation that occur under unidirectional power flow are depicted in Figure 2.6, focusing on the voltages across the inductor.

MODE I (S_1, S_3, S_6, & S_7: on)

In this mode V_1 supplies energy to the load and inductor L as depicted in Figure 2.6 (a).

MODE II (S_2, S_3, S_5, & S_7: on)

In this mode V_2 supplies energy to the load and inductor L as depicted in Figure 2.6 (b).

MODE III (S_2, S_3, S_6, & S_7: on)

In this mode both the power sources are disconnected from the circuit. The energy stored in the inductor is being released to the load. Thus inductor gets de-energized during this mode as depicted in Figure 2.6 (c).

MODE IV (S_1, S_3, S_5, & S_7: on)

In this mode both the power sources supply energy to the load and inductor L. Thus both the sources can operate simultaneously as depicted in Figure 2.6 (d).Voltage across the inductor for different modes of operation is given in Table 2.3.

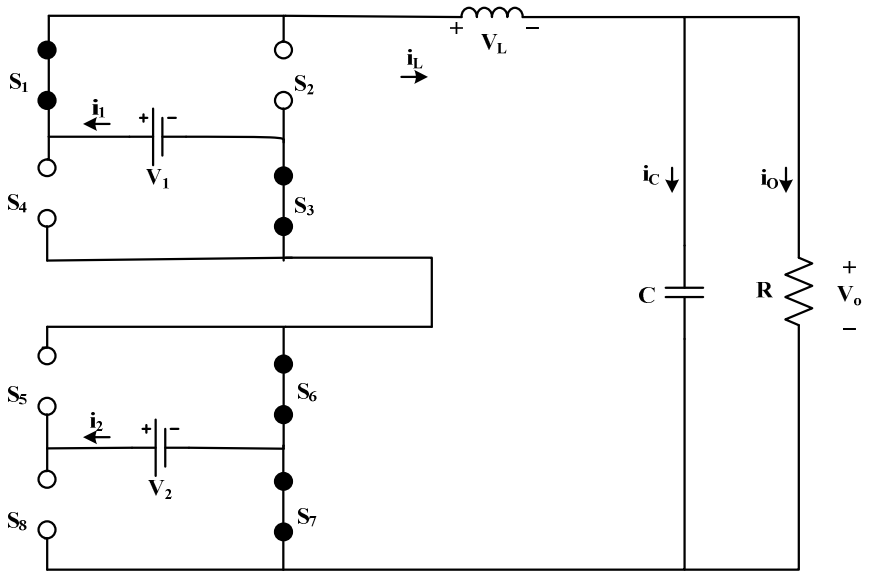

(a) Mode I

Figure 2.6. Different modes of operation of a double-input buck-buck converter using H-bridge cells

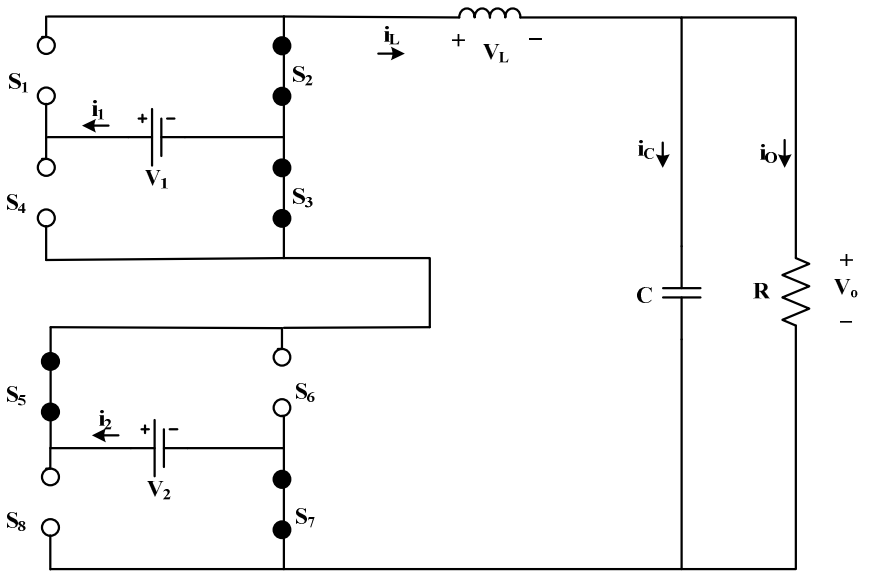

(b) Mode II

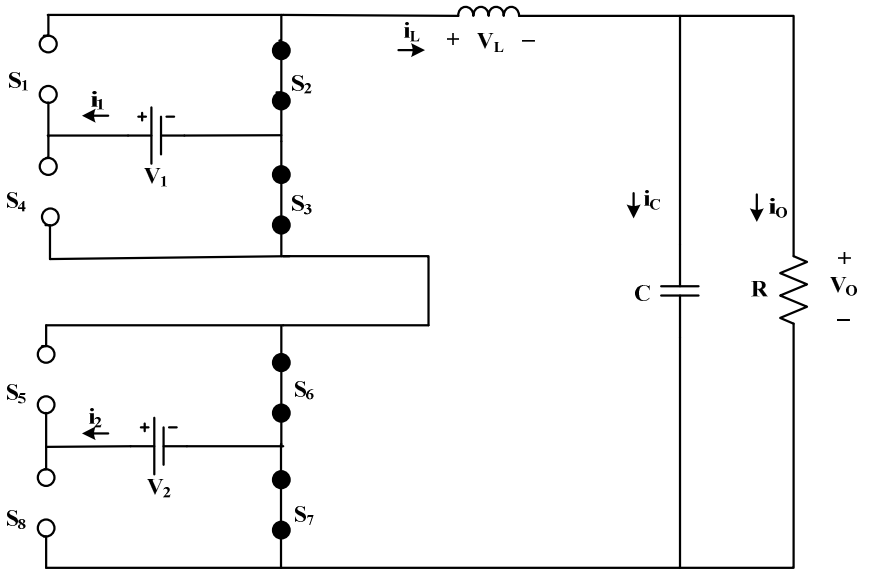

(c) Mode III

Figure 2.6. Different modes of operation of a double-input buck-buck converter using H-bridge cells (continued)

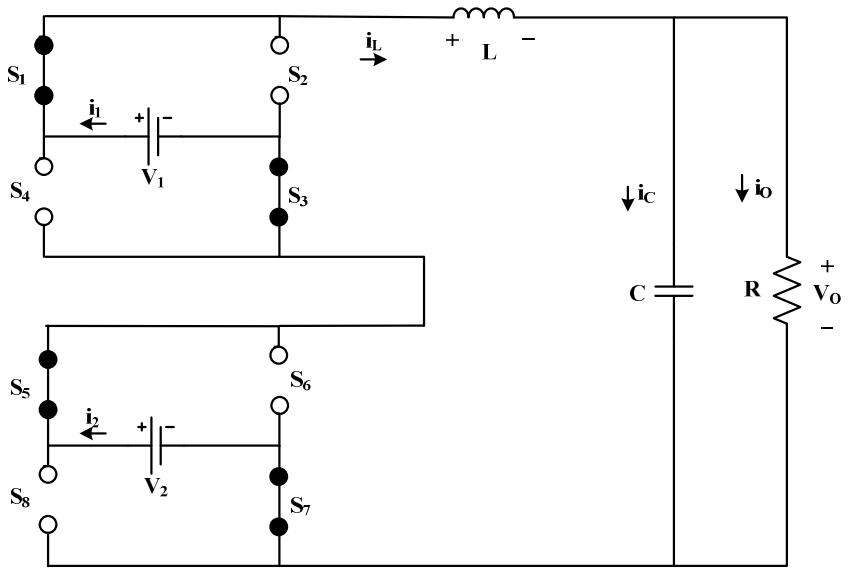

(d) Mode IV

Figure 2.6. Different modes of operation of a double-input buck-buck converter using H-bridge cells (continued)

Table 2.3. Voltage across the inductor for different modes of operation of a double-input buck-buck converter using H-bridge cells

Mode	**V_L**	**Switches ON**
I	$V_1 - V_o$	S_1, S_3, S_6, & S_7
II	$V_2 - V_o$	S_2, S_3, S_5, & S_7
III	$- V_o$	S_2, S_3, S_6, & S_7
IV	$V_1 + V_2 - V_o$	S_1, S_3, S_5, & S_7

It can be seen from the circuit operation that switches S_4 and S_8 are not used at all so they can be eliminated from the circuit. And also switches S_3 and S_7 are always on so

they can be shorted. Hence, the circuit topology can be reduced to Figure 2.7 which consists of only four switches.

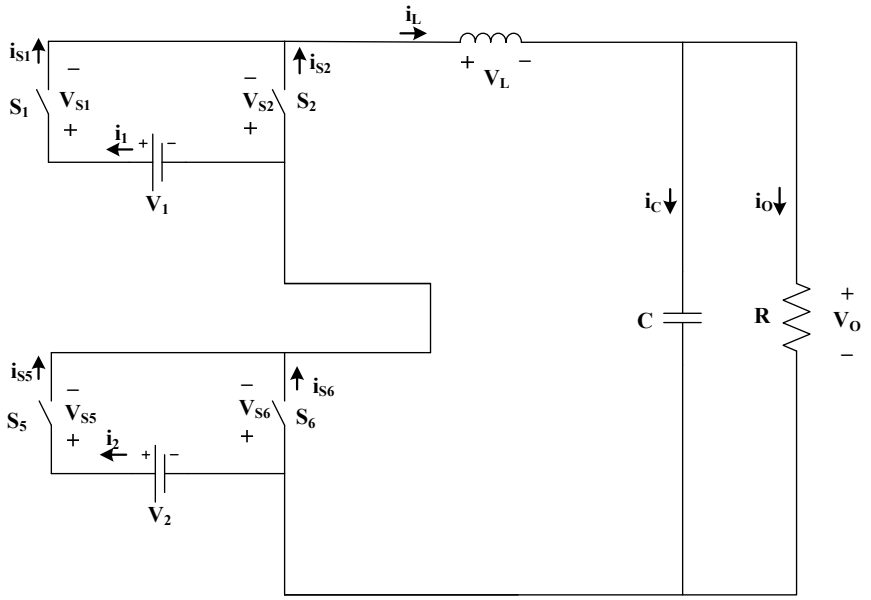

Figure 2.7. Derived topology of a double-input buck-buck converter using H-bridge cells

In the above circuit the switches can be replaced by diodes or transistors. One may obtain the circuit with transistors and diodes by the following explanation. As the power flow through the inductor is unidirectional, i_L should always be positive.

(If S_1 is on ➔ S_2 is off) => ($i_{S1} > 0$ & $V_{S2} < 0$)

(If S_2 is on ➔ S_1 is off) => ($i_{S2} > 0$ & $V_{S1} > 0$)

As switch S_2 conducts positive current and opposes negative voltage it can be replaced by a diode and as switch S_1 conducts positive current and positive voltage it can be replaced by a transistor. Similarly S_6 can be replaced by a diode and S_5 can be replaced by a transistor. So the final circuit that is obtained is shown in Figure 2.8.

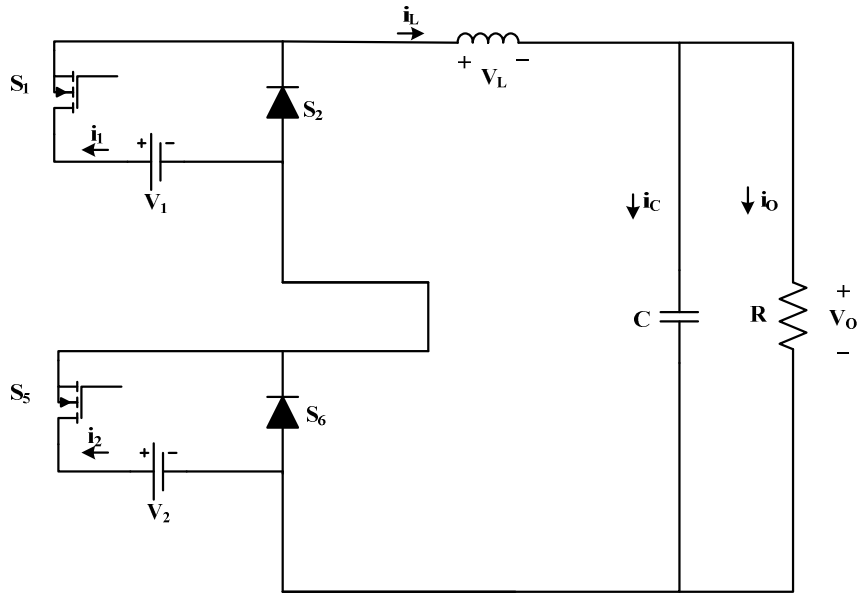

Figure 2.8. Final derived double-input buck-buck converter using H-bridge cells

2.3. DERIVATION OF DOUBLE-INPUT BUCKBOOST-BUCKBOOST CONVERTER USING H-BRIDGE CELLS

A simple outline of new dc-dc converter using H-bridge cells as building blocks is shown in Figure 2.9. It consists of two H-bridge cells which can operate simultaneously or individually. Topology introduced in Figure 2.9, herein after named as buckboost-buckboost converter, resembles the topology of a buckboost converter with two inputs. The advantage of this type of converter is that it contains only one inductor so the size, parts count, weight, and cost are reduced. By replacing H-bridge cells in a buckboost-buckboost converter with their circuit topology, one would obtain Figure 2.10.

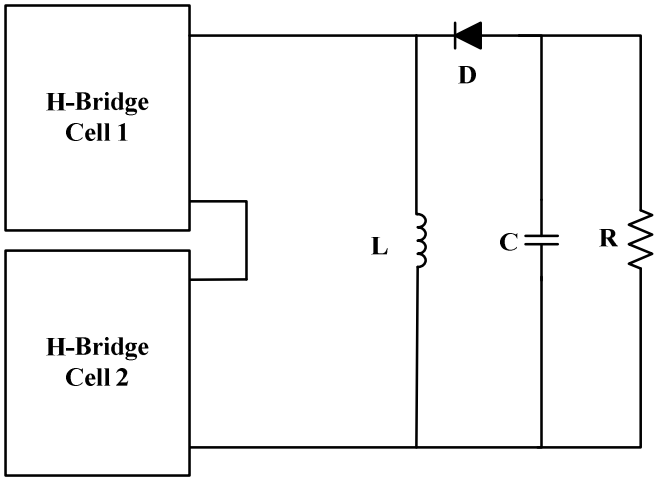

Figure 2.9. Outline of a buckboost-buckboost converter using H-bridge cells

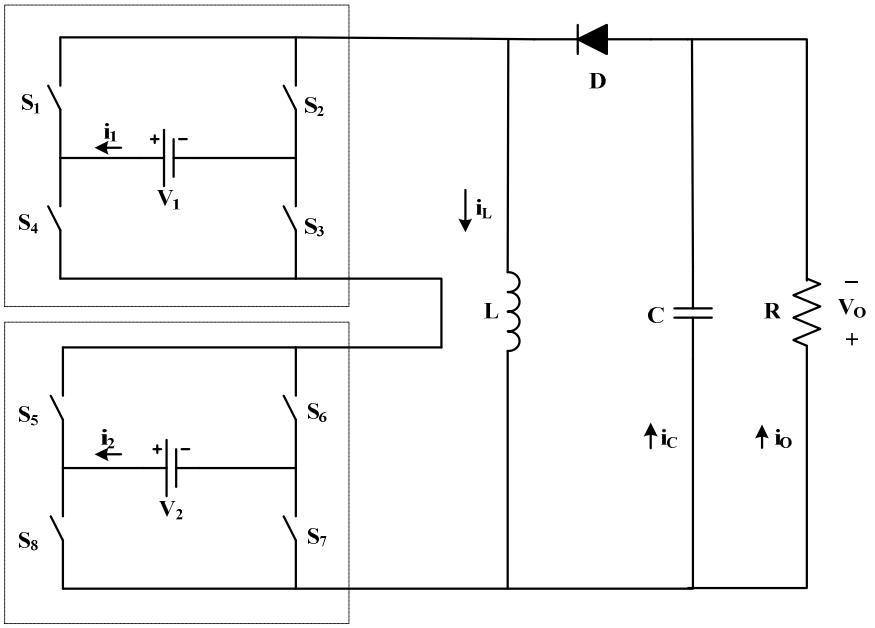

Figure 2.10. Double-input buckboost-buckboost converter using H-bridge cells

Four modes of operation that occur under unidirectional power flow are depicted in Figure 2.11, focusing on the voltages across the inductor.

MODE I (S_1, S_3, S_6, & S_7: on)

In this mode V_1 supplies energy to inductor L. The negative of the sum of voltages V_L and V_O appears across diode D; hence it is reverse biased as depicted in Figure 2.11 (a).

MODE II (S_2, S_3, S_5, & S_7: on)

In this mode V_2 supplies energy to inductor L. The negative of the sum of voltages V_L and V_O appears across diode D; hence it is reverse biased as depicted in Figure 2.11 (b).

MODE III (All are open)

In this mode both of the power sources are disconnected from the circuit. The energy stored in the inductor is being supplied to the load. Thus inductor gets de-energized during this mode. In this mode diode D is forced to conduct, to provide a current path for the inductor as depicted in Figure 2.11 (c).

MODE IV (S_1, S_3, S_5, & S_7: on)

In this mode both of the power sources supply energy to inductor L. Thus both of the sources can operate simultaneously in this mode. Diode D is reverse biased in this case as depicted in Figure 2.11 (d). The voltages across the inductor are shown in Table 2.4.

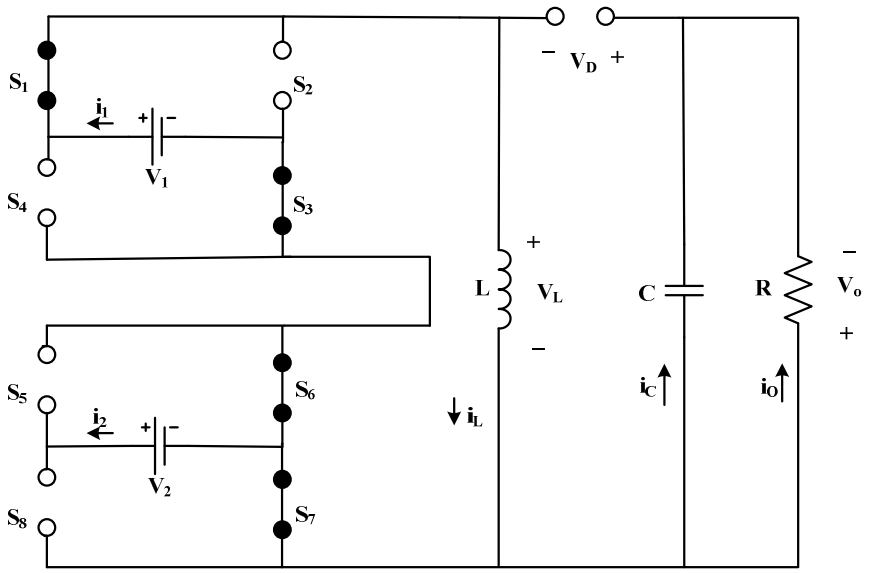

(a) Mode I

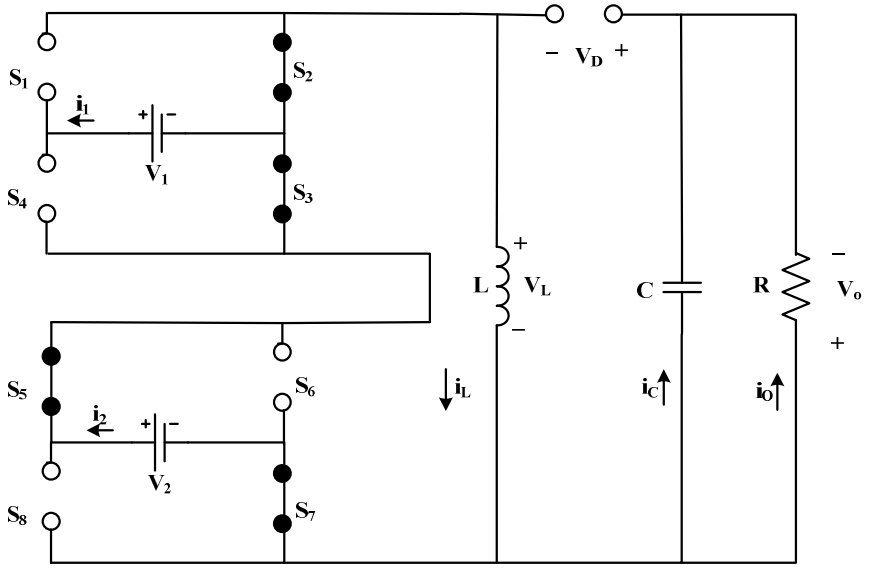

(b) Mode II

Figure 2.11. Different modes of operation of a double-input buckboost-buckboost converter using H-bridge cells

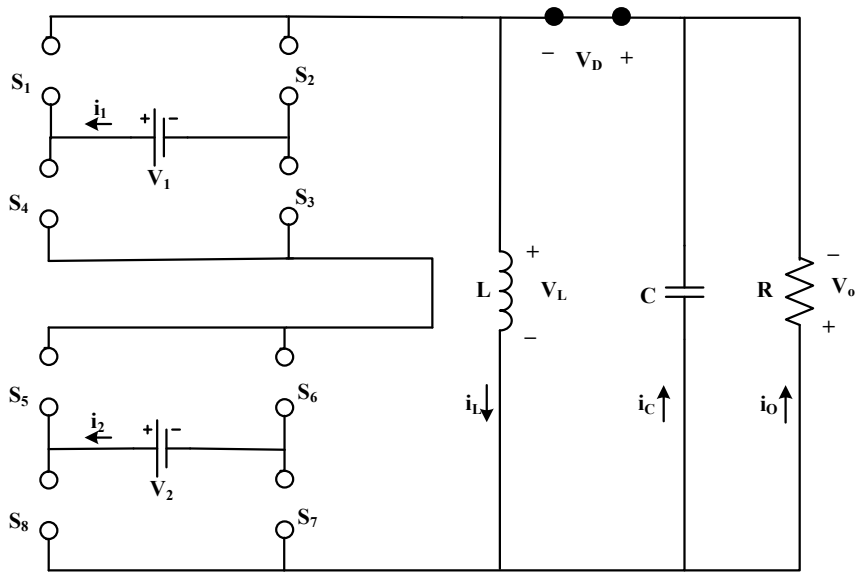

(c) Mode III

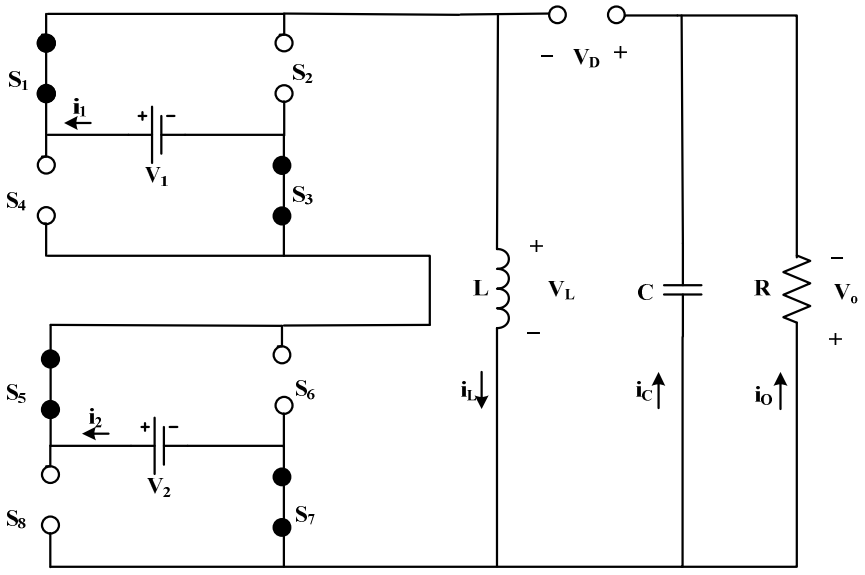

(d) Mode IV

Figure 2.11. Different modes of operation of a double-input buckboost-buckboost converter using H-bridge cells (continued)

Table 2.4. Voltage across the inductor for different modes of operation of a double-input buckboost-buckboost converter using H-bridge cells

Mode	$\mathbf{V_L}$
I	V_1
II	V_2
III	$-V_o$
IV	$V_1+ V_2$

It can be seen from the circuit operation that switches S_4 and S_8 are not used at all so they can be eliminated from the circuit. And also switches S_3 and S_7 can be shorted. Hence the circuit topology can be reduced to Figure 2.12 which consists of only four switches.

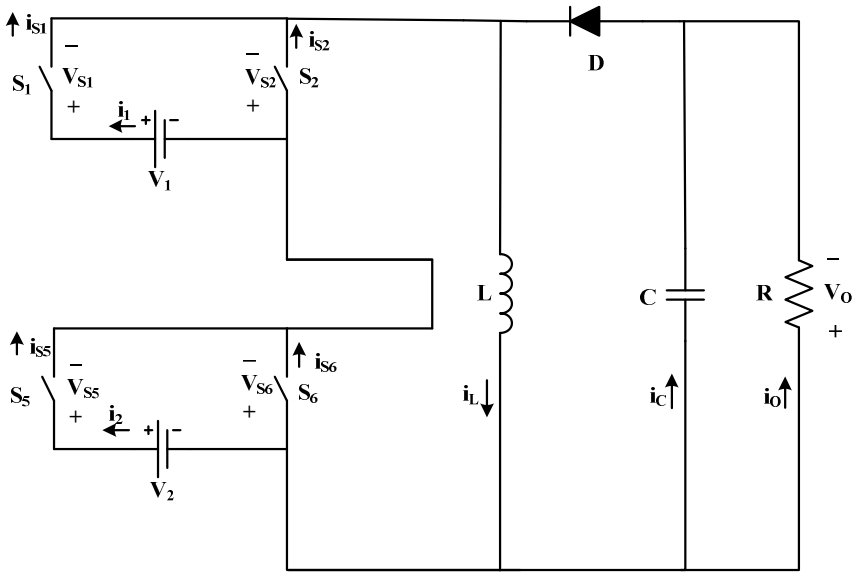

Figure 2.12. Derived topology of a double-input buckboost-buckboost converter using H-bridge cells

In the above circuit the switches can be replaced by diodes or transistors. One may obtain the circuit with transistors and diodes by the following explanation.

(If S_1 is on ➔ S_2 is off) => ($i_{S1} > 0$ & $V_{S2} < 0$)

(If S_2 is on ➔ S_1 is off) => ($i_{S2} > 0$ & $V_{S1} > 0$)

As switch S_2 conducts positive current and opposes negative voltage it can be replaced by a diode and as switch S_1 conducts positive current and positive voltage it can be replaced by a transistor. Similarly S_6 can be replaced by a diode and S_5 can be replaced by a transistor. So the final circuit that is obtained is shown in Figure 2.13. If node O is assumed to be a ground then V_2 and load will have a ground connection but the output voltage is negative, which is a disadvantage.

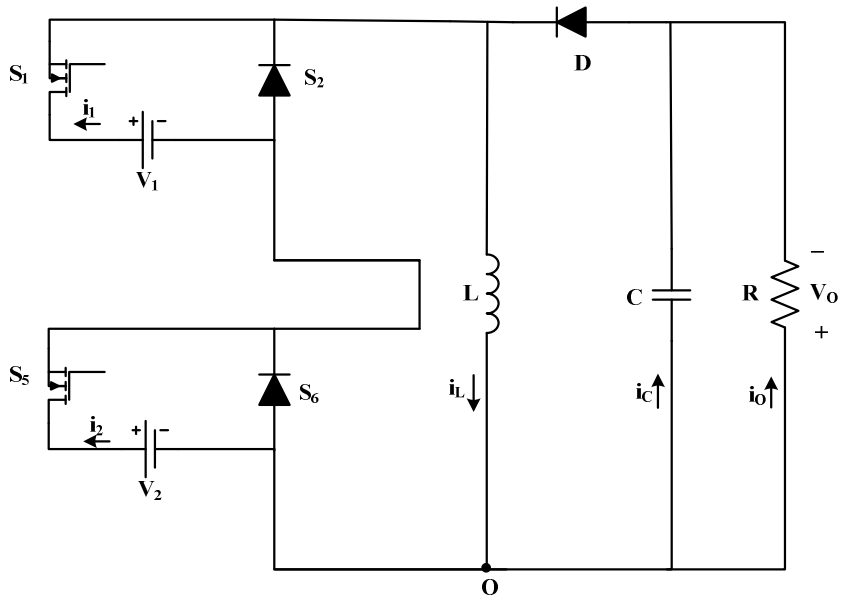

Figure 2.13. Final derived double input buckboost-buckboost converter using H-bridge cells

2.4. A SECOND WAY TO DERIVE DOUBLE-INPUT BUCKBOOST-BUCKBOOST CONVERTER USING H-BRIDGE CELLS

A second way to derive double-input buckboost-buckboost converter is explained here. A simple outline of new dc-dc converter using H-bridge cells as building blocks is shown in Figure 2.14. It consists of two H-bridge cells which can operate simultaneously or individually. Topology introduced in Figure 2.14, herein after named as buckboost-buckboost converter, resembles the topology of a buckboost converter with two inputs. The advantage of this type of converter is that it contains only one inductor so the size, weight, parts count, and cost are reduced. By replacing H-bridge cells in the buckboost-buckboost converter with their circuit topology, one would obtain Figure 2.15.

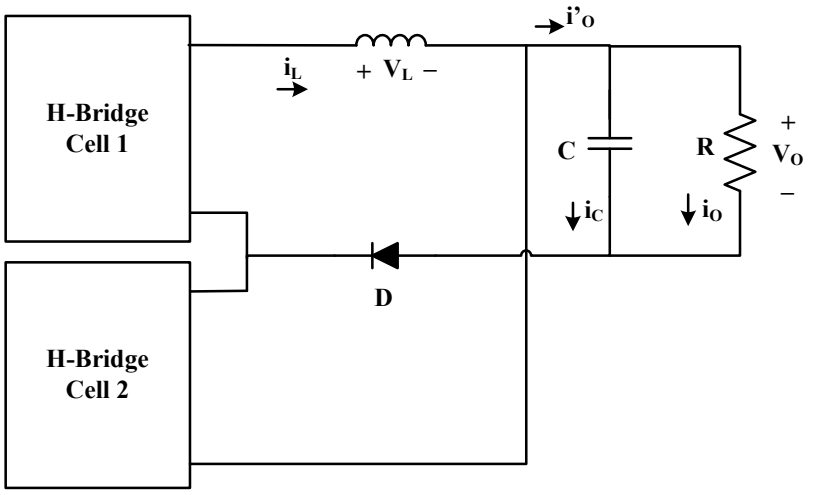

Figure 2.14. Outline of a double-input buckboost-buckboost converter using H-bridge cells

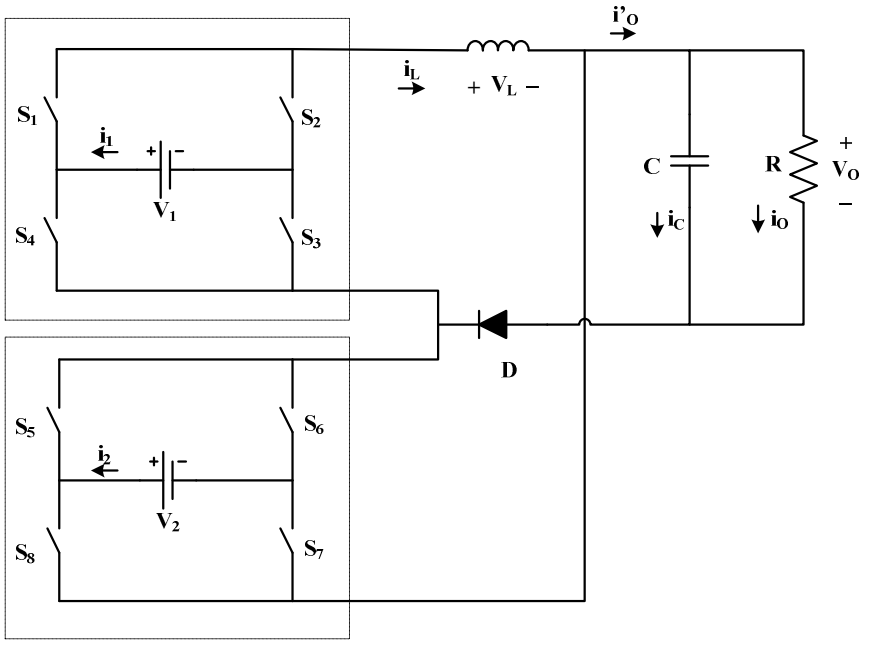

Figure 2.15. Double-input buckboost-buckboost converter using H-bridge cells

Four modes of operation that occur under unidirectional power flow are depicted in Figure 2.16, focusing on the voltages across the inductor.

MODE I (S_1, S_3, S_6, & S_7: on)

In this mode V_1 supplies energy to inductor L. one can see that the negative of the load voltage appears across diode D; hence it is reverse biased as depicted in Figure 2.16 (a).

MODE II (S_2, S_3, S_5, & S_7: on)

In this mode V_2 supplies energy to inductor L. The negative of the sum of the voltages V_O and V_2 appears across diode D; hence it is reverse biased as depicted in Figure 2.16 (b).

.

MODE III (S_2, & S_3: on)

In this mode both of the power sources are disconnected from the circuit. The energy stored in the inductor is being supplied to the load. Thus inductor gets de-energized during this mode as depicted in Figure 2.16 (c). In this mode diode D is forced to conduct to provide current path for the inductor.

Switches S_6 and S_7 are not allowed to be on during this mode, otherwise, diode D will be reverse biased and there will be no energy transfer to the load

MODE IV (S_1, S_3, S_5, & S_7: on)

In this mode both of the power sources supply energy to inductor L. Thus both of the sources can operate simultaneously in this mode as depicted in Figure 2.16 (d). The negative of the sum of the voltages V_O and V_2 appears across diode D; hence it is reverse biased like in modes I and II. Voltages across the inductor for different modes of operation are shown in Table 2.5.

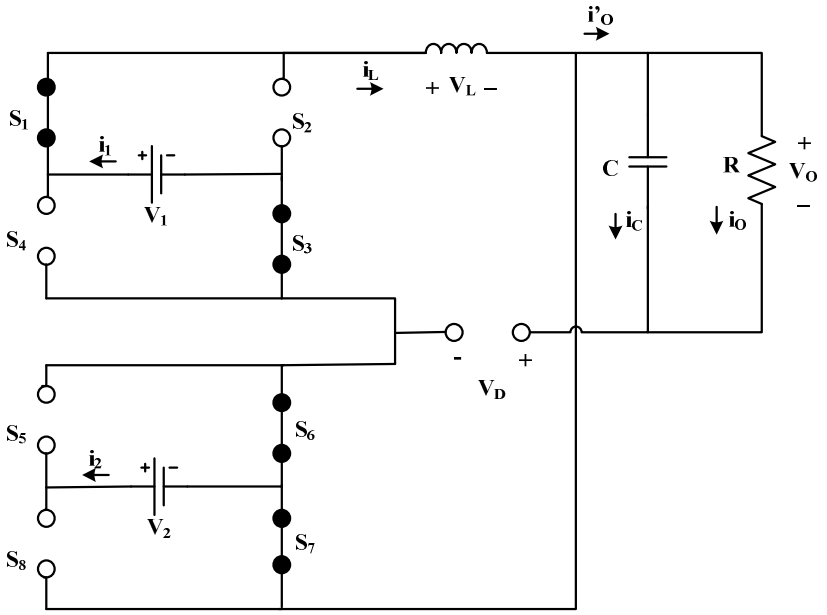

(a) Mode I

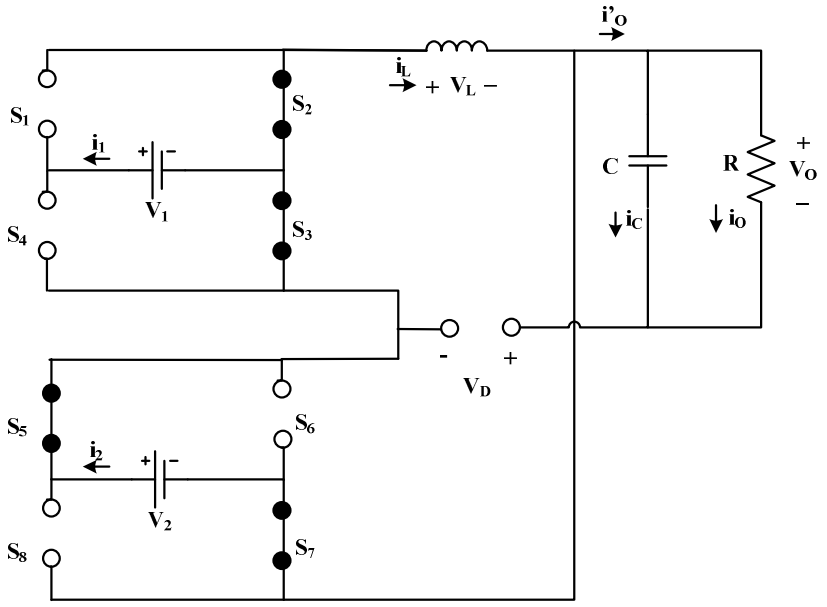

(b) Mode II

Figure 2.16. Different modes of operation of a double-input buckboost-buckboost converter using H-bridge cells

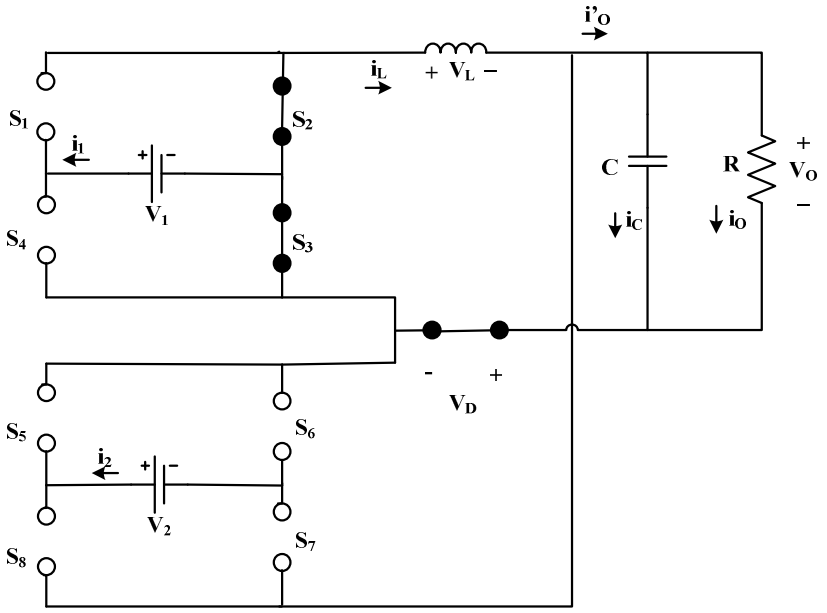

(c) Mode III

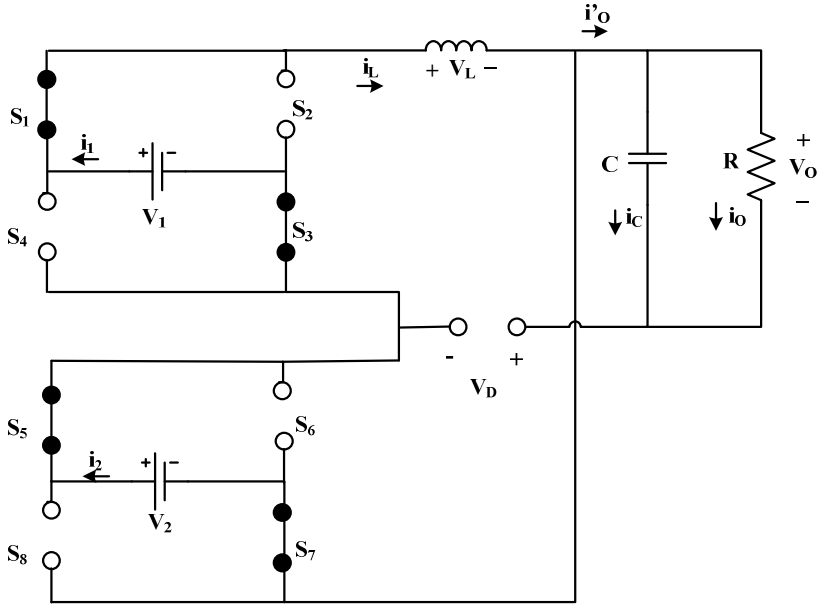

(d) Mode IV

Figure 2.16. Different modes of a operation of double-input buckboost-buckboost converter using H-bridge cells (continued)

Table 2.5. Voltage across the inductor for different modes of operation of a double-input buckboost-buckboost converter using H-bridge cells

Mode	**V_L**
I	V_1
II	V_2
III	$- V_o$
IV	$V_1 + V_2$

It can be seen from the circuit operation that switches S_4 and S_8 are not used at all so they can be eliminated from the circuit. In case of Mode III, S_7 can be shorted as this will not vary the circuit operation. So switches S_3 and S_7 can be shorted. Hence the circuit topology can be reduced to Figure 2.17 which consists of only four switches.

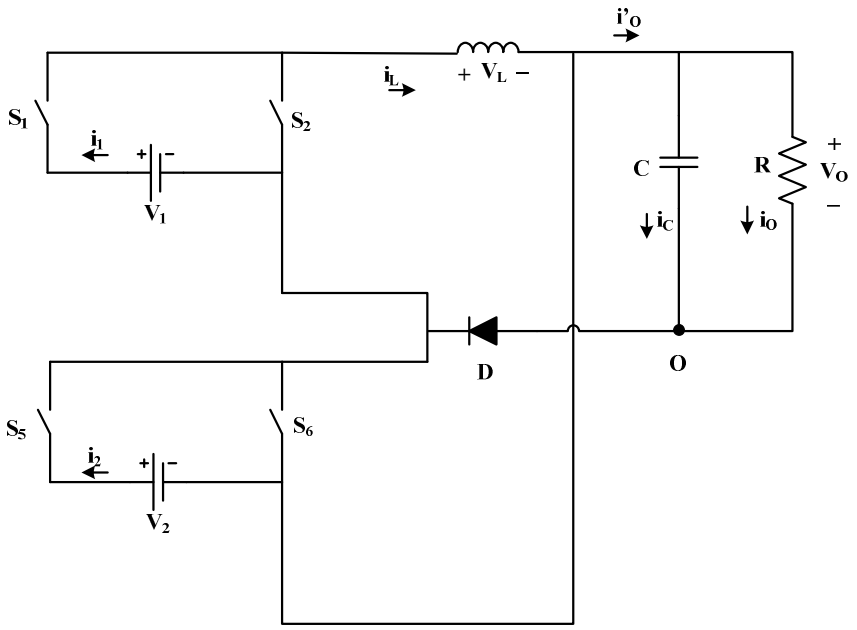

Figure 2.17. Derived topology of a double-input buckboost-buckboost converter using H-bridge cells

In the above circuit the switches can be replaced by diodes or transistors. One may obtain the circuit with transistors and diodes by the following explanation. As the power flow through the inductor is unidirectional, i_L should always be positive.

(If S_1 is on ➔ S_2 is off) => ($i_{S1} > 0$ & $V_{S2} < 0$)

(If S_2 is on ➔ S_1 is off) => ($i_{S2} > 0$ & $V_{S1} > 0$)

As switch S_2 conducts positive current and opposes negative voltage it can be replaced by a diode and as switch S_1 conducts positive current and positive voltage it can be replaced by a transistor. Similarly S_5 can be replaced by a transistor. In case of switch S_6, it cannot be replaced by a diode as this results in diode D to be reverse biased in mode III, hence, it is replaced by a transistor. So the final circuit that is obtained is shown in Figure 2.18.

If node O is assumed to be grounded, then the load will have a ground connection and also output voltage is positive, which is an advantage over the previous circuit of Figure 2.13. But input voltage will not have a ground connection, which is a disadvantage.

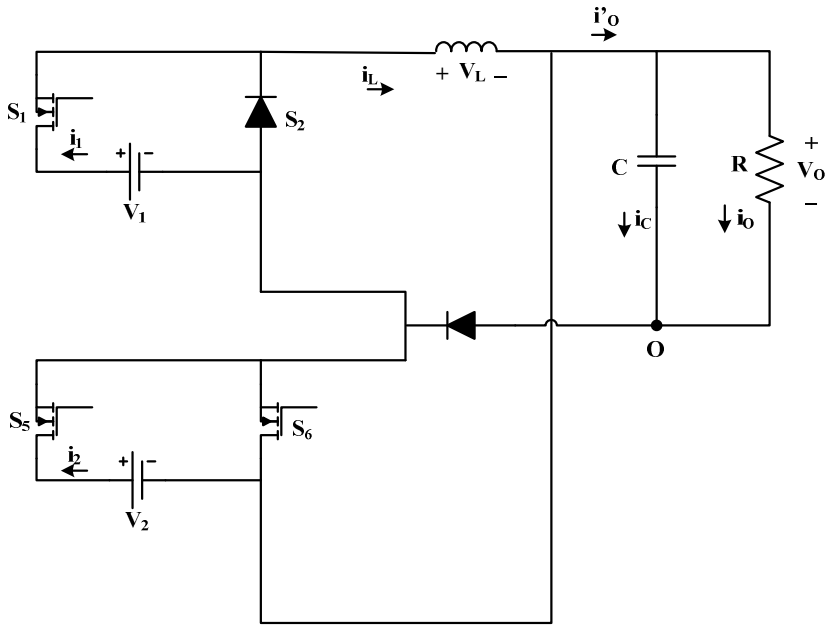

Figure 2.18. Final derived double-input buckboost-buckboost converter using H-bridge cells

A buckboost-buckboost converter has been reported in the literature [50]. This converter as depicted in Figure 2.19 has only two diodes; however, it has a mode limitation. Both switches S_1 and S_5 cannot be turned at the same time as this results in both the voltage sources directly coming in parallel. Different modes of operation of this converter are summarized in Table 2.6. Comparison of Tables 2.4, 2.5 and 2.6 clearly reveals the restriction of the limited buckboost-buckboost converter.

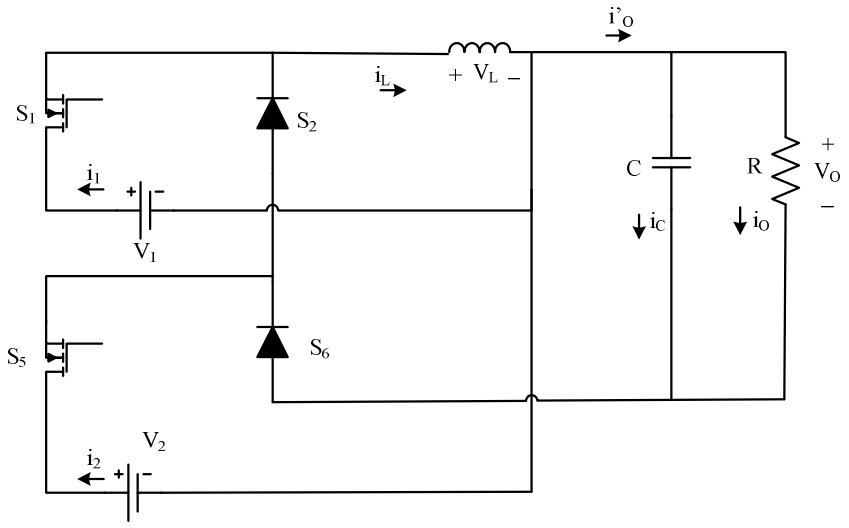

Figure 2.19. Double-input limited buckboost-buckboost converter

Table 2.6. Voltage across the inductor for different modes of operation of a double-input limited buckboost-buckboost converter of [50]

Mode	**Voltage V_L**
I	V_1
II	V_2
III	$-V_O$

2.5. DERIVATION OF DOUBLE-INPUT BUCK-BUCKBOOST CONVERTER USING H-BRIDGE CELLS

The topology introduced in Figure 2.20, herein after named as buck-buckboost converter, resembles the topology of a buck and buckboost converter. The advantage of this type of converter is that it contains only one inductor so the size, weight, parts count, and cost are reduced. By replacing H-bridge cells in a buck-buckboost converter with their circuit topology, one would obtain Figure 2.21.

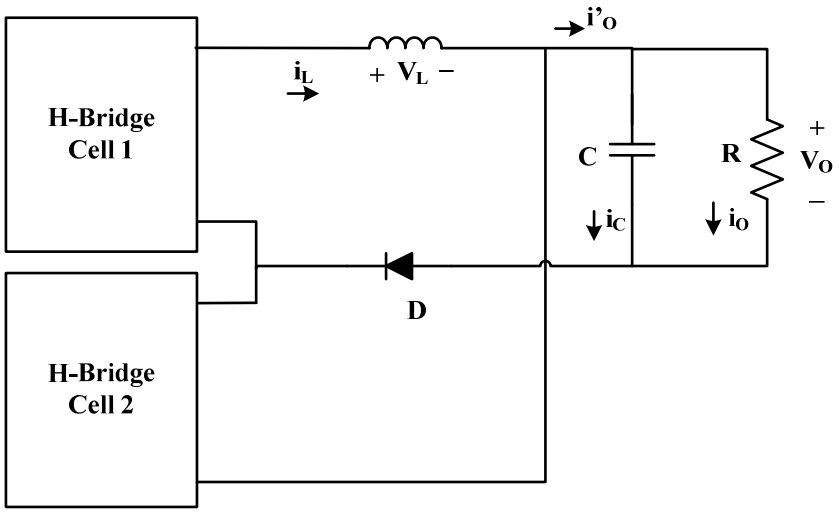

Figure 2.20. Outline of a double-input buck-buckboost converter using H-bridge cells

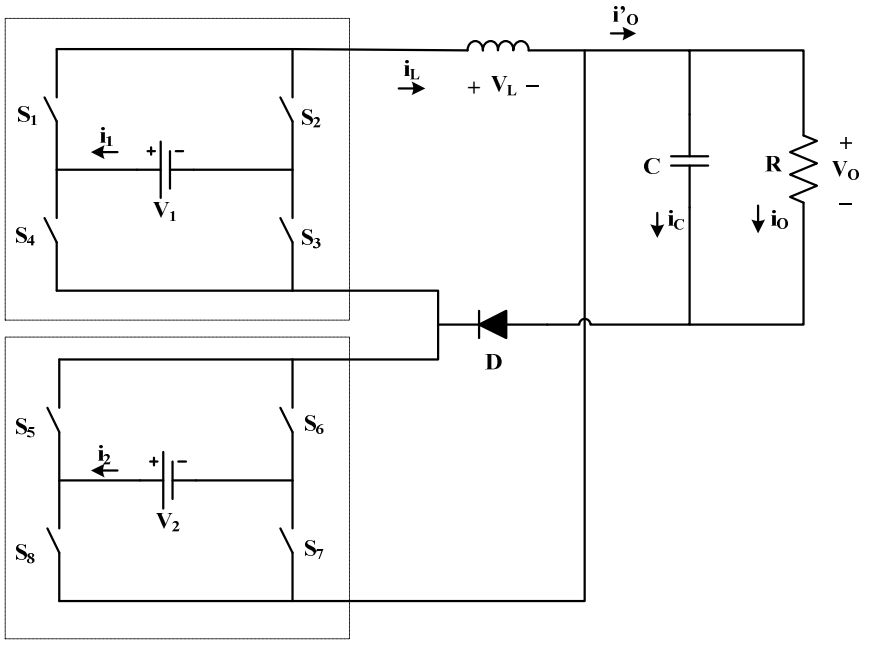

Figure 2.21. Double-input buck-buckboost converter using H-bridge cells

Four modes of operation that occur under unidirectional power flow are depicted in Figure 2.22, focusing on the voltages across the inductor.

MODE I (S_1 & S_3: on)

In this mode V_1 supplies energy to inductor L and the load as depicted in Figure 2.22 (a). Diode D is forward biased because of the positive source voltage and positive output voltage applied across it.

MODE II (S_2, S_3, S_5, & S_7: on)

In this mode V_2 supplies energy to inductor L as depicted in Figure 2.22 (b). The negative of the sum of the voltages V_O and V_2 appears across diode D; hence it is reverse biased.

MODE III (S_2, & S_3: on)

In this mode both of the power sources are disconnected from the circuit as depicted in Figure 2.22 (c). The energy stored in the inductor is being supplied to the load. Thus inductor gets de-energized during this mode. In this mode diode D is forced to conduct to provide current path for the inductor.

MODE IV (S_1, S_3, S_5, & S_7: on)

In this mode both the power sources supply energy to inductor L as depicted in Figure 2.22 (d). The negative of the sum of voltages V_O and V_2 appears across diode D; hence it is reverse biased. Voltages across the inductor for different modes of operation are shown in Table 2.7.

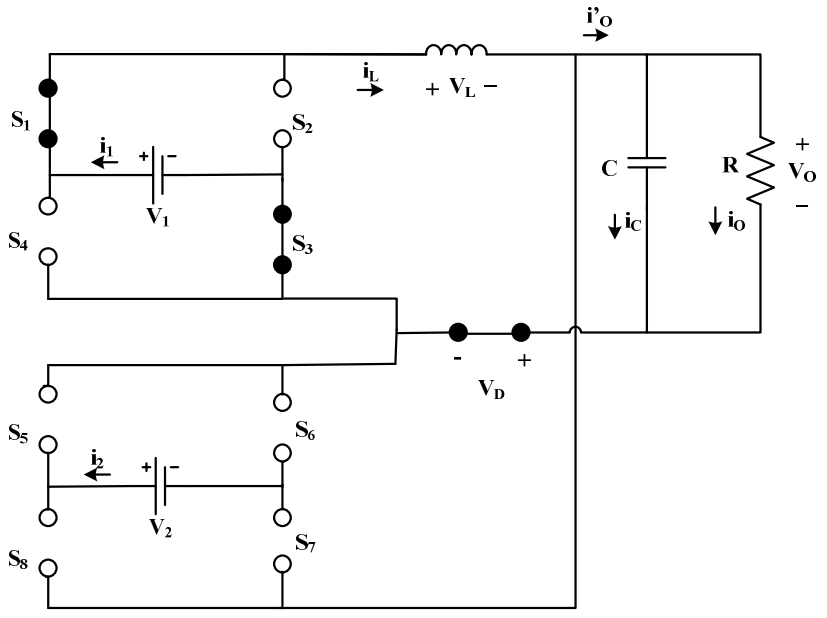

(a) Mode I

Figure 2.22. Different modes of operation of a double-input buck-buckboost converter using H-bridge cells

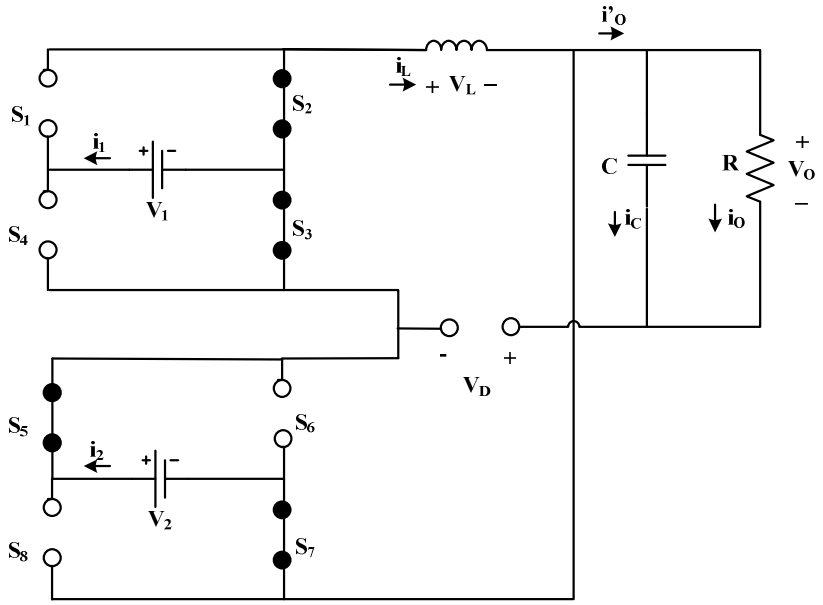

(b) Mode II

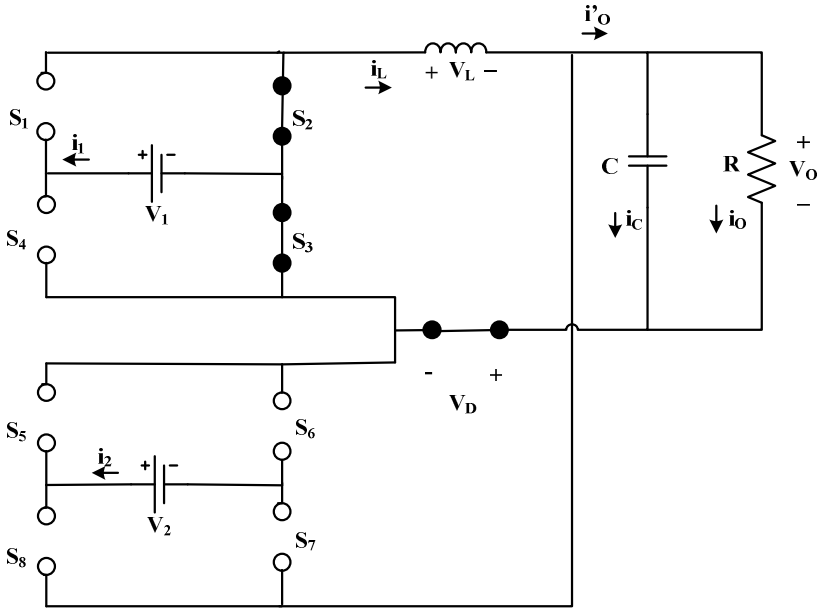

(c) Mode III

Figure 2.22. Different modes of operation of a double-input buck-buckboost converter using H-bridge cells (continued)

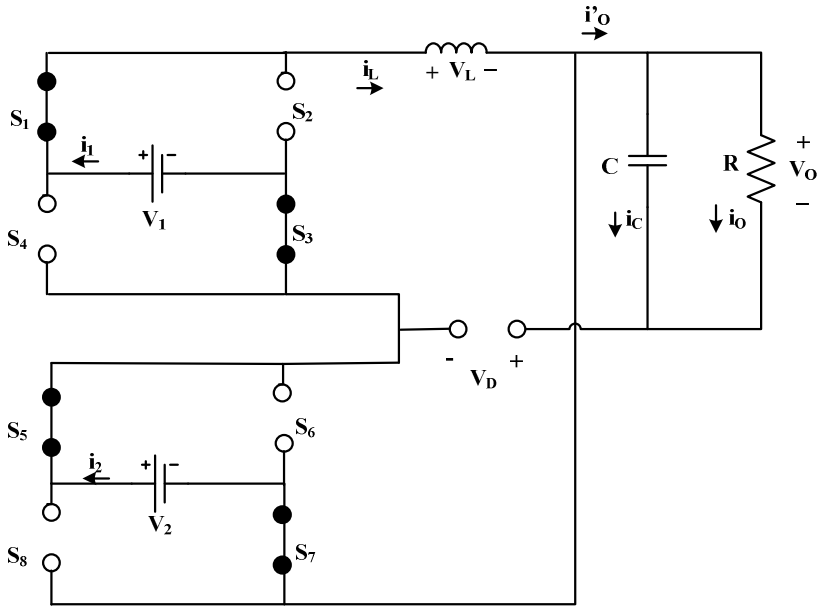

(d) Mode IV

Figure 2.22. Different modes of operation of a double-input buck-buckboost converter using H-bridge cells (continued)

Table 2.7. Voltage across the inductor for different modes of operation of a double-input buck-buckboost converter using H-bridge cells

Mode	**V_L**
I	$V_1 - V_O$
II	V_2
III	$- V_O$
IV	$V_1 + V_2$

It can be seen from the circuit operation that switches S_4, S_6, and S_8 are not used at all so they can be eliminated from the circuit. In case of Mode III, S_7 can be shorted as this will not vary the circuit operation. So switches S_3 and S_7 can be shorted. Hence the circuit topology can be reduced to Figure 2.23 which consists of only three switches.

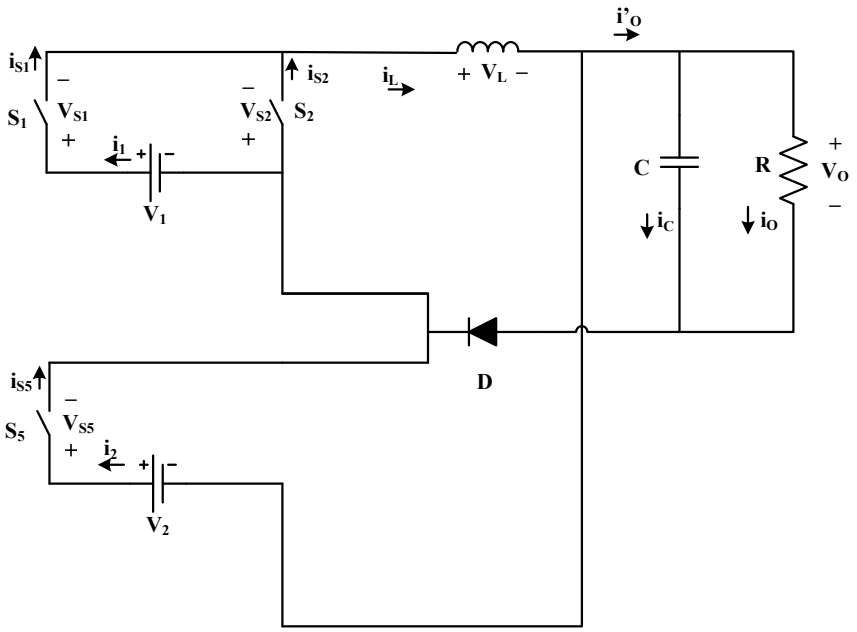

Figure 2.23. Derived topology of a double-input buck-buckboost converter using H-bridge cells

In the above circuit the switches can be replaced by diodes or transistors. One may obtain the circuit with transistors and diodes by the following explanation. As the power flow through the inductor is unidirectional, i_L should always be positive.

(If S_1 is on ➔ S_2 is off) => ($i_{S1} > 0$ & $V_{S2} < 0$)

(If S_2 is on ➔ S_1 is off) => ($i_{S2} > 0$ & $V_{S1} > 0$)

As switch S_2 conducts positive current and opposes negative voltage it can be replaced by a diode and as switch S_1 conducts positive current and positive voltage it can be replaced by a transistor. Similarly S_5 can be replaced by a transistor as it opposes positive current and voltage. So the final circuit that is obtained is shown in Figure 2.24.

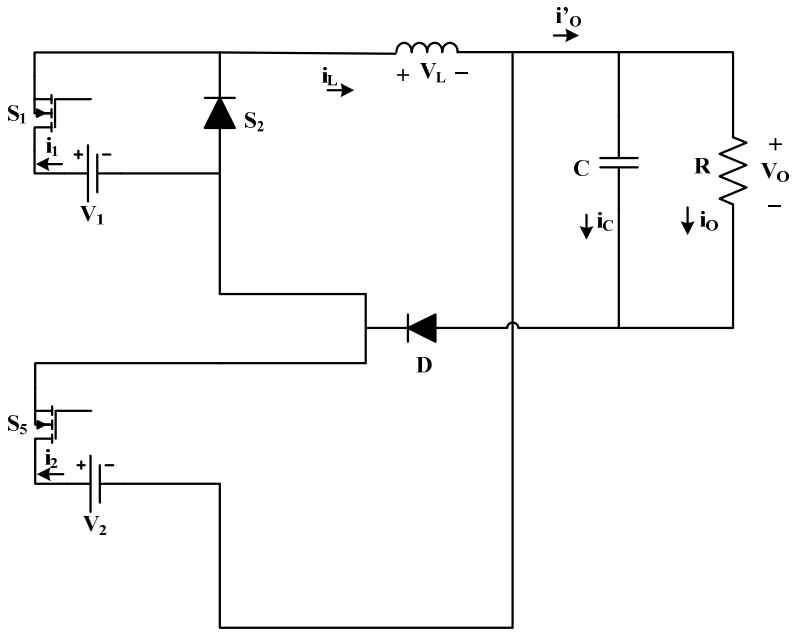

Figure 2.24. Final derived double-input buck-buckboost converter using H-bridge cells

2.6. DERIVATION OF DOUBLE-INPUT BOOST-BOOST CONVERTER USING ENHANCED H-BRIDGE CELLS

Topology introduced in Figure 2.25, herein after named as boost-boost converter, resembles the topology of a boost converter with two inputs. By replacing enhanced H-bridge cells in the boost-boost converter with their equivalent circuit topology, one would obtain Figure 2.26. The restriction of this circuit is that switches S_1, S_3, S_5, and S_7 are not allowed to turn on at the same time as this operation results in both the inductors to align in series and this is not allowed as the inductors have different currents flowing through them at a time.

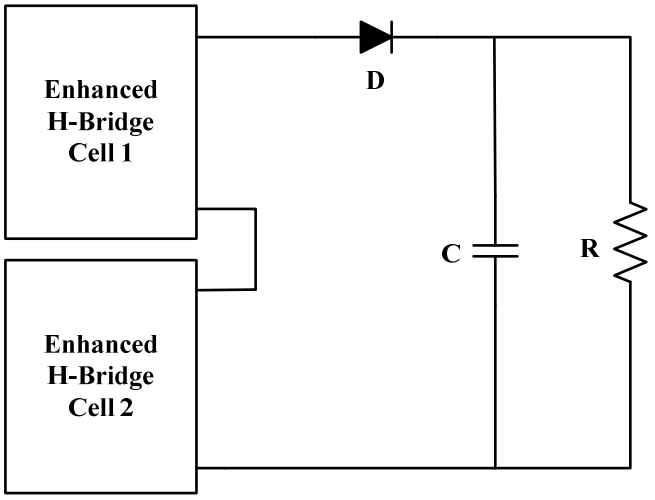

Figure 2.25. Outline of a double-input boost-boost converter using enhanced H-bridge cells

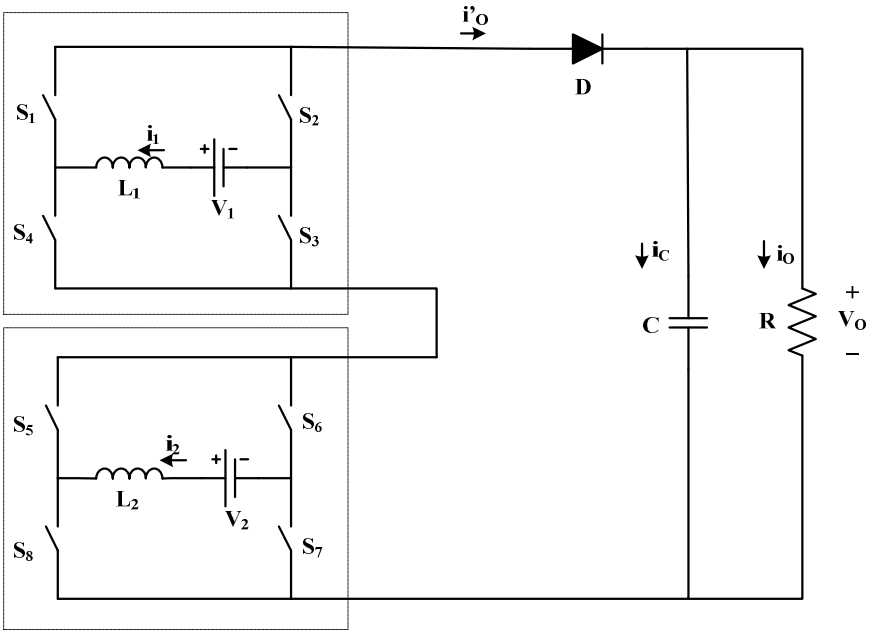

Figure 2.26. Double-input boost-boost converter using enhanced H-bridge cells

Three modes of operation that occur under unidirectional power flow are depicted in Figure 2.27, focusing on the voltages across the inductor.

MODE I (S_1, S_2, S_5, & S_6: on)

In this mode both of the power sources supply energy to both the inductors respectively as depicted in Figure 2.27 (a).

MODE II (S_1, S_3, S_5, S_6 & S_7: on)

In this mode V_1 and inductor L_1 supply energy to the load and also inductor L_2 is charged by source V_2 as depicted in Figure 2.27 (b). One can see that the current flowing through S_6 can only be positive when i_1 is less than i_2. Also diode D is forward biased as $(V_1 – V_O)$ is applied across it which is positive.

MODE III (S_1, S_2, S_3, S_5, & S_7: on)

In this mode V_2 and inductor L_2 supply energy to the load and also inductor L_1 is charged by source V_1 as depicted in Figure 2.27 (c). One can see that the current flowing through S_2 can only be positive when i_2 is less than i_1. To go from mode II to mode III we have to make sure to turn S_2 on first then turn S_6 off as this will not lead to the inductors coming in series. Also diode D is forward biased as ($V_2 - V_O$) is applied across it which is positive. Table 2.8 shows the voltages across the inductor for different modes of operation of the circuit.

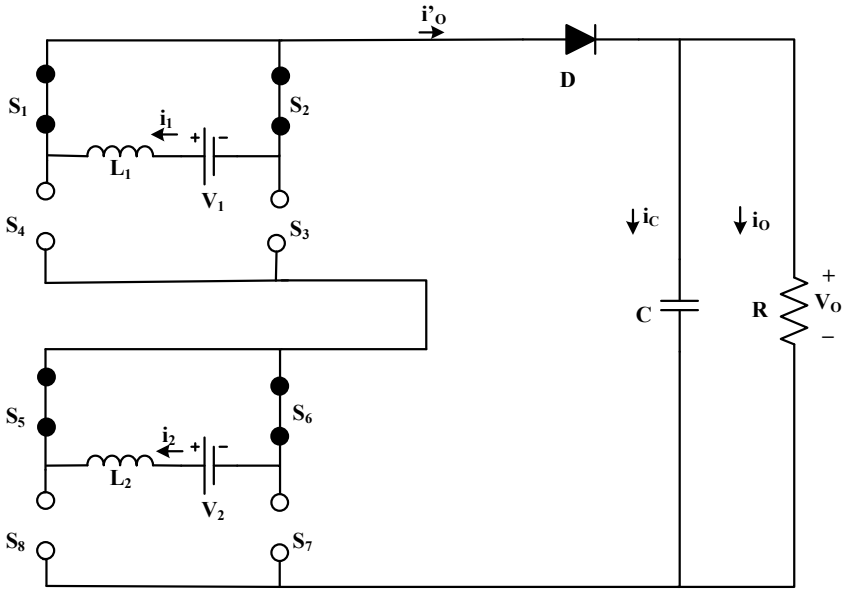

(a) Mode I

Figure 2.27. Different modes of operation of a double-input boost-boost converter using enhanced H-bridge cells

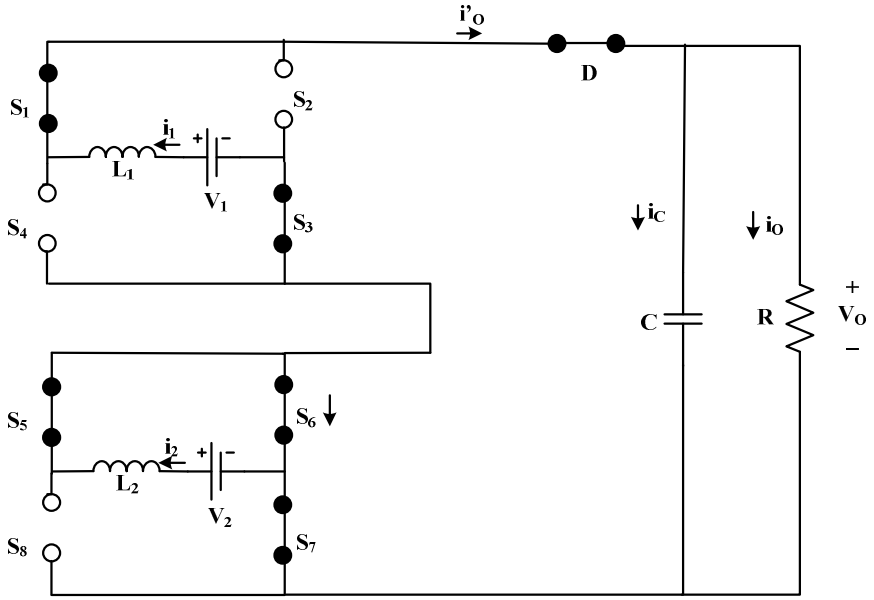

(b) Mode II

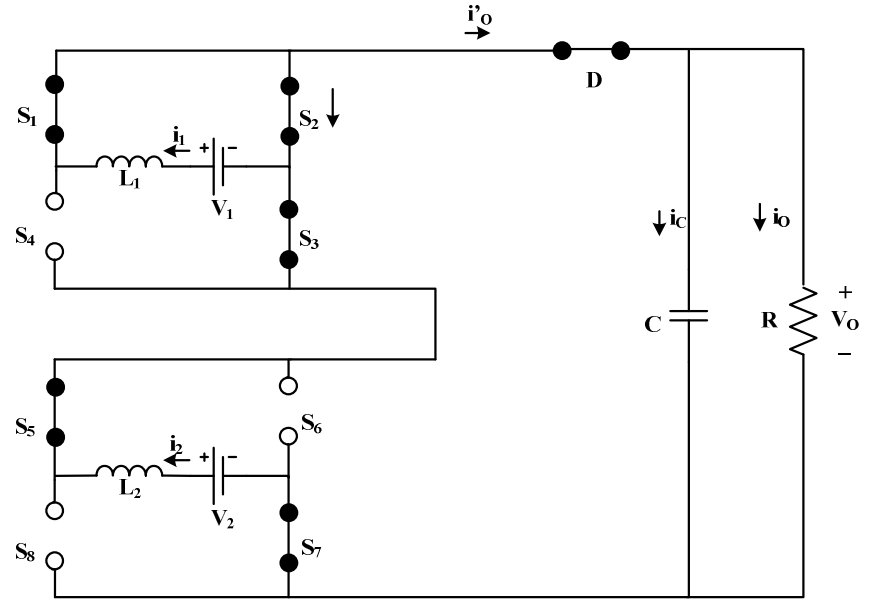

(c) Mode III

Figure 2.27. Different modes of operation of a double-input boost-boost converter using enhanced H-bridge cells (continued)

Table 2.8. Voltage across the inductor for different modes of operation of a double-input boost-boost converter using enhanced H-bridge cells

Mode	$\mathbf{V_{L1}}$	$\mathbf{V_{L2}}$
I	V_1	V_2
II	$V_1 - V_O$	V_2
III	V_1	$V_2 - V_O$

It can be seen from the circuit operation that switches S_4 and S_8 are not used at all so they can be eliminated from the circuit. And also switch S_1, S_3, S_5, and S_7 can be shorted. Hence the circuit topology can be reduced to Figure 2.28 which consists of only two switches.

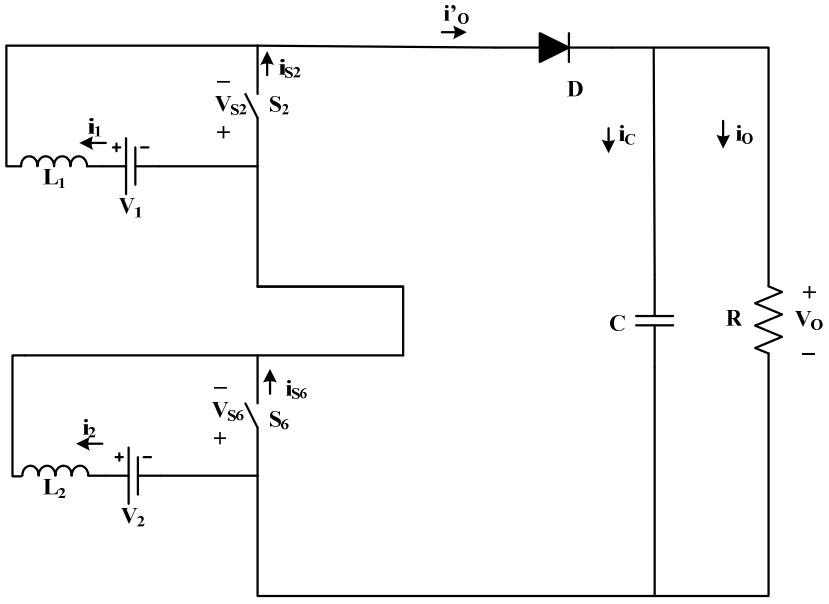

Figure 2.28. Derived topology of a double-input boost-boost converter using enhanced H-bridge cells

Three modes of operation for the derived topology can be explained as follows.

MODE I (S_2 & S_6: on)

In this mode both the power sources supply energy to both the inductors respectively.

MODE II (S_6: on)

In this mode V_1 and inductor L_1 supply energy to the load and also inductor L_2 is charged by source V_2.

MODE III (S_2: on)

In this mode V_2 and inductor L_2 supply energy to the load and also inductor L_1 is charged by source V_1.

Thus the number of switches that are used is reduced to only two in spite of the disadvantage of having two inductors.

In Figure 2.28 switches can be replaced by diodes or transistors depending on the requirement of the system. One may obtain the circuit with transistors and diodes by the following explanation.

(If S_2 is on & S_6 is on) => ($i_{S2} < 0$ & $i_{S6} < 0$)

(If S_2 is on & S_6 is off) => {$V_{S6} < 0$ & $i_{S2} > 0$ (or < 0) if $i_2 > i_1$ (or $i_2 < i_1$)}

(If S_2 is off & S_6 is on) => {$V_{S2} < 0$ & $i_{S6} > 0$ (or < 0) if $i_1 > i_2$ (or $i_1 < i_2$)}

As switch S_2 conducts both positive and negative currents and opposes negative voltage it should be replaced by a bidirectional switch. Similarly switch S_6 conducts both positive and negative currents and opposes negative voltage, so it should be replaced by a bidirectional switch. So the final circuit that is obtained is shown in Figure 2.29.

Bidirectional switch consists of two MOSFETs with parallel diodes so that they can conduct bidirectional current

.

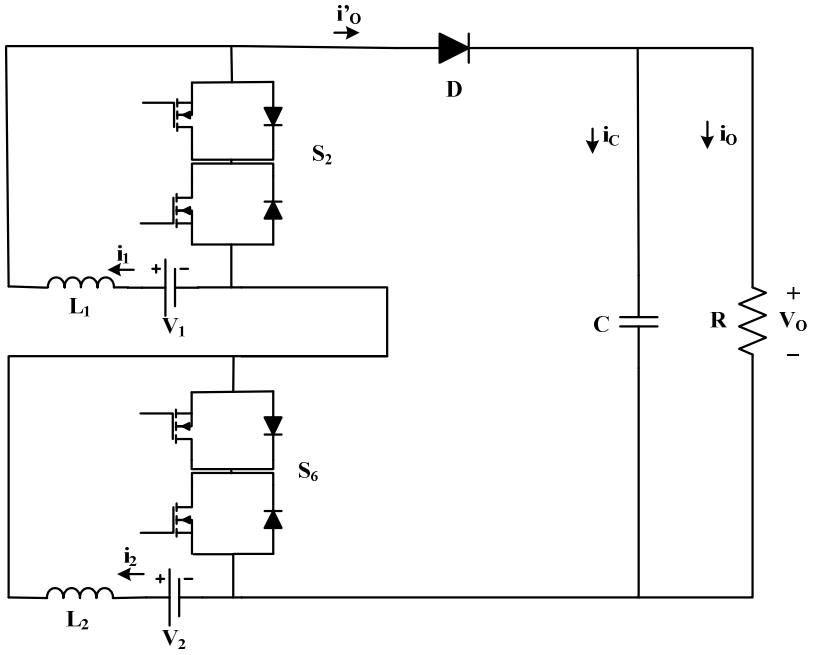

Figure 2.29. Final derived double-input boost-boost converter using enhanced H-bridge cells

2.7. BIDIRECTIONAL DOUBLE-INPUT BUCKBOOST-BUCKBOOST CONVERTER USING H-BRIDGE CELLS

In this chapter, until now sources V_1 and V_2 are assumed to be power sources, which need not be recharged. However, if one of the sources is an energy storage unit, then it needs to be recharged regularly. For this purpose, the converter needs to have bidirectional power transfer capability. In this chapter, only bidirectional buckboost-buckboost converter is derived, however, same approach is applicable to rest of the

converters introduced in this chapter. The converter of Figure 2.15 can have bidirectional capabilities, if we consider the following modes.

MODE I (S_1, S_3, S_6, & S_7: on)

In this mode V_1 supplies energy to inductor L. one can see that the negative of the load voltage appears across diode D; hence it is reverse biased.

MODE II (S_2, S_3, S_5, & S_7: on)

In this mode V_2 supplies energy to inductor L. The negative of the sum of the voltages V_O and V_2 appears across diode D; hence it is reverse biased.

MODE III (S_2 & S_3: on)

In this mode both the power sources are disconnected from the circuit. The energy stored in the inductor is being supplied to the load. Thus inductor gets de-energized during this mode. In this mode diode D is forced to conduct to provide current path for the inductor.

MODE IV (S_1, S_3, S_5, & S_7: on)

In this mode both the power sources supply energy to inductor L. Thus both the sources can operate simultaneously in this mode. The negative of the sum of the voltages V_O and V_2 appears across diode D; hence it is reverse biased like in modes I and II.

MODE V (S_2 & S_4: on)

In this mode voltage source V_1 is charged by the load. The system can be assumed to be a hybrid electric vehicle, so during regenerative braking, the energy is stored back in the power source V_1, which is a battery for example. Voltages across the inductor for different modes of operation are shown in Table 2.9.

Table 2.9. Voltage across the inductor for different modes of operation of Bidirectional double-input buckboost-buckboost converter using H-bridge cell

Mode	**V_L**
I	V_1
II	V_2
III	$- V_o$
IV	$V_1 + V_2$
V	$-(V_1 + V_O)$

It can be seen from the circuit operation that switch S_8 is not used at all, so it can be eliminated from the circuit. In case of Mode III, S_7 can be shorted as this will not vary the circuit operation. So switch S_7 can be shorted. Hence the circuit topology can be reduced to Figure 2.30 which consists of six switches.

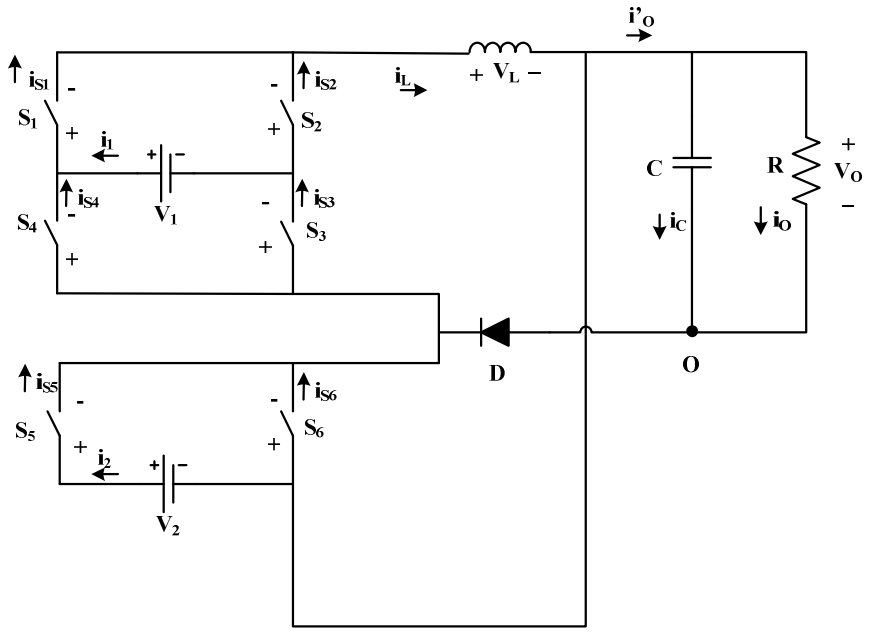

Figure 2.30. Bidirectional double-input buckboost-buckboost converter using H-bridge cells

In the above circuit the switches can be replaced by diodes or transistors. One may obtain the circuit with transistors and diodes by the following explanation.

(If S_1 & S_3 are on ➔ S_2 & S_4 are off) => ($i_{S1} > 0$, $i_{S3} > 0$, $V_{S2} < 0$ & $V_{S4} < 0$)

(If S_2 & S_4 are on ➔ S_1 & S_3 are off) => ($i_{S2} > 0$, $i_{S4} > 0$, $V_{S1} > 0$& $V_{S3} > 0$)

(If S_5 is on ➔ S_6 is off) => ($i_{S5} > 0$ & $V_{S6} < 0$)

(If S_6 is on ➔ S_5 is off) => ($i_{S6} > 0$ & $V_{S5} > 0$)

As switch S_2 conducts positive current and opposes negative voltage it can be replaced by a diode and as switch S_1 conducts positive current and positive voltage it can be replaced by a transistor. Similarly S_3 and S_4 can be replaced by a transistor and diode respectively. In case of switch S_6, it cannot be replaced by a diode as this results in diode D to be reverse biased in mode III, hence, it is replaced by a transistor. Switch S_5 can be

replaced by a transistor as it conducts positive current and opposes positive voltage. So the final circuit that is obtained is shown in Figure 2.31. This principle can be applied to other converters if bidirectional power flow is needed.

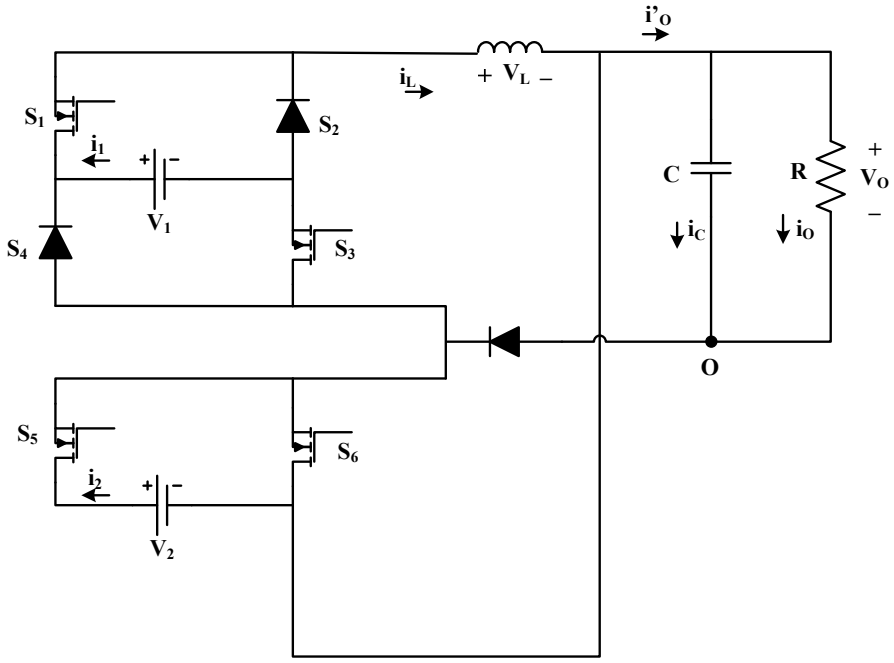

Figure 2.31. Final circuit of bidirectional double-input buckboost-buckboost converter using H-bridge cells

In this chapter, new converters including buck-buck, buckboost-buckboost, buck-buckboost, and boost-boost are derived using H-bridge cells. These converters except boost-boost consist of only one inductor and two switches, so they eliminate the complex structure of the converter circuits that are already available. Boost-boost converter has its own advantages, inspite of having two inductors. As the two voltage sources are dependent on each other in a boost-boost converter, one of the sources can be replaced by

an ultracapacitor. The converter can be changed accordingly to accommodate ultracapacitor. The voltage transfer ratios and simulation results of these converters will be discussed in chapter three.

3. VOLTAGE TRANSFER RATIOS AND SIMULATION RESULTS OF MULTI-INPUT DC-DC CONVERTERS DERIVED USING H-BRIDGE CELLS

Voltage transfer ratio is the relationship between input and output voltages of a circuit described by the duty ratios. Voltage transfer ratio is obtained in steady-state mode of operation.

3.1. VOLTAGE TRANSFER RATIO OF DOUBLE-INPUT DC-DC BUCK-BUCK CONVERTER

Double-input buck-buck converter using H-bridge cells, shown in Figure 3.1 consists of two switches and two diodes. Switching pattern of switches S_1 and S_5 of the converter are shown in Figure 3.2. The pattern is true for all the possible arrangements of the converter as it consists of all the four modes. Table 3.1 shows the voltage across inductor for different modes of operation of the circuit.

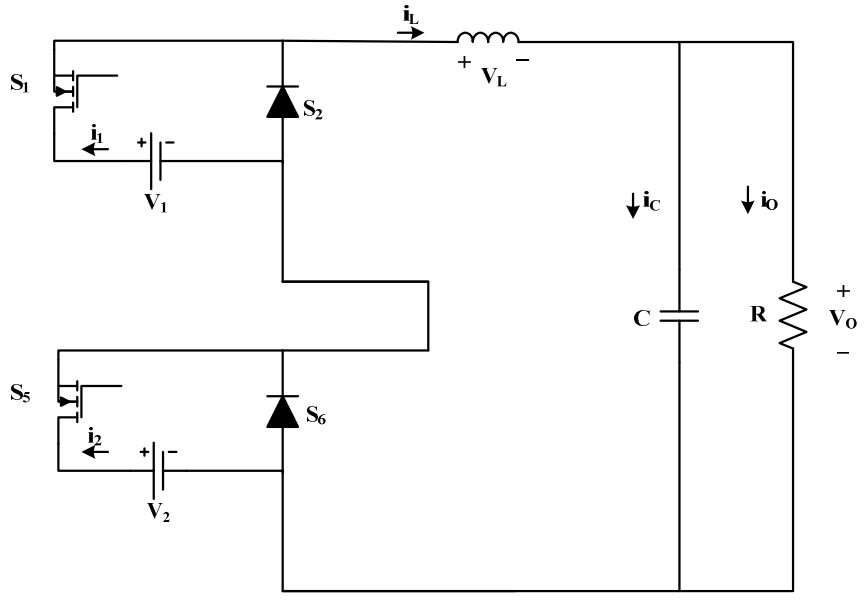

Figure 3.1. Double-input buck-buck converter using H-bridge cells

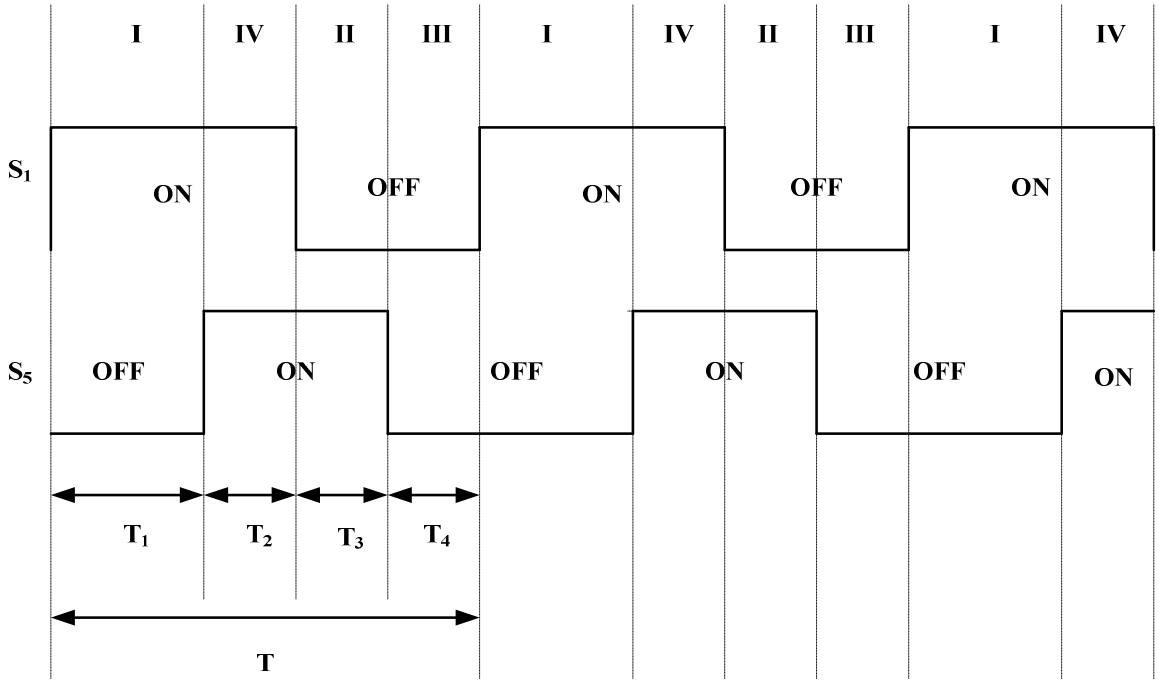

Figure 3.2. Switching pattern of buck-buck double input dc-dc converter derived using H-bridge cells

Table 3.1. Voltage across the inductor for different modes of operation of buck-buck converter

	T_1	T_2	T_3	T_4
S_1	ON	ON	OFF	OFF
S_5	OFF	ON	ON	OFF
V_L	$V_1 - V_O$	$V_1 + V_2 - V_O$	$V_2 - V_O$	$- V_O$

One can see from Figure 3.2 that the sum of T_1 and T_2 is the on time of switch S_1 and sum of T_2 and T_3 is the on time of switch S_5. Duty cycle is defined as the ratio of switch on time to the period.

$$T_1 + T_2 = d_1 * T \tag{1}$$

$$T_2 + T_3 = d_2 * T \tag{2}$$

T is the time period of the switching patterns of S_1 or S_5, and d_1 and d_2 are the duty cycles of switches S_1 and S_5 respectively. One can write the following equations based on Figure 3.2, Table 3.1, and volt-second balance equation of inductor.

$$T_1 + T_2 + T_3 + T_4 = T \tag{3}$$

$$T_1 * (V_1 - V_O) + T_2 * (V_1 + V_2 - V_O) + T_3 (V_2 - V_O) + T_4 * (-V_O) = 0 \tag{4}$$

This can be simplified as the following equation.

$$V_1 * (T_1 + T_2) + V_2 * (T_2 + T_3) = V_O * (T_1 + T_2 + T_3 + T_4) \tag{5}$$

Combining equations (1), (2), and (5) one can obtain the following equation which gives the relation between input and output.

$$V_1 * d_1 + V_2 * d_2 = V_O * 1$$

$$V_O = d_1 * V_1 + d_2 * V_2 \tag{6}$$

Equation (6) determines the transfer function of the double-input buck-buck dc-dc converter using H-bridge cells. It can also be observed that the output is positive as long as the two sources are positive.

Following the above procedure for other converters, one can obtain the transfer functions of all the converters which are shown in the following Table 3.2.

Table 3.2. Transfer function ratios of double-input dc-dc converters

Double-input converter topology	**Voltage transfer ratio**	**Range of V_O**
Buck-buck	$V_O = d_1 * V_1 + d_2 * V_2$	$0 < V_O < V_1 + V_2$
Buckboost-buckboost	$V_O = \frac{d_1}{1 - d_1 - d_2 + \frac{T_2}{T}} * V_1 + \frac{d_2}{1 - d_1 - d_2 + \frac{T_2}{T}} * V_2$	$0 < V_O < \infty$
Limited buckboost-buckboost	$V_O = \frac{d_1}{1 - d_1 - d_2} * V_1 + \frac{d_2}{1 - d_1 - d_2} * V_2$	$0 < V_O < \infty$
Buck-buckboost	$V_O = \frac{d_1}{1 - d_2} * V_1 + \frac{d_2}{1 - d_2} * V_2$	$0 < V_O < \infty$
Boost-boost	$V_O = \frac{1}{1 - d_1} * V_1 = \frac{1}{1 - d_2} * V_2$	$V_1, V_2 < V_O < \infty$

One can observe from Table 3.2, output voltage V_O is positive as long as the input sources V_1 and V_2 are positive. And also the Table suggests that the voltage transfer ratio of the buckboost-buckboost converter depends on T_2, where T_2 is the overlap between the conduction of the two switches. If T_2 is chosen to be zero, then the voltage transfer ratio will be similar to that of a limited buckboost-buckboost converter [50]. One can also see that voltages V_1 and V_2 of a boost-boost converter are not independent of each other if d_1 and d_2 are already defined. This feature can be used to replace one of the sources with a capacitor.

3.2. SIMULATION RESULTS OF DOUBLE-INPUT DC-DC CONVERTERS

Figure 3.3 shows the typical simulation results of the buck-buck converter using Matlab-simulink. Two dc voltage sources V_1 = 100 V and V_2 = 150 V are used for the input voltage sources. The switching commands for S_1 and S_5 have fixed duty ratios of 0.5 at the switching frequency of 100 KHz. From top to bottom are the waveforms of switching commands S_1 and S_5, inductor voltage V_L, inductor current i_L, capacitor current i_C, output current i_O, and the output voltage. One can observe from the waveforms that the average value of output voltage is around 125 V which can also be obtained from the transfer function of Table 3.2.

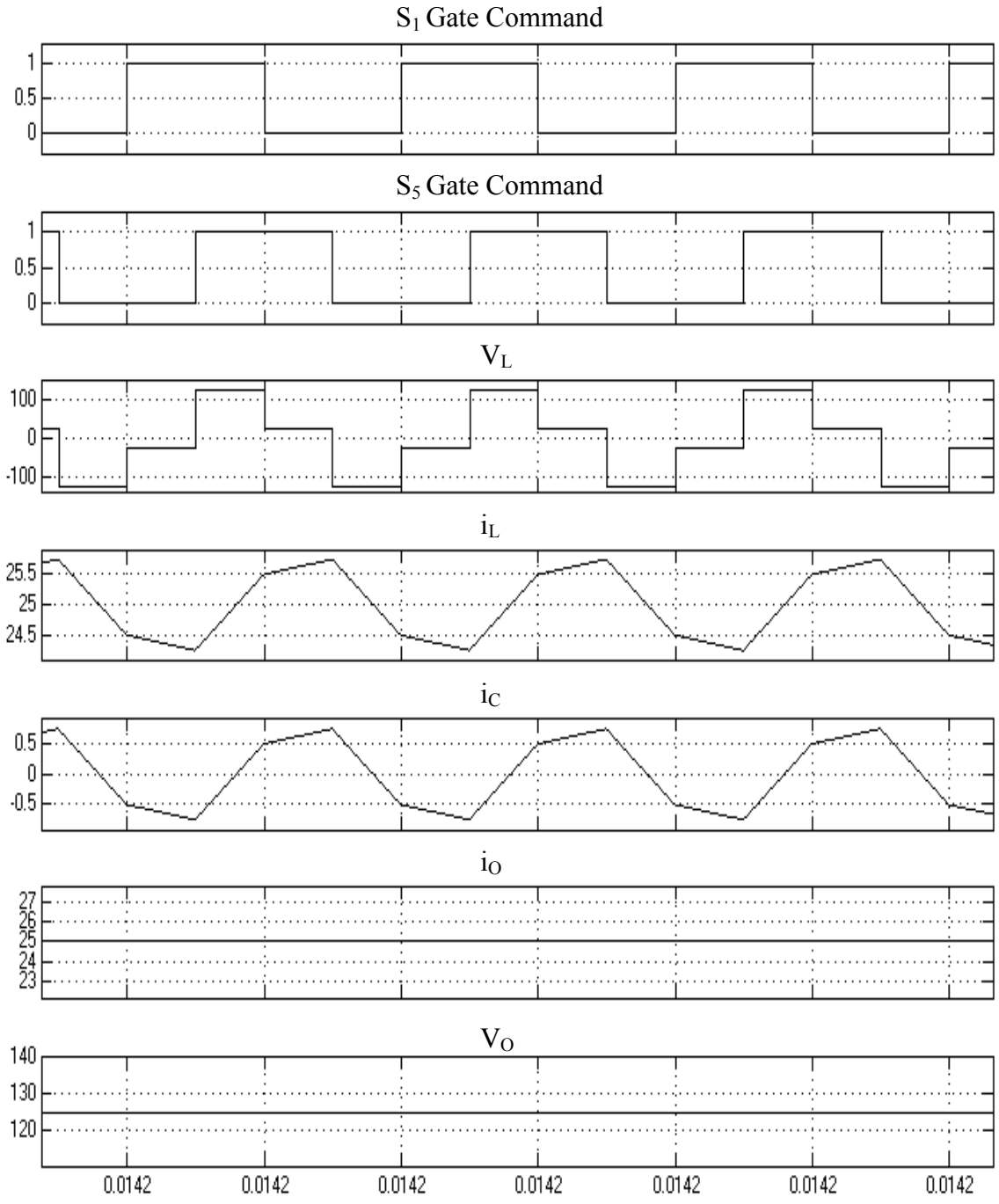

Figure 3.3. Simulation waveforms of double-input buck-buck converter

Figure 3.4 shows the typical simulation results of the buckboost-buckboost converter using Matlab-simulink. Two dc voltage sources V_1 = 100 V and V_2 = 150 V are used for the input voltage sources. The switching commands S_1 and S_2 have fixed duty ratios of 0.5 at a switching frequency of 100 KHz. From top to bottom are the waveforms of switching commands S_1 and S_2, inductor voltage V_L, inductor current i_L, capacitor current i_C, output current i_O, and the output voltage.

One can observe from the waveforms that the average of output voltage is around 500 V which can also be obtained from the transfer function of Table 3.2. One can also observe that the output voltage can be varied simply by changing T_2 (the overlap of conduction of both the switches) without actually changing the time periods of the gate commands. This can be verified from Figure 3.5, which shows that the average value of output voltage is around 625 V because T_2 which was originally 0.25 was changed to 0.2, which can also be obtained from Table 3.2.

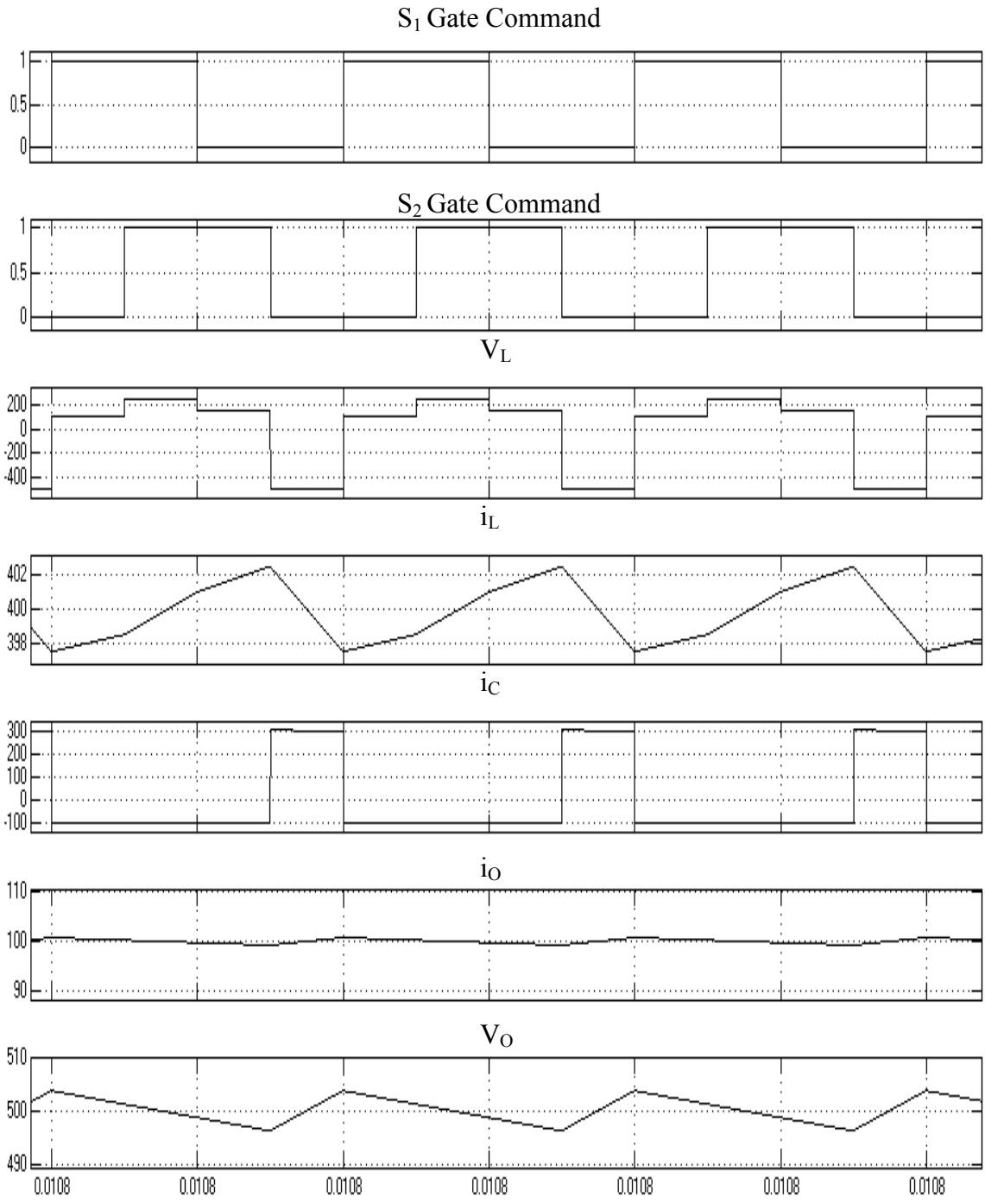

Figure 3.4. Simulation waveforms of double-input buckboost-buckboost converter

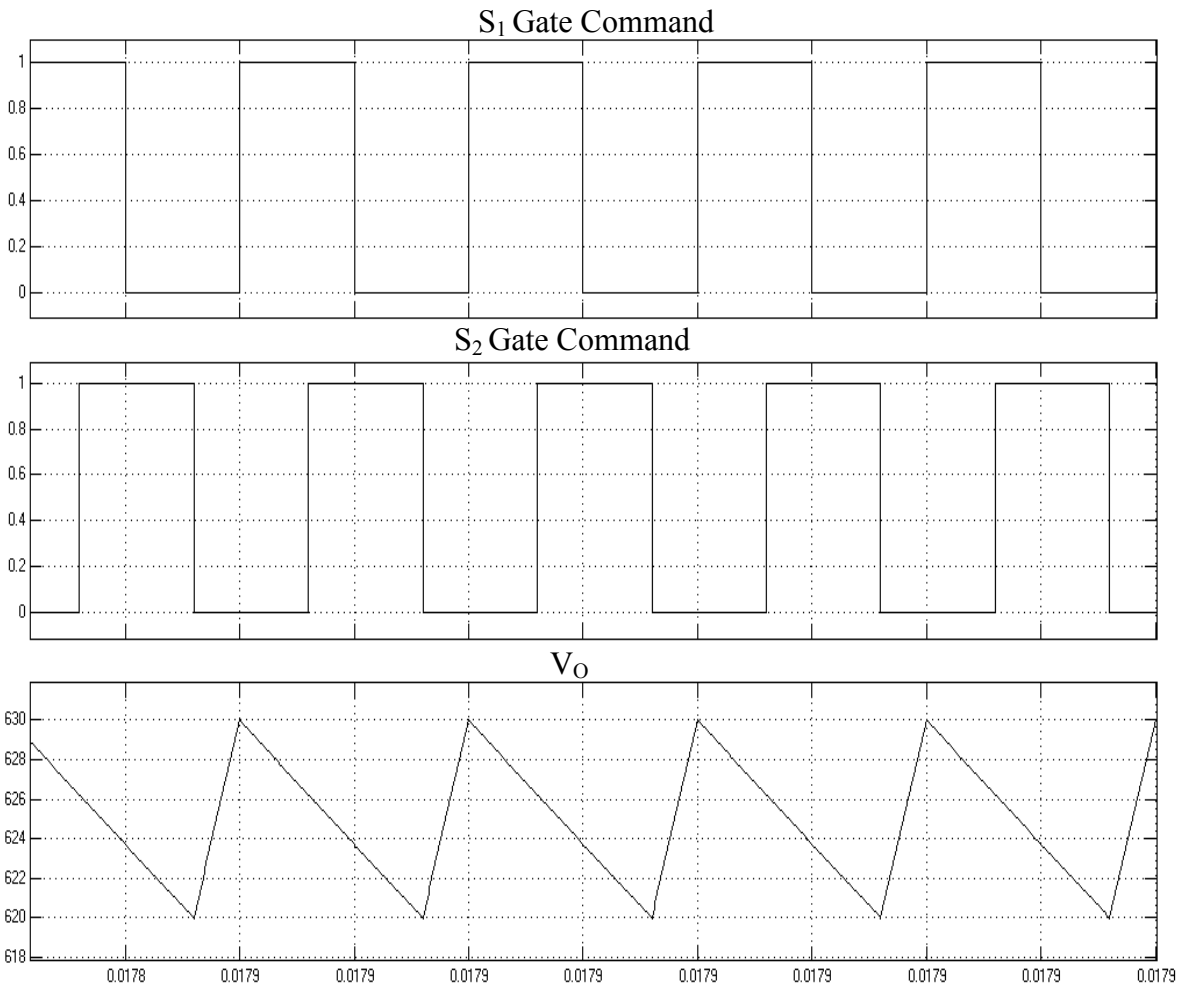

Figure 3.5. Simulation waveforms of double-input buckboost-buckboost converter with different value of T_2

Figure 3.6 shows the typical simulation results of the buck-buckboost converter using Matlab-simulink. Two dc voltage sources V_1 = 100 V and V_2 = 150 V are used for the input voltage sources. The switching commands for S_1 and S_2 have fixed duty ratios of 0.5 at the switching frequency of 100 KHz. From top to bottom are the waveforms of switching commands S_1 and S_2, inductor voltage V_L, inductor current i_L, capacitor current i_C, output current i_O, and the output voltage. One can observe from the waveforms that

the average of output voltage is around 250 V which can also be obtained from the transfer function of Table 3.2.

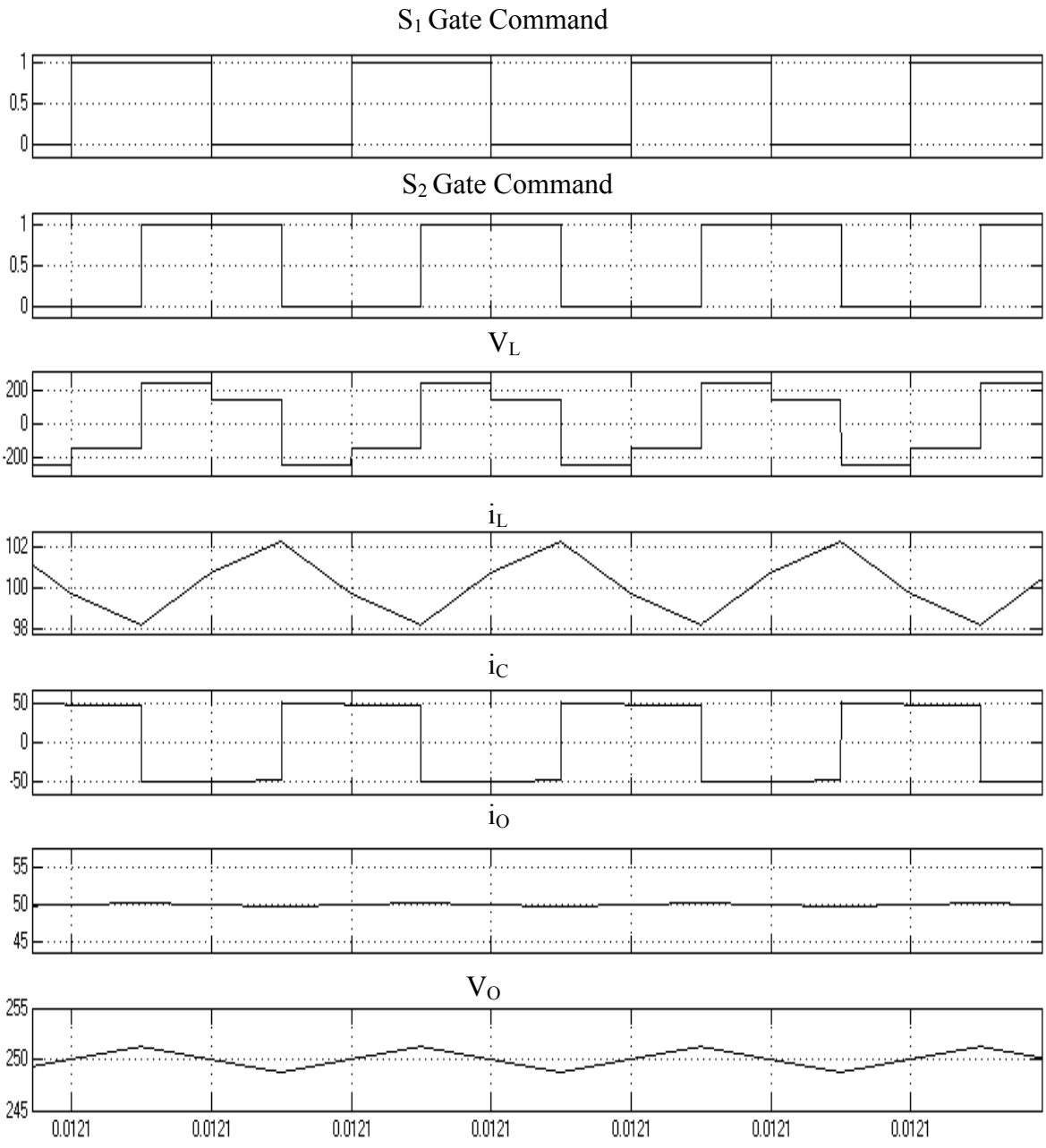

Figure 3.6. Simulation waveforms of double-input buck-buckboost converter

Figure 3.7 shows the typical simulation results of the boost-boost converter using Matlab-simulink. Two dc voltage sources V_1 = 200 V and V_2 = 100 V are used for the input voltage sources. The switching commands for S_1 and S_2 have fixed duty ratios of 0.5 and 0.75 at the switching frequency of 100 KHz, respectively. From top to bottom are the waveforms of switching commands S_1 and S_2, inductor voltages V_{L1} and V_{L2}, inductor currents i_{L1} and i_{L2}, capacitor current i_C, and the output voltage V_O. One can observe from the waveforms that the average of output voltage is around 400 V which can also be obtained from the transfer function of Table 3.2.

The simulation results are presented for all the four converters and the results are verified with the voltage ratios of table 3.2. Buckboost-buckboost converter has the advantage of changing the output voltage without actually changing the switching periods. Also this converter compared to the limited converter, has no limitation of connecting both the voltage sources in the circuit at the same time. In chapter 4, a new approach will be used to synthesize multi-input converters.

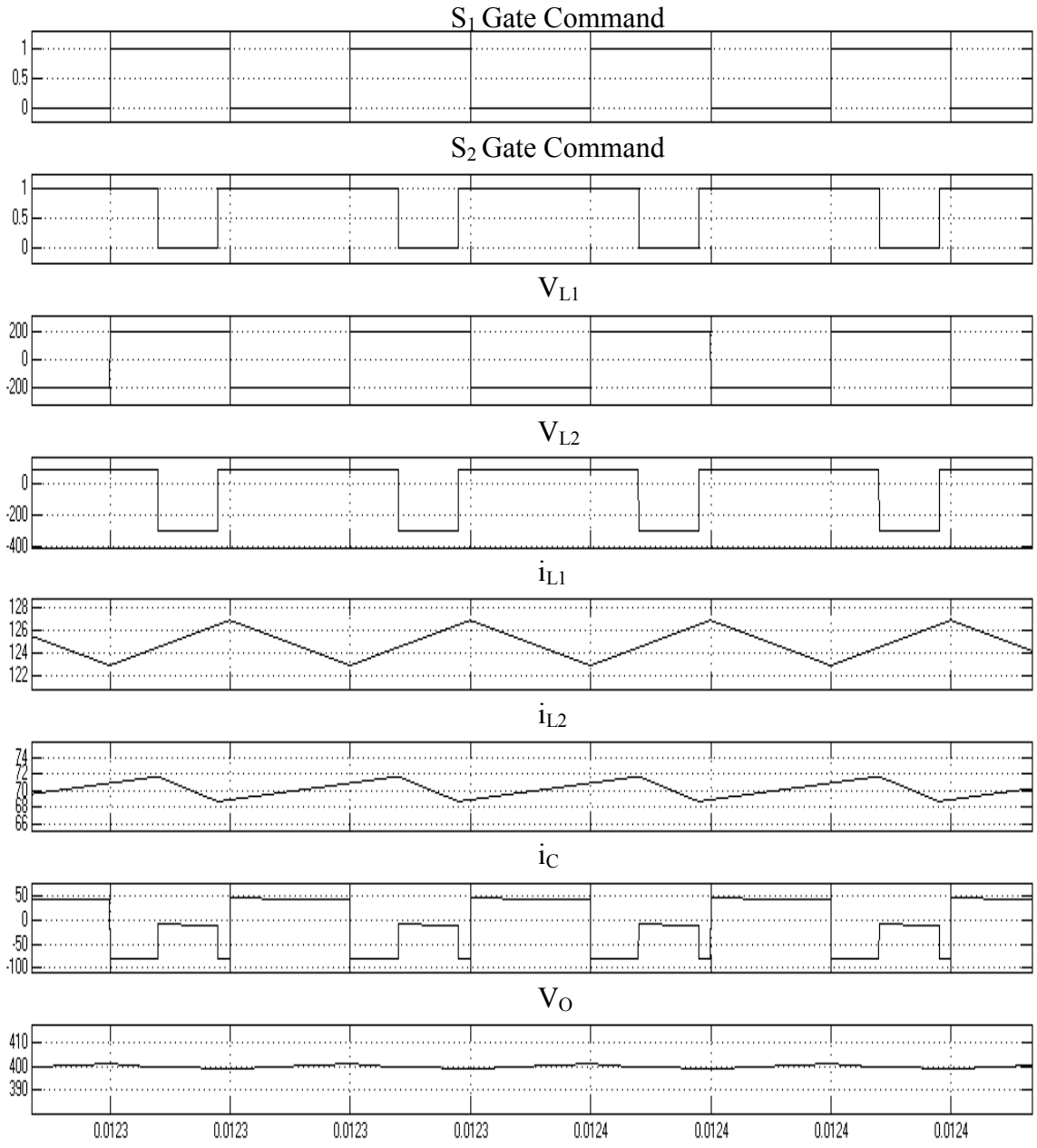

Figure 3.7. Simulation waveforms of double-input boost-boost converter

4. DERIVATION OF DOUBLE-INPUT DC-DC CONVERTERS USING A SINGLE-POLE TRIPLE-THROW SWITCH

4.1. INTRODUCTION

In order to combine the main source of power with the energy storage unit, either several independent converters or a single double-input converter can be used. The advantages of using a double-input converter are high efficiency, reduced component count, low cost, and simple control. In this chapter a single-pole triple-throw (SP3T) switch is used as the building block to realize four new double-input dc-dc converters. These new converters are named as double-input buck, double-input buckboost, double-input buckboost-buck, and double-output boost converters.

As the name suggests, SP3T switch consists of a single pole ‘P’ and three throws 1, 2, and 3. Figure 4.1 shows basic representation of an SP3T switch that can be turned on with any of the three positions in contact with the pole. An SP3T switch can be realized by using three single-pole single-throw (SPST) switches, as depicted in Figure 4.2. It is worth mentioning that one and only one of the three switches is on at any time instant [64].

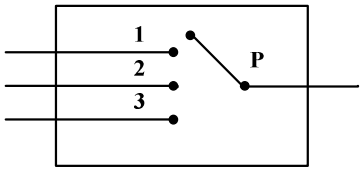

Figure 4.1. Single-pole triple-throw switch

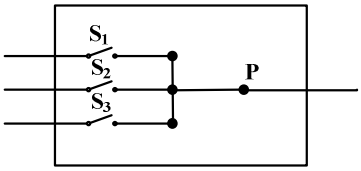

Figure 4.2. SP3T switch realized using three SPST switches

4.2. DERIVATION OF DOUBLE-INPUT BUCK CONVERTER USING AN SP3T SWITCH

Figure 4.3 shows the circuit diagram of the double-input buck converter using an SP3T switch [65, 66]. Voltage source V_1 delivers power by keeping the switch at position 1, voltage source V_2 delivers power by keeping the switch at position 2, and position 3 can be used for free wheeling purposes. Figure 4.4 shows the circuit diagram of the double-input buck converter using three SPST switches instead of a single SP3T switch. It consists of three single SPST switches S_1, S_2, and S_3 which can be turned on and off individually.

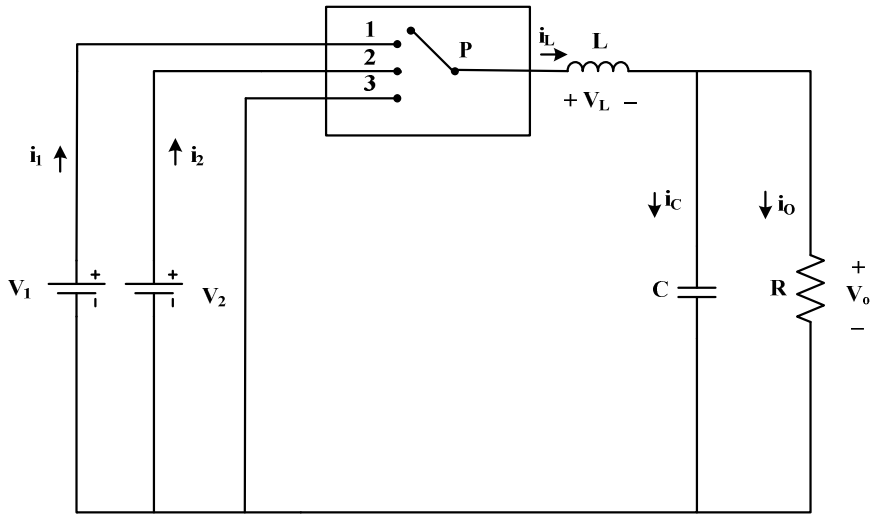

Figure 4.3. Double-input buck converter using an SP3T switch

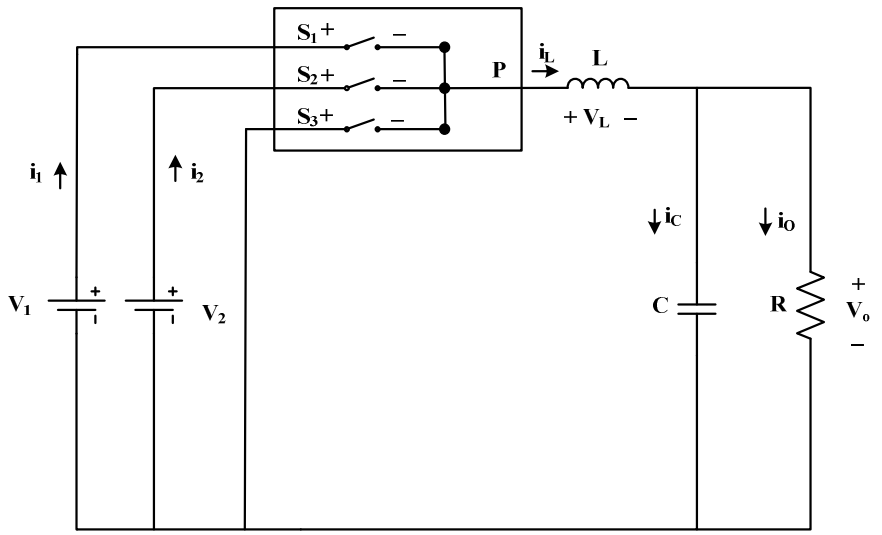

Figure 4.4. Double-input buck converter using three SPST switches

Figure 4.5 shows the switching patterns of three switches S_1, S_2, and S_3. The pattern is true for all the possible arrangements of the converter. The three modes of operation that occur under regular circumstances are discussed below

MODE I (S_1: on)

In this mode V_1 supplies energy to the load and inductor L.

MODE II (S_2: on)

In this mode V_2 supplies energy to the load and inductor L.

MODE III (S_3: on)

In this mode both the power sources are disconnected from the circuit. The energy stored in the inductor is being released to the load. Thus inductor gets de-energized during this mode.

Voltage across the inductor for different modes of operation is given in Table 4.1.

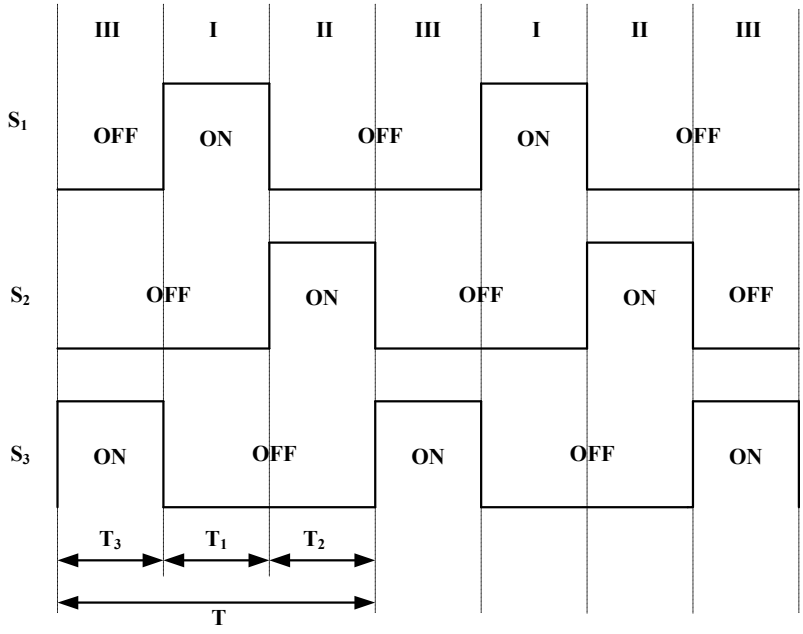

Figure 4.5. Switching patterns of double-input buck converter using three SPST switches

Table 4.1. Voltage across the inductor for different modes of operation of buck-buck converter using three SPST switches

	I	**II**	**III**
S_1	ON	OFF	OFF
S_2	OFF	ON	OFF
S_3	OFF	OFF	ON
V_L	V_1-V_O	V_2-V_O	-V_O

One can see from Figure 4.5 that T_1 is the on time of switch S_1, T_2 is the on time of switch S_2, and T_3 is the on time of switch S_3. T is the time period of the switching patterns of S_1 or S_2 or S_3, and d_1, d_2, and d_3 are the duty cycles of switches S_1, S_2 and S_3

respectively. One can write the following equations based on Figure 4.5, Table 4.1, and volt-second balance equation of the inductor.

$$T_1 = d_1 * T \tag{1}$$

$$T_2 = d_2 * T \tag{2}$$

$$T_3 = d_3 * T \tag{3}$$

$$T_1 + T_2 + T_3 = T \tag{4}$$

$$T_1 * (V_1 - V_O) + T_2 * (V_2 - V_O) + T_3 (-V_O) = 0 \tag{5}$$

This can be simplified as the following equation.

$$V_1 * T_1 + V_2 * T_2 = V_O * (T_1 + T_2 + T_3) \tag{6}$$

Combining equations (1), (2), (3), and (6) one can obtain the following equation which gives the relation between input and output.

$$V_1 * d_1 + V_2 * d_2 = V_O * 1$$

$$V_O = d_1 * V_1 + d_2 * V_2 \tag{7}$$

Equation (7) determines the voltage transfer ratio of the double-input buck converter using three SPST switches. One can observe from (7) that this expression is equal to the voltage transfer ratio obtained in chapter three for a buck-buck converter, inspite of not having the mode where both the voltage sources supply energy to the load. Also the voltage transfer ratios that are obtained in this chapter will be the same as that for the previously proposed double-input converters. Hence, the focus here is the derivation of new circuit topologies using SP3T switch and the simulation results are not provided.

4.3. SWITCH REALIZATION OF DOUBLE-INPUT BUCK CONVERTER USING AN SP3T SWITCH

In Figure 4.4, the switches can be replaced by diodes or transistors depending on the voltage levels of the system. One may obtain the circuit with transistors and diodes by the following explanation. As the power flow through the inductor is unidirectional, i_L should always be positive.

(If S_1 is on ➔ S_2 and S_3 off) => ($i_{S1} > 0$, $V_{S2} = V_2 - V_1$, and $V_{S3} = -V_1$)

(If S_2 is on ➔ S_1 and S_3 off) => ($i_{S2} > 0$, $V_{S1} = V_1 - V_2$, and $V_{S3} = -V_2$)

(If S_3 is on ➔ S_1 and S_2 off) => ($i_{S3} > 0$, $V_{S1} = V_1$, and $V_{S2} = V_2$)

One can observe that switch S_1 conducts positive current but opposes either positive or negative voltages depending on the magnitude of V_1 and V_2; hence it can be replaced by a diode in series with a transistor. Similarly switch S_2 can be replaced by a diode in series with a transistor. Switch S_3, which conducts positive current and opposes negative voltage, can be replaced by a diode. So the final circuit that is obtained is shown in Figure 4.6.

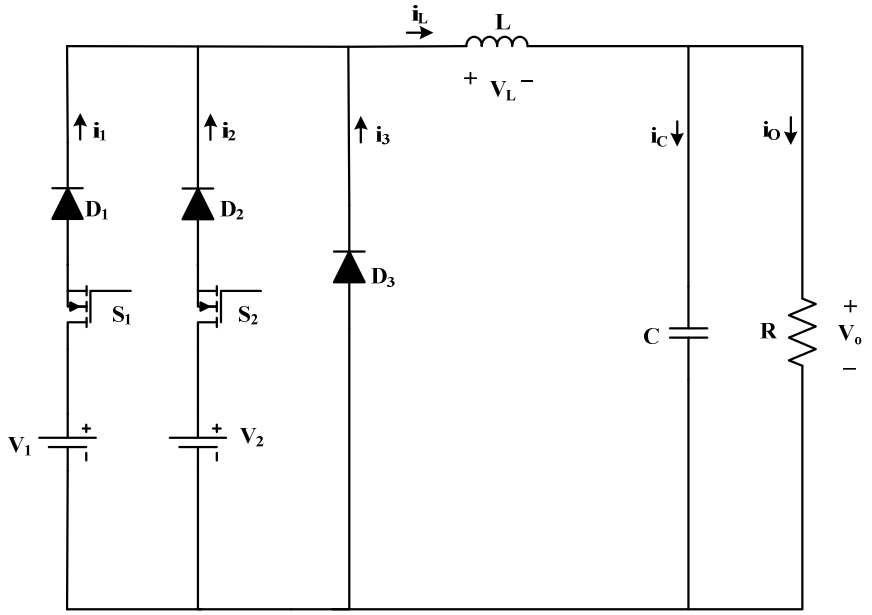

Figure 4.6. Final double-input buck converter using an SP3T switch

The structure of the double-input buck converter can be simplified if V_1 is greater than V_2 ($V_1 > V_2$). The switch realization equations changes accordingly

(If S_1 is on ➔ S_2 and S_3 off) => ($i_{S1} > 0$, $V_{S2} = V_2 - V_1 < 0$, and $V_{S3} = -V_1 < 0$)

(If S_2 is on ➔ S_1 and S_3 off) => ($i_{S2} > 0$, $V_{S1} = V_1 - V_2 > 0$, and $V_{S3} = -V_2 < 0$)

(If S_3 is on ➔ S_1 and S_2 off) => ($i_{S3} > 0$, $V_{S1} = V_1 > 0$, and $V_{S2} = V_2 > 0$)

One can observe that switch S_1 conducts positive current and opposes positive voltage; hence it can be replaced by a transistor. Similarly switch S_2, which conducts positive current and opposes either positive or negative voltages, can be replaced by a diode in series with a transistor. Switch S_3, which conducts positive current and opposes negative voltage, can be replaced by a diode. So the final circuit that is obtained is shown in Figure 4.7.

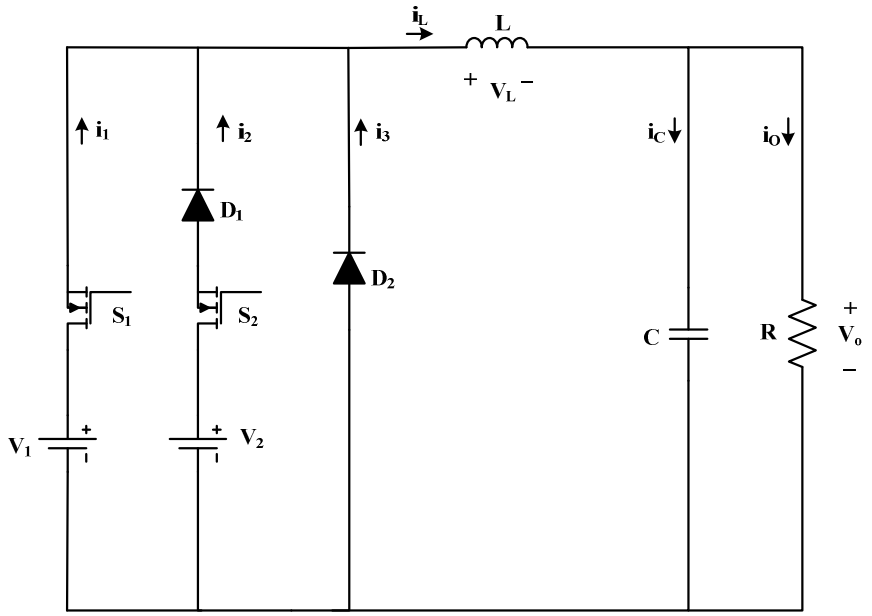

Figure 4.7. Simplified double-input buck converter using an SP3T switch

The structure of the double-input buck converter can be further simplified if V_1 is greater than V_2 ($V_1 > V_2$) and mode III never occurs in the system. The switch realization equations changes accordingly

(If S_1 is on ➔ S_2 off) => ($i_{S1} > 0$ and $V_{S2} = V_2 - V_1 < 0$)

(If S_2 is on ➔ S_1 off) => ($i_{S2} > 0$ and $V_{S1} = V_1 - V_2 > 0$)

One can observe that switch S_1 conducts positive current and opposes positive voltage; hence it can be replaced by a transistor. Switch S_2 can be replaced by a diode as it conducts positive current and opposes negative voltage. So the final circuit that is obtained is shown in Figure 4.8. This converter is similar to a ti-buck (two-input buck) converter [65-68].

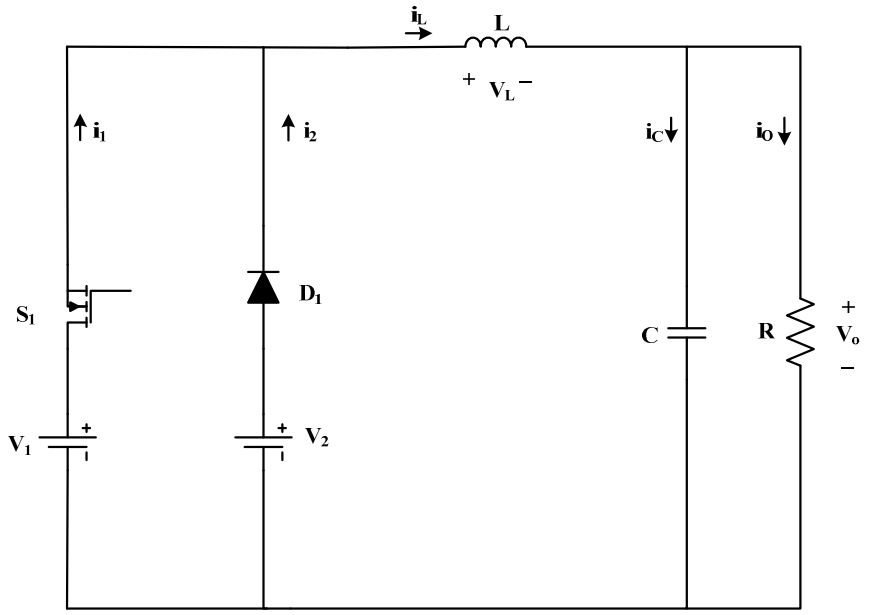

Figure 4.8. Simplified double-input buck converter using an SP3T switch with no mode III

4.4. DERIVATION OF DOUBLE-INPUT BUCKBOOST CONVERTER USING AN SP3T SWITCH

Figure 4.9 shows the circuit diagram of a double-input buckboost converter using an SP3T switch. In this topology negative terminal of the input sources is connected to the positive terminal of the output voltage. Figure 4.10 shows the circuit diagram of a double-input buckboost converter using three SPST switches instead of a single SP3T switch. It consists of three single SPST switches S_1, S_2, and S_3 which can be turned on and off individually.

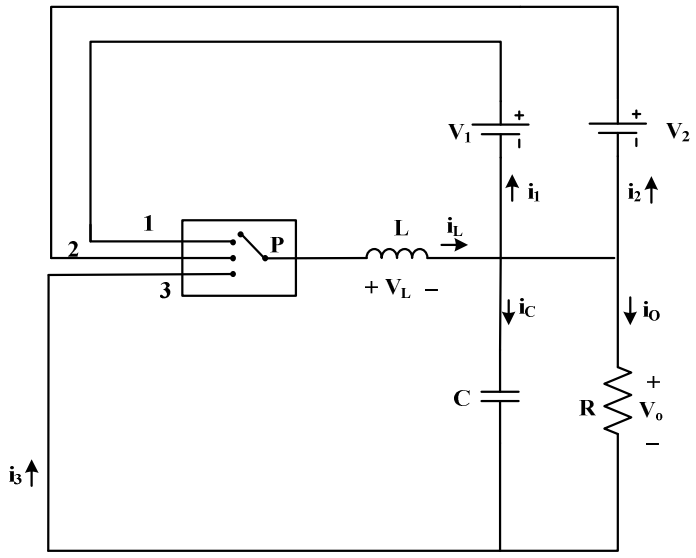

Figure 4.9. Double-input buckboost converter using an SP3T switch

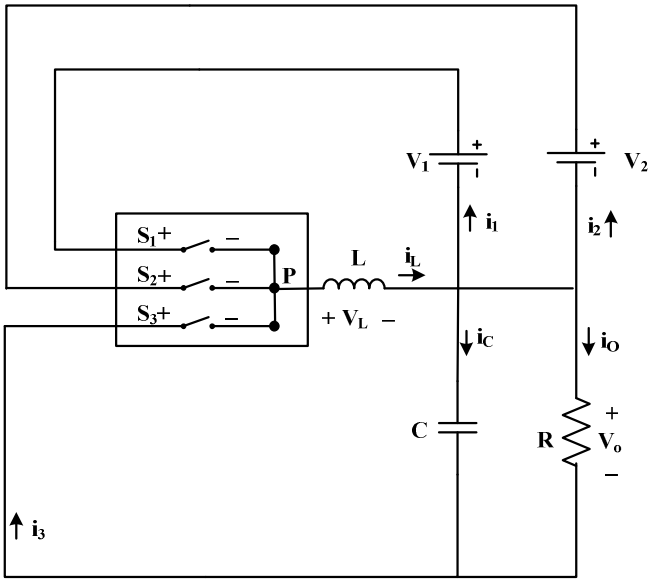

Figure 4.10. Double-input buckboost converter using three SPST switches

The switching patterns of the three switches are the same as shown in Figure 4.5. The three modes of operation under regular circumstances are discussed below

MODE I (S_1: on)

In this mode V_1 supplies energy to inductor L.

MODE II (S_2: on)

In this mode V_2 supplies energy to inductor L.

MODE III (S_3: on)

In this mode both the power sources are disconnected from the circuit. The energy stored in the inductor is being released to the load. Thus inductor gets de-energized during this mode. Voltage across the inductor for different modes of operation is given in Table 4.2.

Table 4.2. Voltage across the inductor for different modes of operation of a double-input buckboost converter using three SPST switches

	I	**II**	**III**
S_1	ON	OFF	OFF
S_2	OFF	ON	OFF
S_3	OFF	OFF	ON
V_L	V_1	V_2	$-V_O$

One can see from Figure 4.5 that T_1 is the on time of switch S_1, T_2 is the on time of switch S_2, and T_3 is the on time of switch S_3. T is the time period of the switching patterns of S_1 or S_2 or S_3, and d_1, d_2, and d_3 are the duty cycles of switches S_1, S_2 and S_3 respectively. One can write the following equations based on Figure 4.5, Table 4.2, and volt-second balance equation of the inductor.

$$T_1 = d_1 * T \tag{8}$$

$$T_2 = d_2 * T \tag{9}$$

$$T_3 = d_3 * T \tag{10}$$

$$T_1 + T_2 + T_3 = T \tag{11}$$

$$T_1 * (V_1) + T_2 * (V_2) + T_3 (-V_O) = 0 \tag{12}$$

This can be simplified as the following equation.

$$V_1 * T_1 + V_2 * T_2 = V_O * (T_3) \tag{13}$$

Combining equations (8), (9), (10), and (13) one can obtain the following equation which gives the relation between input and output.

$$V_1 * d_1 + V_2 * d_2 = V_O * (1 - d_1 - d_2)$$

$$V_O = \frac{d_1}{1 - d_1 - d_2} * V_1 + \frac{d_2}{1 - d_1 - d_2} * V_2 \tag{14}$$

Equation (14) determines the voltage transfer ratio of the double-input buckboost converter using three SPST switches. One can observe from (14), that it is equal to the voltage transfer ratio of limited buckboost-buckboost converter discussed in chapter three (see Table 3.2).

4.5. SWITCH REALIZATION OF DOUBLE-INPUT BUCKBOOST CONVERTER USING AN SP3T SWITCH

In the circuit of Figure 4.10, the switches can be replaced by diodes or transistors depending on the voltage levels of the system. One may obtain the circuit with transistors and diodes by the following explanation. As the power flow through the inductor is unidirectional, i_L should always be positive.

(If S_1 is on ➔ S_2 and S_3 off) => ($i_{S1} > 0$, $V_{S2} = V_2 - V_1$, and $V_{S3} = -(V_1 + V_O)$)

(If S_2 is on ➔ S_1 and S_3 off) => ($i_{S2} > 0$, $V_{S1} = V_1 - V_2$, and $V_{S3} = -(V_2 + V_O)$)

(If S_3 is on ➔ S_1 and S_2 off) => ($i_{S3} > 0$, $V_{S1} = V_1 + V_O$, and $V_{S2} = V_2 + V_O$)

One can observe that switch S_1 conducts positive current but opposes either positive or negative voltages depending on the magnitude of V_1 and V_2; hence it can be replaced by a diode in series with a transistor. Similarly switch S_2 can be replaced by a diode in series with a transistor. Switch S_3 which conducts positive current and opposes negative voltage, can be replaced by a diode. So the final circuit that is obtained is shown in Figure 4.11. The structure of this topology may also be further simplified like in the case of the double-input buck converter.

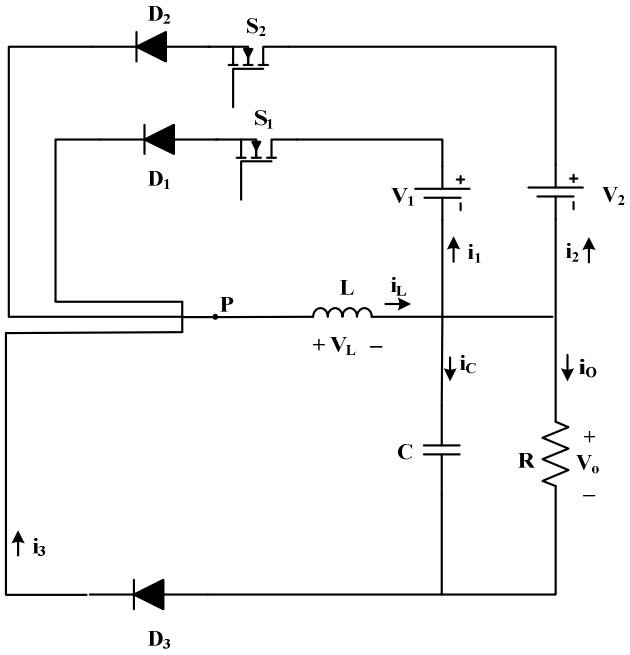

Figure 4.11. Final double-input buckboost converter using an SP3T switch

The circuit diagram of Figure 4.11 can be redrawn in a more familiar format as depicted in Figure 4.12.

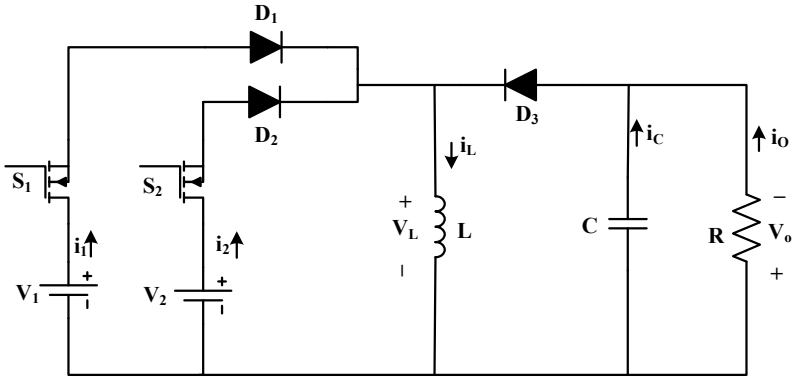

Figure 4.12. Redrawn double-input buckboost converter using an SP3T switch

4.6. DERIVATION OF DOUBLE-INPUT BUCKBOOST-BUCK CONVERTER USING AN SP3T SWITCH

Figure 4.13 shows the circuit diagram of a double-input buckboost-buck converter using an SP3T switch. The circuit diagrams of Figures 4.9 and 4.13 are more or less the same with only difference being that source V_2 in Figure 4.9 is connected between the load and the switch, whereas in Figure 4.13, it is connected between the ground and the switch. Figure 4.14 shows the circuit diagram of a double-input buckboost-buck converter using three SPST switches instead of a single SP3T switch. It consists of three single SPST switches S_1, S_2, and S_3 which can be turned on and off individually.

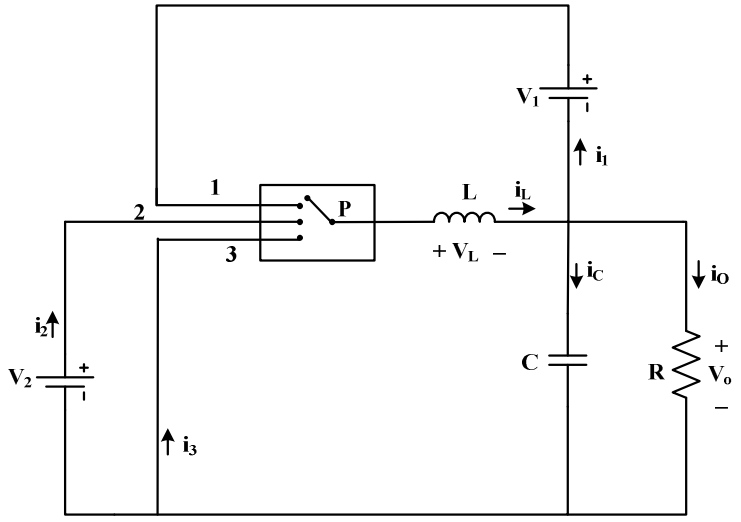

Figure 4.13. Double-input buckboost-buck converter using an SP3T switch

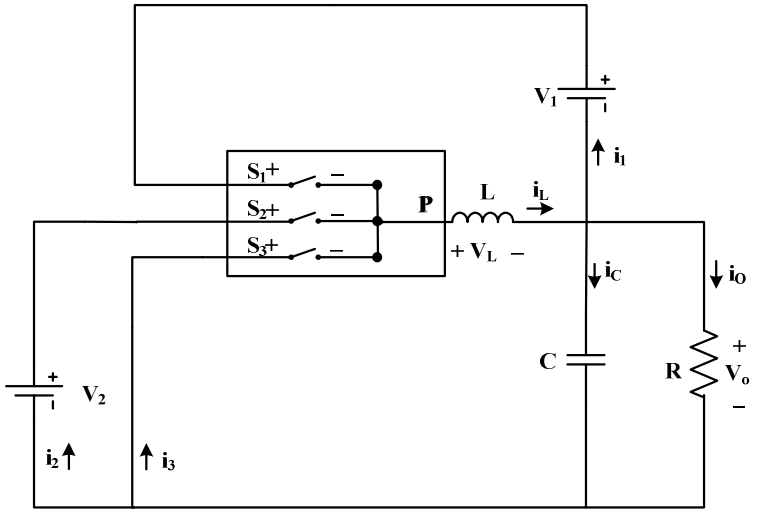

Figure 4.14. Double-input buckboost-buck converter using three SPST switches

The switching patterns of the three switches are the same as shown in Figure 4.5. The three modes of operation that occur under regular circumstances are discussed below

MODE I (S_1: on)

In this mode V_1 supplies energy to inductor L.

MODE II (S_2: on)

In this mode V_2 supplies energy to the load and inductor L.

MODE III (S_3: on)

In this mode both the power sources are disconnected from the circuit. The energy stored in the inductor is being released to the load. Thus inductor gets de-energized during this mode. Voltage across the inductor for different modes of operation is given in Table 4.3.

Table 4.3. Voltage across the inductor for different modes of operation of buckboost-buck converter using three SPST switches

	I	**II**	**III**
$\mathbf{S_1}$	ON	OFF	OFF
$\mathbf{S_2}$	OFF	ON	OFF
$\mathbf{S_3}$	OFF	OFF	ON
$\mathbf{V_L}$	V_1	$V_2 - V_O$	$-V_O$

One can see from Figure 4.5 that T_1 is the on time of switch S_1, T_2 is the on time of switch S_2, and T_3 is the on time of switch S_3. T is the time period of S_1 or S_2 or S_3, and d_1, d_2, and d_3 are the duty cycles of switches S_1, S_2 and S_3 respectively. One can write the following equations based on Figure 4.5, Table 4.3, and volt-second balance equation of the inductor.

$$T_1 = d_1 * T \tag{15}$$

$$T_2 = d_2 * T \tag{16}$$

$$T_3 = d_3 * T \tag{17}$$

$$T_1 + T_2 + T_3 = T \tag{18}$$

$$T_1 * (V_1) + T_2 * (V_2 - V_O) + T_3 (-V_O) = 0 \tag{19}$$

This can be further simplified as the following equation.

$$V_1 * T_1 + V_2 * T_2 = V_O * (T_3 + T_2) \tag{20}$$

Combining equations (15), (16), (17), and (20) one can obtain the following equation which gives the relation between input and output.

$$V_1 * d_1 + V_2 * d_2 = V_O * (1 - d_1)$$

$$V_O = \frac{d_1}{1 - d_1} * V_1 + \frac{d_2}{1 - d_1} * V_2 \tag{21}$$

Equation (21) determines the voltage transfer ratio of the double-input buckboost-buck converter using three SPST switches. One can observe from (21), that it is equal to the voltage transfer ratio obtained in chapter three for buck-buckboost converter expect that the sources are interchanged. It can also be observed that the output is positive as long as the two sources are positive.

4.7 SWITCH REALIZATION OF DOUBLE-INPUT DC-DC BUCKBOOST-BUCK CONVERTER USING AN SP3T SWITCH

In Figure 4.14, the switches can be replaced by diodes or transistors depending on the voltage levels of the system. One may obtain the circuit with transistors and diodes by the following explanation. As the power flow through the inductor is unidirectional, i_L should always be positive.

(If S_1 is on ➔ S_2 and S_3 off) => ($i_{S1} > 0$, $V_{S2} = V_2 - (V_1 + V_O)$, and $V_{S3} = -(V_1 + V_O)$)

(If S_2 is on ➔ S_1 and S_3 off) => ($i_{S2} > 0$, $V_{S1} = V_1 + V_O - V_2$, and $V_{S3} = -(V_2)$

(If S_3 is on ➔ S_1 and S_2 off) => ($i_{S3} > 0$, $V_{S1} = V_1 + V_O$, and $V_{S2} = V_2$)

One can observe that switch S_1 conducts positive current but opposes either positive or negative voltages depending on the magnitude of V_1, V_2 and V_O; hence it should be replaced by a diode in series with a transistor. Similarly switch S_2 can be replaced by a diode in series with a transistor. Switch S_3 which conducts positive current and opposes negative voltage, can be replaced by a diode. So the final circuit that is

obtained is shown in Figure 4.15. The structure of this topology can also be simplified like in the case of the double-input buck converter.

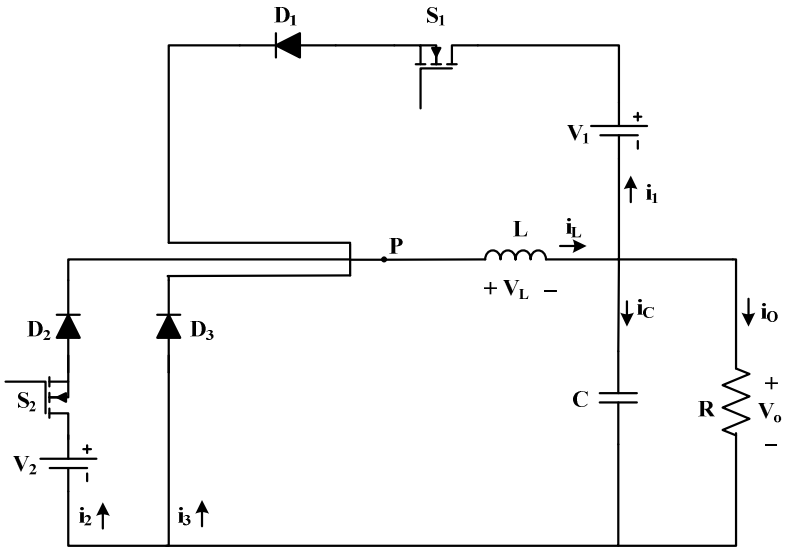

Figure 4.15. Final double-input buckboost-buck converter using an SP3T switch

4.8. DERIVATION OF DOUBLE-OUTPUT BOOST CONVERTER USING AN SP3T SWITCH

Figure 4.16 shows the circuit diagram of a double-output boost converter using an SP3T switch. Load R_1 consumes power by keeping the switch at position 1, load R_2 consumes power by keeping the switch at position 2, and position 3 can be used for free wheeling purposes. Figure 4.17 shows the circuit diagram of a double-output boost converter using three SPST switches instead of a single SP3T switch.

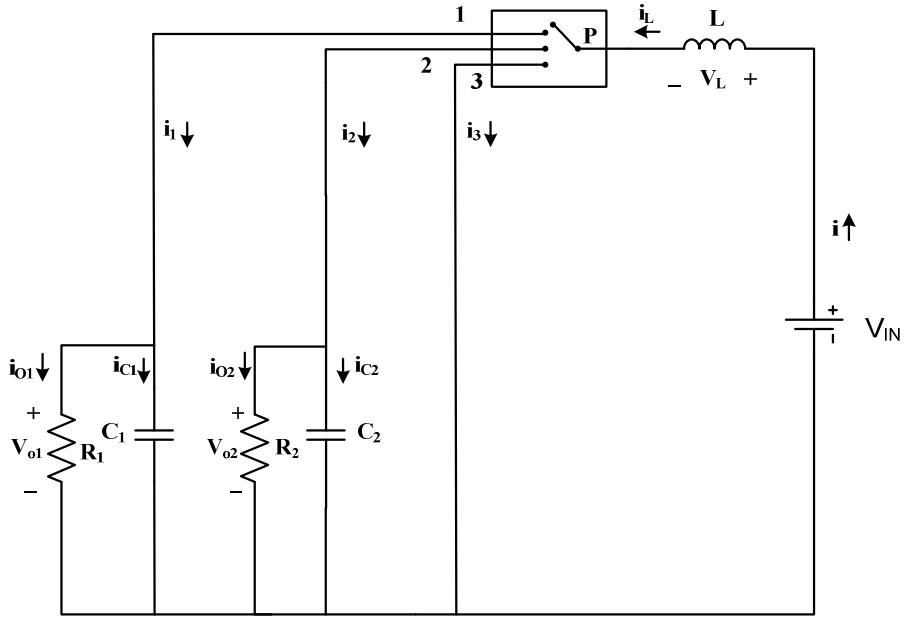

Figure 4.16. Double-output boost converter using an SP3T switch

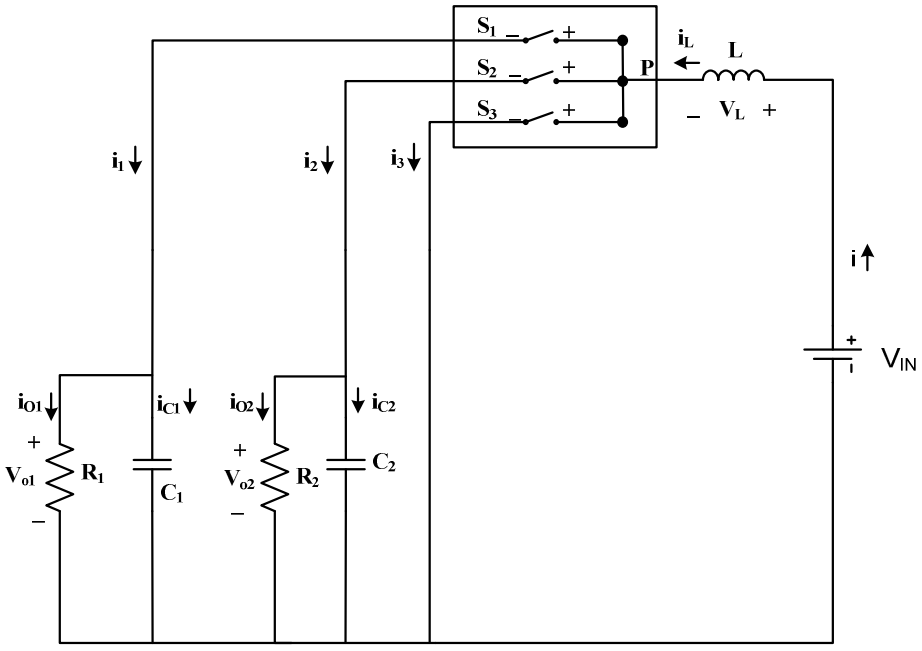

Figure 4.17. Double-output boost converter using three SPST switches

The switching patterns of the three switches are the same as the previous converter which is shown in Figure 4.5. The three modes of operation that occur under regular circumstances are discussed below

MODE I (S_1: on)

In this mode V_{IN} supplies energy to inductor L and load 1.

MODE II (S_2: on)

In this mode V_{IN} supplies energy to inductor L and load 2.

MODE III (S_3: on)

In this mode both the loads are disconnected from the circuit and inductor is being charged. Voltage across the inductor for different modes of operation is given in Table 4.4.

Table 4.4. Voltage across the inductor for different modes of operation of double-output boost converter using three SPST switches

	I	**II**	**III**
S_1	ON	OFF	OFF
S_2	OFF	ON	OFF
S_3	OFF	OFF	ON
V_L	V_{IN} - V_{O1}	V_{IN} - V_{O2}	V_{IN}

One can see from Figure 4.5 that T_1 is the on time of switch S_1, T_2 is the on time of switch S_2, and T_3 is the on time of switch S_3.

$$T_1 = d_1 * T \tag{22}$$

$$T_2 = d_2 * T \tag{23}$$

$$T_3 = d_3 * T \tag{24}$$

T is the time period of S_1 or S_2 or S_3, and d_1, d_2, and d_3 are the duty cycles of switches S_1, S_2 and S_3 respectively. One can write the following equations based on Figure 4.5, Table 4.4, and volt-second balance equation of the inductor.

$$T_1 + T_2 + T_3 = T \tag{25}$$

$$T_1 * (V_{IN} - V_{O1}) + T_2 * (V_{IN} - V_{O2}) + T_3 (V_{IN}) = 0 \tag{26}$$

This can be simplified as the following equation.

$$V_{O1} * T_1 + V_{O2} * T_2 = V_{IN} * (T_1 + T_2 + T_3) \tag{27}$$

Combining equations (22), (23), (24), and (27) one can obtain the following equation which gives the relation between input and output.

$$V_{O1} * d_1 + V_{O2} * d_2 = V_{IN}$$

$$V_{IN} = d_1 * V_{O1} + d_2 * V_{O2} \tag{28}$$

Equation (28) determines the voltage transfer ratio of the double-output boost converter using three SPST switches. One can observe from (28), that the output voltages are independent of each other. But a limitation was there for the source voltages of the double-input boost-boost converter in chapter three. At first glance, (28) may look different than the voltage transfer ratio of a single output boost converter. The difference lies beneath the way the duty ratios are defined.

4.9. SWITCH REALIZATION OF DOUBLE-OUTPUT BOOST CONVERTER USING AN SP3T SWITCH

In Figure 4.17, the switches can be replaced by diodes or transistors depending on the system. One may obtain the circuit with transistors and diodes by the following explanation. As the power flow through the inductor is unidirectional, i_L should always be positive.

(If S_1 is on ➔ S_2 and S_3 off) => ($i_{S1} > 0$, $V_{S2} = V_{O1} - V_{O2}$, and $V_{S3} = V_{O1}$)

(If S_2 is on ➔ S_1 and S_3 off) => ($i_{S2} > 0$, $V_{S1} = V_{O2} - V_{O1}$, and $V_{S3} = V_{O2}$)

(If S_3 is on ➔ S_1 and S_2 off) => ($i_{S3} > 0$, $V_{S1} = - V_{O1}$, and $V_{S2} = - V_{O2}$)

One can observe that switch S_1 conducts positive current and opposes either positive or negative voltage depending on the magnitude of the load voltages; hence it can be replaced by a diode in series with a transistor. Similarly switch S_2 can be replaced

by a diode in series with a transistor. Switch S_3 which conducts positive current and opposes positive voltage, can be replaced by a transistor. So the final circuit that is obtained is shown in Figure 4.18. It is worth mentioning that it is necessary to commutate S_1 by turning the switch S_3 and then turning switch S_2, instead of directly turning switch S_2 after S_1. This is because as the inductor current is continuous S_2 cannot be turned on by turning off S_1 as this results in discontinuous inductor current, instead S_1 is commutated by turning on S_3 and then S_2 is turned on.

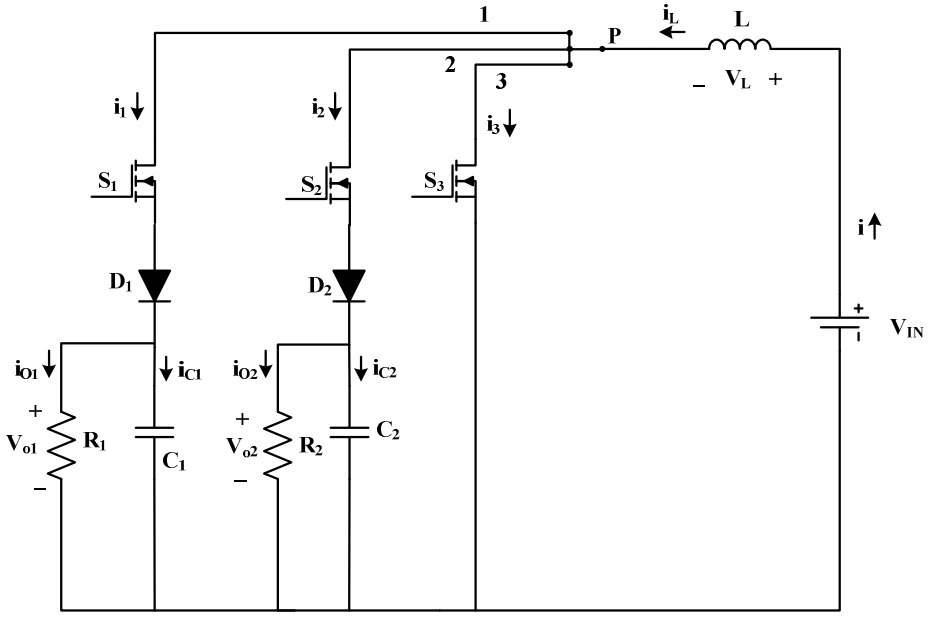

Figure 4.18. Final double-output boost converter using an SP3T switch

4.10. SIMULATION RESULT OF DOUBLE-OUTPUT BOOST CONVERTER

Figure 4.19 shows the typical simulation result of the double-output boost converter using Matlab-simulink. A dc voltage source V_{IN} = 100 V is used. The switching commands S_1, S_2, and S_3 have duty ratios of 0.35, 0.35 and 0.5 at a switching frequency of 10 KHz, 10 KHz, and 20 KHz respectively. From top to bottom are the waveforms of switching commands S_1, S_2, and S_3, inductor voltage V_L, inductor current i_L, and the output voltages V_{O1} and V_{O2}. Effective value for d_1 is the non overlapping part of S_1 and S_3 gate commands which is 0.25. Similarly, effective value for d_2 is 0.25. This is the reason that the sum of output voltages which is around 400 V cannot be directly obtained from the transfer function expressed by (28). Instead, it can be obtained when the exact duty ratios are substituted. In this case d_1 and d_2 are each 0.25.

Different converter topologies are realized using a single-pole triple-throw switch. As the voltage transfer ratios of double-input buck, buckboost, and buckboost-buck are similar to those obtained in chapter three, their simulation results are almost the same which are not discussed here.

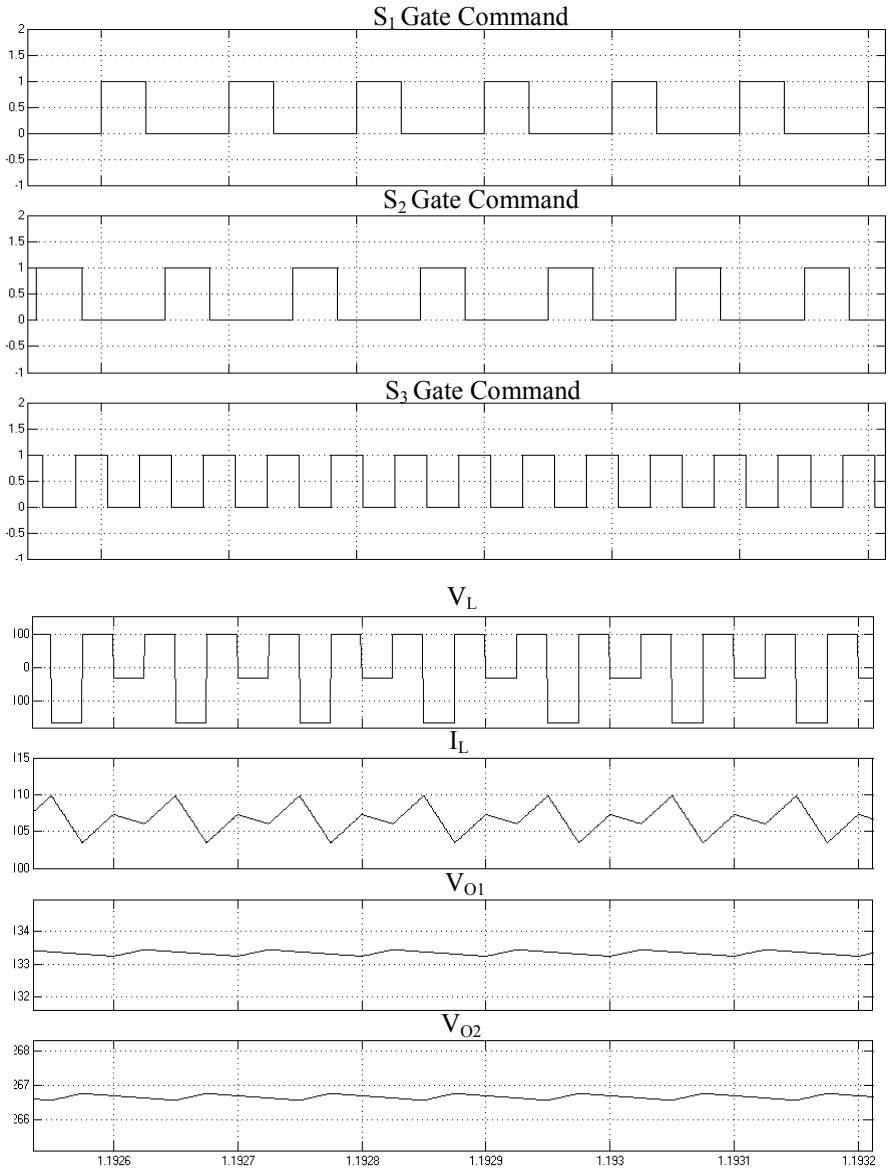

Figure 4.19. Simulation waveforms of double-output boost converter

5. CONCLUSION

In this thesis, several new double-input converters have been proposed using H-bridge cells or single-pole triple-throw switches as building blocks. The operating modes of the converters and their switch realization are discussed. The double-input converters that are derived using H-bridge cells are buck-buck, buckboost-buckboost, buck-buckboost, and boost-boost. All of these converters except for the boost-boost converter consist of only one inductor. This results in reduced size, weight, losses, and ultimately increased efficiency of the converters. The voltage transfer ratios of these converters are obtained and simulation results are used to verify the voltage transfer ratios and the operating characteristics. The proposed converters can also be modified to acquire bidirectional power transfer capabilities. Buckboost-buckboost converter with bidirectional power transfer capabilities is realized in chapter two. The switch realization of this converter is also explained in this chapter.

Furthermore, double-input buck, buckboost, buckboost-buck, and double-output boost converters are proposed using a single-pole triple-throw switch. All of these converters consist of only one inductor; hence, they share the same advantages as the converters that are derived using H-bridge cells. Switch realization and voltage transfer ratios of these converters are obtained accordingly. Simulation results of double-output boost converter are also provided. The converters that are proposed in this thesis can be used in ultracapacitor enhancement of battery packs in automotive applications or hybridizing photovoltaic or fuel cell systems.

BIBLIOGRAPHY

[1] C. C. Chan, "The state of the art of electric and hybrid vehicles," Proc. IEEE, vol. 90, no. 2, pp. 247-275, Feb. 2002

[2] C. C. Chan, "The state of the art of electric, hybrid, and fuel cell vehicles," Proc. IEEE, vol. 95, pp. 704-718, April 2007

[3] C. C. Chan, **"**An overview of electric vehicle technology**,"** Proc. IEEE, vol. 81, pp. 1202-1213, Sept. 1993

[4] C. C. Chan, K. T. Chau, **"**An overview of power electronics in electric vehicles**,"** IEEE Transactions on Industrial Electronics, vol. 44, Feb. 1997, pp. 3-13

[5] M. K. C. Marwali, N. M. Maricar, S. K. Shrestha, "Battery capacity tests evaluation for stand-alone photovoltaic systems," IEEE Power Engineering Society Winter Meeting, vol. 1, pp. 540-545, Jan. 2000

[6] M. Glavin, W. G. Hurley, "Battery Management System for Solar Energy Applications**,"** IEEE Universities Power Engineering Conference, vol. 1, Sept. 2006, pp. 79-83

[7] K. Hirachi, M. Yamanaka, T. Takada, T. Mii, M. Nakaoka, "Feasible developments of utility-interactive multi-functional bidirectional converter for solar photovoltaic generating system incorporating storage batteries," IEEE Power Electronics Specialists Conference, 1995, vol. 1, pp. 536-541

[8] S. Sopitpan, P. Changmoang, S. Panyakeow, "PV systems with/without grid back-up for housing applications," IEEE Photovoltaic Specialists Conference, Sept. 2000, pp. 1687-1690

[9] B. Ozpineci, L. M. Tolbert, D. Zhong, "Multiple input converters for fuel cells," in proc. Industry Applications Conference, 2004, vol. 2, pp. 791-797, 3-7 Oct. 2004

[10] R. U. Haque, M. T. Iqbal, J. E. Quaicoe, "Sizing, Dynamic Modeling and Power Electronics of a Hybrid Energy System," IEEE Canadian Conference on Electrical and Computer Engineering, Ottawa, May 2006, pp. 1135-1138

[11] A. D. Napoli, F. Crescimbini, F. G. Capponi, L. Solero, "Control strategy for multiple input DC-DC power converters devoted to hybrid vehicle propulsion systems," IEEE Industrial Electronics International Symposium, vol. 3, May 2002, pp. 1036-1041

[12] L. Solero, A. Lidozzi, J. A. Pomilio, "Design of multiple-input power converter for hybrid vehicles," IEEE Transactions on Power Electronics, vol. 20, pp. 1007-1016, Sept. 2005

[13] A. Lidozzi, L. Solero, "Power balance control of multiple-input DC-DC power converter for hybrid vehicles," IEEE Industrial Electronics International Symposium, vol. 2, pp. 1467-1472

[14] M. Amirabadi, S. Farhangi, "Fuzzy Control of a Hybrid Power Source for Fuel Cell Electric Vehicle using Regenerative Braking Ultra-capacitor," IEEE International Power Electronics and Motion Control Conference, 2006 pp. 1389-1394

[15] M. B. Camara, H. Gualous, F. Gustin, A. Berthon, "Control strategy of Hybrid sources for Transport applications using super capacitors and batteries," Power Electronics and Motion Control Conference, 2006, vol. 1, pp. 1-5

[16] H. Tao, A. Kotsopoulos, J. L. Duarte, M. A. M. Hendrix, "Family of multi-port bidirectional DC-DC converters," IEEE Proc. on Electric Power Applications, vol. 153, pp. 451-458

[17] B. Ozpineci, L. M. Tolbert, D. Zhong, "Optimum fuel cell utilization with multilevel inverters," Power Electronics Specialists Conference, vol. 6, June 2004, pp. 4798-4802

[18] Y. M. Chen, Y. C. Liu, F. Y. Wu, "Multi-input converter with power factor correction, maximum power point tracking, and ripple-free input currents," Power Electronics, IEEE Transactions, Volume 19, May 2004, pp. 631-639

[19] Y. M. Chen, Y. C. Liu, F. Y. Wu, "Multi-input DC-DC converter based on the multi-winding transformer for renewable energy applications," IEEE Transactions on Industry Applications, vol. 38, pp. 1096-1104, July-Aug. 2002

[20] Y. M. Chen, Y. C. Liu, F. Y. Wu, T. F. Wu, "Multi-input DC-DC converter based on the flux additivity," IEEE proc. on Industry Applications Conference, vol. 3, Sept. 2001, pp. 1866-1873

[21] S. Mariethoz, A. Rufer, "Multi-source DC-DC converter for the supply of hybrid multilevel converter," IEEE Industry Applications Conference, vol. 2, Oct. 2006, pp. 982-987

[22] Y. M. Chen, Y. C. Liu, F. Y. Wu, Y. E. Wu, "Multi-input converter with power factor correction and maximum power point tracking features," Applied Power Electronics Conference and Exposition, vol. 1, March 2002, pp. 490-496

[23] K. Kobayashi, H. Matsuo, Y. Sekine, "Novel Solar-Cell Power Supply System Using a Multiple-Input DC–DC Converter," IEEE Industrial Electronics Transactions, vol. 53, pp. 281-286, Dec. 2005

[24] S. Kirn, S. Mun, J. Kirn, S. Jang, C. Won, "A new sepic-flyback converter," IEEE Industrial Electronics Society Annual Conference, vol. 2, Nov. 2004, pp. 1004-1007

[25] M. Jinno, P. Chen, K. Lin, "An efficient active LC snubber for multi-output converters with flyback synchronous rectifier," Power Electronics Specialist Conference, vol. 2, June 2003, pp. 622-627

[26] S. Kim, D. Choi, S. Jang, T. Lee, C. Won, "The Active Clamp Sepic-Flyback Converter," Power Electronics Specialists Conference, 2005, pp. 1209-1212

[27] S. Arulselvi, K. Deepa, G. Uma, "Design, analysis and control of a new multi-output flyback CF-ZVS-QRC," International Conference on Industrial Technology, Dec. 2005, pp. 413-418

[28] C. Kim, W. Oh, H. Kim, "Alternately zero voltage switched forward, flyback multi resonant converter topology," Industrial Electronics Society Annual Conference, vol. 1, Nov. 2002, pp. 300-304

[29] L. Yao, H. Mao, J. Liu, I. Batarseh, "Zero-voltage-switching buck-flyback isolated DC-DC converter with synchronous rectification," IEEE Applied Power Electronics Conference and Exposition, March 2006, pp. 6-11

[30] S. Lee, H. Kim, H. Lee, S. Yang, G. Choe, H. Mok, "A New Automatic Synchronous Switch Post Regulator for Multi-Output Converters," IEEE Power Electronics Specialists Conference, 18-22 June 2006, pp. 1-4

[31] H. S. Chung, S. Y. R. Hui, W. H. Wang, "A zero-current-switching PWM flyback converter with a simple auxiliary switch," IEEE Power Electronics Transactions, vol. 14, pp. 329-342, March 1999

[32] F. Zhang, L. Xiao, Y. Yan, "Bi-directional forward-flyback DC-DC converter," Power Electronics Specialists Conference, vol. 5, 20-25 June 2004, pp. 4058-4061

[33] M. Nakaoka, G. Yu, A. Chibani, H. Yonemori, H. Ueda, Y. Ogino, "Resonant flyback switched-mode DC-DC converters using static induction power devices," Power Electronics and Variable-Speed Drives conference, 13-15 Jul 1988, pp. 466-474

[34] K. W. Ma, Y. S. Lee, "An integrated flyback converter for DC uninterruptible power supply," IEEE Transactions on Power Electronics, vol. 11, pp. 318-327, March 1996

[35] C. M. Wang, C. H. Su, C. H. Yang, "ZVS-PWM flyback converter with a simple auxiliary circuit," IEEE Proc. on Electric Power Applications, vol. 153, pp. 116-121, Jan. 2006

[36] H. S. H. Chung, W. L. Cheung, K. S. Tang, "A ZCS bidirectional flyback converter," Power Electronics Specialists Conference, vol. 2, 20-25 June 2004, pp. 1506-1512

[37] H. Chung, S. Y. R. Hui, W. H. Wang, "An isolated fully soft-switched flyback converter with low voltage stress," Power Electronics Specialists Conference, vol. 2, 22-27 June 1997, pp. 1417-1423

[38] Hongmei Wang, Chunying Gong, Haixiao Ma, Yangguang Yan, "Research on a Novel Interleaved Flyback DC/DC Converter," IEEE Industrial Electronics and Applications Conference, May 2006 pp. 1-5

[39] Y. Chen, Y. Liu, "Development of multi-port converters for hybrid wind-photovoltaic power system," IEEE Electrical and Electronic Technology Proceedings of International Conference, vol. 2, 19-22 Aug. 2001, pp. 804-808

[40] H. Shiji, K. Harada, Y. Ishihara, T. Todaka, G. Alzamora, "A zero-voltage-switching bidirectional converter for PV systems," IEEE Telecommunications Energy Conference, 19-23 Oct. 2003, pp. 14-19

[41] D. Liu, H. Li, "A ZVS Bi-Directional DC–DC Converter for Multiple Energy Storage Elements," IEEE Transactions on Power Electronics, vol. 21, pp. 1513-1517, Sept. 2006

[42] D. Liu, H. Li, "A novel multiple-input ZVS bidirectional DC-DC converter," Industrial Electronics Society Conference, 6-10 Nov. 2005, pp. 6

[43] H. Tao, A. Kotsopoulos, J.L. Duarte, M.A.M. Hendrix, "Multi-input bidirectional DC-DC converter combining DC-link and magnetic-coupling for fuel cell systems," Industry Applications Conference, vol. 3, 2-6 Oct. 2005, pp. 2021-2028

[44] N.D. Benavides, P.L. Chapman, "Power budgeting of a multiple-input buck-boost converter," IEEE Transactions on Power Electronics, vol. 20, pp. 1303-1309, Nov. 2005

[45] H. Tao, A. Kotsopoulos, J. L. Duarte, M. A. M. Hendrix, "Family of multi-port bidirectional DC-DC converters," IEEE Proc. on Electric Power Applications, vol. 153, pp. 451 - 458, May 2006

[46] B.G. Dobbs, P.L. Chapman, "A multiple-input DC-DC converter topology," Power Electronics Letters, vol. 1, pp. 6-9 March 2003

[47] N. D. Benavides, T. Esram, P. L. Chapman, "Ripple Correlation Control of a Multiple-Input Dc-Dc Converter," Power Electronics Specialists Conference, 2005, pp. 160-164

[48] K. P. Yalamanchili, M. Ferdowsi, "Review of multiple input DC-DC converters for electric and hybrid vehicles," Vehicle Power and Propulsion IEEE Conference, 7-9 Sept. 2005, pp. 160-163

[49] Y. M. Chen, Y. C. Liu, S. H. Lin, "Double-Input PWM DC/DC Converter for High/Low-Voltage Sources," IEEE Transactions on Industrial Electronics, vol. 53, pp. 1538-1545, Oct. 2006

[50] Y. P. Krishna, Mehdi Ferdowsi, and Keith Corzine, "New Double Input DC-DC Converters for Automotive Applications", Power Electronics and Motor Drives Laboratory, University of Missouri-Rolla

[51] K. P. Yalamanchili, L. Shuai, M. Ferdowsi, and K. Corzine, "New bidirectional double-input dc-dc converters for automotive applications," to be submitted to IEEE Transactions on Vehicular Technology, 2007

[52] K. P. Yalamanchili, "Multi-input dc-dc converters for combined energy storage systems in hybrid electric vehicles," M. S. Thesis, University of Missouri-Rolla, Dec. 2006

[53] F. Caricchi, F. Crescimbini, F. G. Capponi, and L. Solero, "Study of bidirectional buck-boost converter topologies for application in electrical vehicle motor drives," Applied Power Electronics Conference, 15-19 Feb. 1998, vol. 1, pp. 287-293

[54] M. Becherif, M.Y. Ayad, A. Miraoui, "Modeling and Passivity-Based Control of Hybrid Sources: Fuel Cell and Supercapacitors," Industry Applications Conferenc, vol. 3, Oct. 2006, pp. 1134 - 1139

[55] X. Yan, D. Patterson, "Improvement of drive range, acceleration and deceleration performance in an electric vehicle propulsion system," Power Electronics Specialists Conference, vol. 2, June 1999, pp. 638-643

[56] X. Yan, A. Seckold, D. Patterson, "Development of a zero-voltage-transition bidirectional DC-DC converter for a brushless DC machine EV propulsion system," Power Electronics Specialists Conference, vol. 4, 23-27 June 2002, pp. 1661-1666

[57] S. Lu, K. A. Corzine, M. Ferdowsi, "High Efficiency Energy Storage System Design for Hybrid Electric Vehicle with Motor Drive Integration" IEEE Industry Applications Conference, vol. 5, Oct. 2006, pp. 2560-2567

[58] Y.M. Chen, S.C. Hung, C.S. Cheng, Y.C. Liu, "Multi-input inverter for grid-connected hybrid PV/wind power system," Applied Power Electronics Conference and Exposition, vol. 2, 6-10 March 2005, pp. 850-856

[59] H. Al-Atrash, F. Tian, I. Batarseh, "Tri-Modal Half-Bridge Converter Topology for Three-Port Interface," IEEE Transactions on Power Electronics, vol. 22, pp. 341-345, Jan. 2007

[60] A. D. Napoli, F. Caricchi, F. Crescimbini, O. Honorati, E. Santini, "Testing of a new DC-DC converter topology for integrated wind-photovoltaic generating systems," IEEE Fifth European Conference on Power Electronics and Applications, vol.8, Sept. 1993, pp. 83-88

[61] A. D. Napoli, F. Crescimbini, S. Rodo, L. Solero, "Multiple input DC-DC power converter for fuel-cell powered hybrid vehicles," IEEE Power Electronics Specialists Conference, vol. 4, June 2002, pp. 1685-1690

[62] A. D. Napoli, F. Crescimbini, L. Solero, F. Carricchi, F. G. Capponi, "Multiple-input DC-DC power converter for power-flow management in hybrid vehicles," IEEE Conference on Industry Applications, vol. 3, Oct. 2002, pp. 1578-1585

[63] H. Nikkhajoei, M. Saeedifard, R. Iravani, "A three-level converter based micro-turbine distributed generation system," Power Engineering Society General Meeting, June 2006

[64] P. Wood, *Switching Power Converters*. Van Nostrand Reinhold Co, 1981, Chap. 3

[65] J. Sebastian, P. Villegas, M. M. Hernando, S. Ollero, "High quality flyback power factor corrector based on a two input buck post-regulator," IEEE Applied Power Electronics Conference, Feb. 1997, vol. 1, pp. 23-27

[66] A. Davoudi, J. Jatskevich, and P. L. Chapman, "Parametric average-value modeling of multiple-input buck converters," IEEE Canadian Conference, 22-26 April 2007, pp. 990-993

[67] S. B. Galateanu, "Buck-flyback dc-dc converter," IEEE transactions on Aerospace and Electronic Systems, vol. 24, pp. 800-807, Nov. 1988

[68] G. Spiazzi, S. Buso, "Power factor preregulators based on combined buck-flyback topologies," IEEE transactions on Power Electronics, vol. 15, pp. 197-204, March 2000

VITA

Karteek Gummi was born on 23rd April, 1984 in the heart of Hyderabad city located in the state of Andhra Pradesh, the southern part of India. He obtained his Bachelor's degree in Electrical and Electronics Engineering from Mathuri Venkata Subba Rao engineering college affiliated to Osmania University in May 2006. He came to University of Missouri – Rolla in fall 2006 to pursue his Master's degree in Electrical Engineering specializing in Power Electronics and Power Systems. He graduated in May 2008. His areas of interest are modeling, analysis, design, and control of power electronic converters**,** economic operation and power quality of power systems, hybrid electric vehicles, multi-input converters, photovoltaic systems, automotive power electronics and motor drives, design of electric machines, dc-dc and ac-dc converters. He plans to pursue a career in the field of power.